Journal of Environmental Chemical Engineering 11 (2023) 110467

Contents lists available at ScienceDirect

Journal of Environmental Chemical Engineering

journal homepage: www.elsevier.com/locate/jece

Electrochemical system design for CO_2 conversion: A comprehensive review

M.S. Sajna [a], Sifani Zavahir [a], Anton Popelka [a], Peter Kasak [a], Ali Al-Sharshani [b], Udeogu Onwusogh [b], Miao Wang [c], Hyunwoong Park [c,*], Dong Suk Han [a,d,**]

[a] Center for Advanced Materials, Qatar University, Doha, Qatar
[b] Qatar Shell Research and Technology Center (QSRTC), Qatar Science and Technology Park (QSTP), Doha, Qatar
[c] School of Energy Engineering, Kyungpook National University, Daegu 41566, Republic of Korea
[d] Department of Chemical Engineering, College of Engineering, Qatar University, Doha, Qatar

ARTICLE INFO

Editor: Despo Kassinos

Keywords:
Carbon dioxide
Electrochemical conversion
Electrolyzer
Electrocatalyst
Circular economy

ABSTRACT

This paper reviews the electrochemical reduction of CO_2 and the design of CO_2 electrolyzer cells using advanced materials and novel configurations to improve efficiency and reduce costs. It examines various system types based on geometry and components, analyzing key performance parameters to offer valuable insights into effective and selective CO_2 conversion. Techno-economic analysis is employed to assess the commercial viability of electrochemical CO_2 reduction (eCO_2R) products. Additionally, the paper discusses the design of eCO_2R reactors, addressing challenges, benefits, and developments associated with reactant supply in liquid and gas phases. It also explores knowledge gaps and areas for improvement to facilitate the development of more efficient eCO_2R systems. To compete with gas-fed electrolyzers, the paper presents various approaches to enhance the performance of liquid-fed electrolyzers, leveraging their operation simplicity, scalability, low costs, high selectivity, and reasonable energy requirements. Furthermore, recent reports summarizing the performance parameters of reliable and effective electrocatalysts under ideal operating conditions, in conjunction with different electrolyzer configurations, are highlighted. This overview provides insights into the current state of the field and suggests future research directions for producing valuable chemicals with high energy efficiency (low overpotential). Ultimately, this review equips readers with fundamental knowledge and understanding necessary to improve and optimize eCO_2R beyond lab-scale applications, fostering advancements in the promising field.

1. General overview: CO_2 emission and reduction

Carbon dioxide (CO_2) is a colorless, odorless gas essential for plant photosynthesis but, along with other greenhouse gases (GHGs) (e.g., methane, nitrous oxide, and industrial gases), contributes to global warming and air pollution. CO_2 is the most common GHG, primarily released from fossil fuel combustion. As industries grow, more CO_2 enters the atmosphere, worsening climatic change. The 6th Assessment Report (AR6) of the Intergovernmental Panel on Climate Change (IPCC) warns that without significant emissions reductions, Earth's average temperature will rise by 1.5 °C within 20 years and 2 °C by mid-century [1].

Various techniques have been developed to address the negative impact of rising atmospheric CO_2 levels. These includes improving energy efficiency, CO_2 capture and utilization (CCU), bioenergy with carbon capture and storage (BECCS) (such as algae cultivation for CO_2 capture and reduction), geological sequestration through carbon capture and storage (CCS), carbon mineralization, photocatalytic CO_2 reduction, chemical looping conversion, and using non/low-carbon energy sources (e.g., solar and wind) [2–4]. Among these, CO_2 conversion is particularly promising, as it reduces emissions while converting CO_2 into valuable materials or fuels. Increased government funding worldwide show importance of addressing CO_2 emissions.

Gulzar et al. have proposed and summarized several strategies to minimize anthropogenic CO_2 emissions (Fig. 1) [5].

Fig. 2 **(a)** illustrates the significant progress achieved in electrochemical CO_2 conversion research over the past decade, as evidenced by the growing number of relevant publications. Keywords play a crucial

* Correspondence to: Kyungpook National University, Daegu, Republic of Korea.
** Corresponding author at: Center for Advanced Materials, Qatar University, Doha, Qatar.
E-mail addresses: hwp@knu.ac.kr (H. Park), dhan@qu.edu.qa (D.S. Han).

https://doi.org/10.1016/j.jece.2023.110467
Received 7 February 2023; Received in revised form 26 June 2023; Accepted 28 June 2023
Available online 29 June 2023

role in summarizing an article's main ideas [6], and identifying them is essential for bibliometric analysis (BA). To analyze the thematic content of the publication set from 2010 to 2022, we utilized VOSviewer software developed by Eck and Waltman [7], enabling co-occurrence analysis and network map visualization, as shown in Fig. 2**(b)**. The software clusters related topics and represent them by colored circles, with size indicating keyword frequency and distance reflecting topic similarity. From 5896 papers on "electrochemical CO_2 conversion," we set a minimum keyword occurrence threshold of 15, resulting in 571 keywords that met the criterion. Analyzing keyword co-occurrences reveals research potential and trending topics in various disciplines. Fig. 2**(b)** presents the interconnectedness and relevance of keywords within the electrochemical CO_2 conversion field.

Converting CO_2 into valuable fuel products and chemicals effectively reduces atmospheric CO_2 levels, and various processes have been extensively studied for this purpose. CO_2 reduction (CO_2R) methods, including electrochemical, thermal, photochemical, plasma-based biochemical, photocatalytic, chemo-enzymatic, and photo-electrochemical reduction, have been investigated [8–14]. The combination of affordable renewable electricity and the need to reduce carbon intensity provides an ideal environment for CO_2R development. Therefore, it is crucial to examine the technical feasibility of all current methods and establish state-of-the-art (SOT) technology. CO_2 capture, conversion, and utilization are among the most practical and promising research areas in the energy and environment fields.

Recent review papers on electrochemical CO_2 reduction (eCO_2R) focus on electrocatalytic materials [15,16] and the eCO_2R mechanism [17,18]. However, fewer articles address CO_2 electrolyzer design, structure, and optimization, which are crucial topics to investigate.

In their study, Sean et al. [19] focused on reactor engineering to improve the reaction rate and scalability, and they examined reaction mechanisms using in situ and operando techniques. Their research emphasizes the importance of overcoming technical barriers for CO_2 electrolysis technology's commercial deployment. Our review covers various aspects of eCO_2R, including potential reaction pathways, research interest, techno-economic feasibility evaluation, and figure of merit parameters, offering a comprehensive understanding of the subject. The primary focus is electrolytic cell design and engineering based on geometry and CO_2 feed form. Various subsections, such as separator membrane design, electrolyte selection, and catalyst choice, are also discussed. This review highlights the advantages and challenges of the CO_2R reaction in both aqueous and gas-fed electrochemical cells, providing a foundation for further exploration and implementation of these technologies to address critical issues such as mass transfer, stability, and durability in eCO_2R processes.

2. Electrochemical CO_2 reduction (eCO_2R)

Electrochemical CO_2 reduction (eCO_2R) is a valuable technology that mitigates CO_2 emissions, making it essential for tackling global environmental challenges. Electrochemistry uses electrical input to drive chemical reactions, with various reaction pathways leading to value-added products. The circular carbon economy (CCE) is part of the "4 R" strategy: reduce, reuse, recycle, and remove [20]. The eCO_2R contributes to CCE management, as illustrated in Fig. 3, by producing various gas-phase (e.g., CO, CH_4, and C_2H_4) and liquid-phase (e.g., HCOOH, CH_3OH, C_2H_5OH, and C_3H_7OH) products.

Formic acid, for example, has potential applications as a safe, portable chemical and energy storage material, either used directly or reformed in a formic acid fuel cell [21–23]. It can also be biochemically transformed into various materials, such as fuels, plastic monomers, and solvents [24]. Key limiting factors for the eCO_2R reaction include mass transfer dynamics, CO_2 solubility, CO_2 supply, electrolyte pH, electrocatalytic properties, and electrolyzer system design [25,26]. Therefore, developing improved catalysts, electrolyzers, and optimized electrolytic processes is essential for achieving highly selective CO_2R.

2.1. Possible reaction pathways in eCO_2R

The eCO_2R process involves multiple electron and proton transfer steps, including two, four, six, eight, and twelve-electron pathways, as shown in Fig. 4 [28]. Various products are generated depending on the specific reaction pathway, solvent, and catalysts [29]. However, selectively producing a specific product with high yield is challenging due to the similar thermodynamic oxidation-reduction potentials of several CO_2 reaction pathways, reducing selectivity toward the target product. Table 1 presents the standard potentials of selected eCO_2R products under normal conditions, calculated using the standard Gibbs free energy. These potential shows that numerous CO_2R reactions competing with the hydrogen evolution reaction (HER) have a narrow range of standard potentials (E_0), making it difficult to achieve high selectivity.

2.2. Economics of CO_2 reduction products

Determining which CO_2 reduction product to prioritize for commercialization is essential, as CO_2 can be eletrochemically reduced to various compounds at similar potentials. Supply, demand, and cutting-edge technology can impact total cost and production rate. Key economic factors help address this issue. The global market plays a significant role in eCO_2R research, and the techno-economic analysis of target products is important. Jouny et al. [31] report that under current conditions, carbon monoxide and formic acid are commercially viable products with respective end-of-life net present values (NPV) of $13.5 million and $39.4 million at a production rate of 100 tons/day. Higher-order alcohols like ethanol and n-propanol could become more attractive with improved electrocatalytic performance. These products are desirable due to their high energy densities and large market capacities. To be profitable, parameters like current density, overpotential,

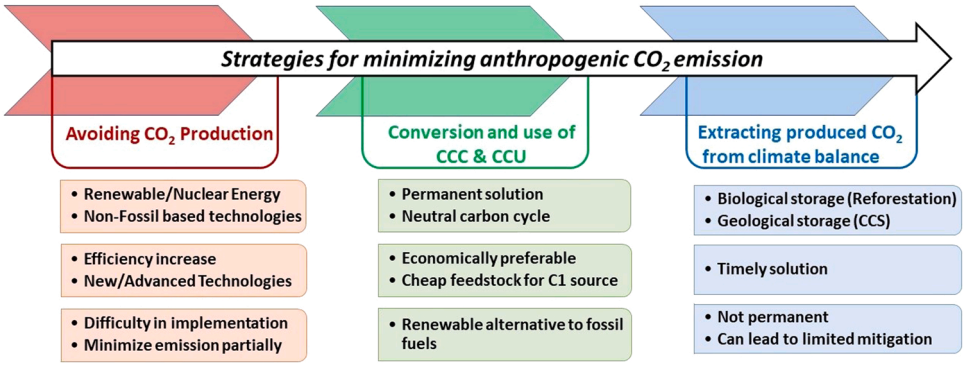

Fig. 1. Strategies for minimizing CO_2 emissions (Redrawn from [5]).

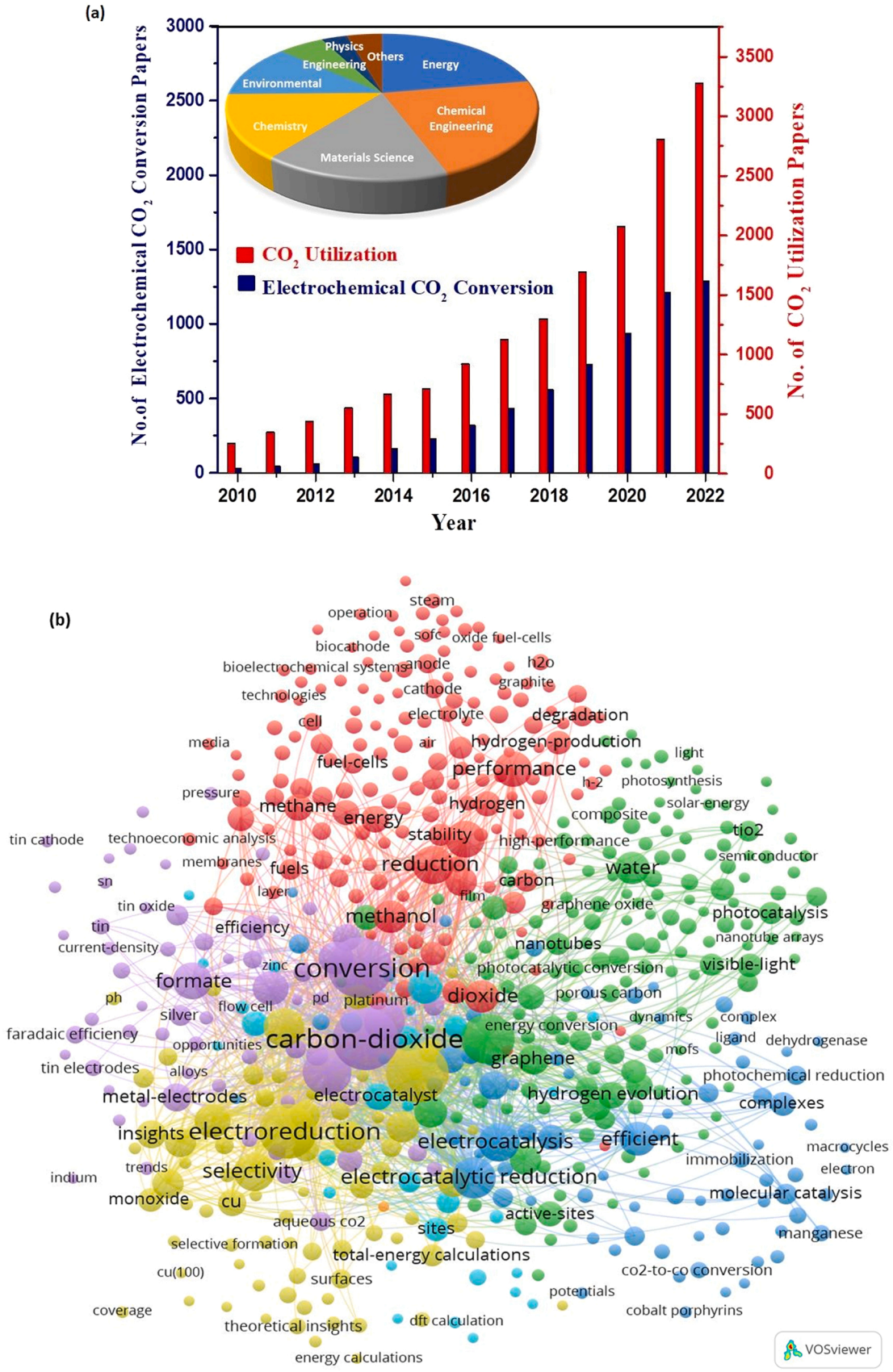

Fig. 2. (a) Bar diagram representing the number of publications with two different keyword combinations, i.e., "CO_2 utilization" and "electrochemical CO_2 conversion," reported over the past decade, with the distribution of core content of the publications over the subject area (embedded pie chart). (b) VOSviewer network map of co-occurrence of keywords with thematic content electrochemical CO_2 conversion (For the plots and mapping, data adapted from Web of Science database).

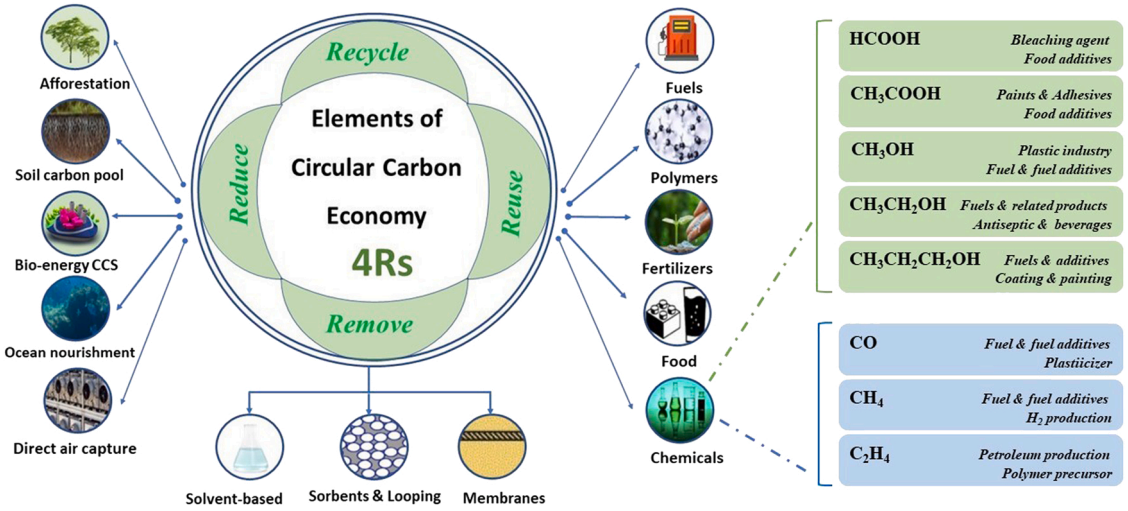

Fig. 3. Schematic of CCE elements and chemical products of typical CO_2R electrocatalysis (Redrawn from [20,27]).

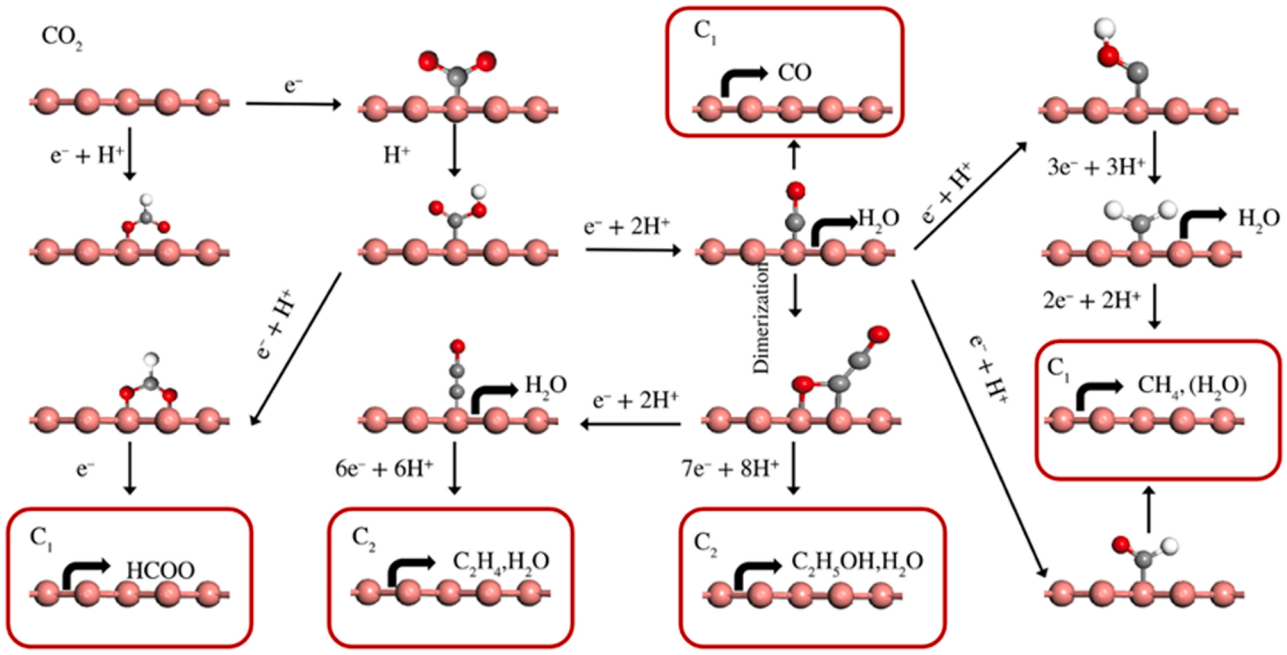

Fig. 4. Scheme for possible electrochemical carbon dioxide reduction routes that result in C_1 products, such as CO, HCOOH, and CH_4, and C_2 products, such as C_2H_4 and C_2H_5OH
(Adapted with permission from [30], Copyright (2019) Wiley Periodicals, Inc.).

and Faradaic efficiency (FE) must reach certain benchmarks. Achieving these targets could make eCO_2R an economically viable option within the renewable energy infrastructure.

Fig. 5 shows a modeling study by Nitopi et al. [32] on the economics and energetics of potential CO_2 reduction products. Values are presented for the minimum energy required for CO_2R to be balanced with the oxygen evolution reaction (OER). Indicator size represents the logarithmic global market size, and all economic variables are normalized to carbon mass. Production cost is shown for two electricity price scenarios ($20 and $50 per MWh). The study assumes CO_2 capture at a power plant costs $200 per ton of carbon. Products above the lines, including formic acid, propanol, ethanol, acetaldehyde, ethylene, methanol, and carbon monoxide, are economically feasible. Ethanol and ethylene are notable for their high energy content, market price, and volume. The study emphasizes that not all products are value-added when considering CO_2 capture costs. Current research focuses on primary eCO_2R products: single-carbon compounds (C1) like formic acid, CO, and propanol, and multiple-carbon products (C_{2+}) with high energy and attractive market prices [33].

2.3. Performance parameters of the eCO_2R system

An efficient CO_2 electrolyzer must be durable with low ohmic resistance and good mass transfer quality under reaction conditions while using a highly active, stable, and selective catalyst. Characterizing each specific aspect of an electrolyzer is tedious. However, several metrics, such as the Faradaic efficiency (FE), energy efficiency (EE), current density (CD), catalyst activity, overpotential, and reactor stability, are used to quantify the CO_2R system, regardless of the electrochemical properties of a particular reaction [34,35].

Table 1
Standard equilibrium potentials for the hydrogen evolution half-cell reaction and several other half-cell reactions used to reduce CO_2 into various products (Adapted with permission from [31], Copyright (2018) American Chemical Society).

Product: -	Half-cell electrochemical reactions	Potential E/V vs. SHE (V)
$CO_{(g)}$	$CO_{2(g)}+ 2\ H^+ + 2e^- \leftrightarrow CO_{(g)} + H_2O_{(l)}$	-0.106
$HCOOH_{(l)}$	$CO_{2(g)}+ 2\ H^+ + 2e^- \leftrightarrow HCOOH_{(l)}$	-0.250
$CH_3OH_{(l)}$	$CO_{2(g)}+ 6\ H^+ + 6e^- \leftrightarrow CH_3OH_{(l)} + H_2O_{(l)}$	0.016
$CH_{4(g)}$	$CO_{2(g)}+ 8\ H^+ + 8e^- \leftrightarrow CH_{4(g)} + 2\ H_2O_{(l)}$	0.169
$C_2H_{4(g)}$	$CO_{2(g)}+ 12\ H^+ + 12e^- \leftrightarrow C_2H_{4(g)} + 4\ H_2O_{(l)}$	0.064
$C_2H_5OH_{(l)}$	$CO_{2(g)}+ 12\ H^+ + 12e^- \leftrightarrow C_2H_5OH_{(l)} + 3\ H_2O_{(l)}$	0.084
$C_3H_7OH_{(l)}$	$CO_{2(g)}+ 18\ H^+ + 18e^- \leftrightarrow C_3H_7OH_{(l)} + 5\ H_2O_{(l)}$	0.095
$H_{2(g)}$	$2\ H+ 2e^- \leftrightarrow H_{2\ (g)}$	0.000

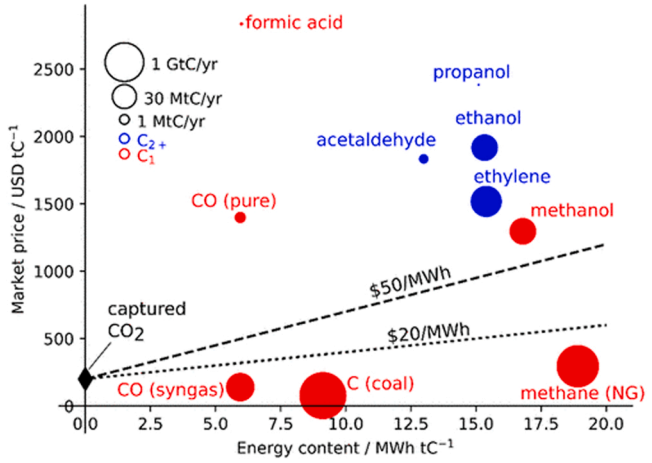

Fig. 5. Energy content versus the market price of selected CO_2 reduction products. The lines reflect the minimum energy cost required for CO_2 capture and conversion using commercially available technologies; capital costs are excluded
(Adapted with permission from [32], Copyright (2019) American Chemical Society).

2.3.1. Faradaic efficiency

The target product's FE (or current efficiency) is an essential performance metric. It is the ratio of the total charge flowing between the electrodes to the charge used to generate the desired product, as follows.

$$(\mathrm{FE})_{\mathrm{product}} = \frac{ynF}{Q} \tag{1}$$

where, y is the number of moles of the targeted product, n is the number of electrons required for a half-cell reaction per mole of product, and F is the Faradaic constant (96485 C/mol electrons, Q is the total charge supplied through the electrodes during the process [36]. Numerous factors, such as the catalyst, electrode potential, pH, and electrolyte species, affect the faradaic efficiency and selectivity of the reaction [29]. The FE reflects the selectivity for a given product, and an increase in the FE can effectively enhance CO_2 conversion into the final product. This improvement, in turn, minimizes production extraction costs and reduces energy losses in electrocatalysis.

2.3.2. Current density

CD, which is the total current (I, amps) per unit area (A) of the cathode (active electrode area, m^2 or typically cm^2) at a given potential, is an essential parameter for production output. Since the electrons exchanged in a chemical reaction are related to the reaction's scale, this parameter indicates the reaction rate of a specific product under certain conditions (i.e., the number of moles of reactant reduced). The CD is a vital input for estimating the electrolyzer size and the cost-effectiveness of the CO_2R process, as it represents the overall reaction rate [37]. Additionally, several other factors can influence the CD, including catalyst type, catalyst loading, and the rates at which reactants and products are transported to and from the electrode.

In an electrochemical system, a higher CD corresponds to a higher reactant reduction rate, while a higher partial CD indicates a higher product generation rate. A high CD is desirable because it reduces the overall size of the electrolyzer and decreases the capital expenditure required to achieve the target production rate.

$$CD = \frac{I}{A} \tag{2}$$

The partial CD of a particular product is evaluated as follows.

$$j_{product} = FE_{product} \times CD \tag{3}$$

2.3.3. Onset potential and overpotential

The onset potential refers to the lowest negative potential at which the reaction product or Faradaic current is detected. Essentially, the voltage applied to the electrocatalyst relative to the reference electrode determines the conditions under which the desired product is produced in detectable amounts.

The difference between the standard potential and the potential at which the redox event occurs is called the overpotential (η) of the electrochemical reaction. Essentially, it is the additional potential required by the system, compared to that predicted using thermodynamics, to induce the redox reaction. Note that the overpotential should generally be low. The overpotential is often divided into two parts: the activation polarization ($\eta_{activation}$), which is required to overcome the activation energy barrier for the reaction to proceed on the catalytic electrode surface, and the constraint on the mass transport of dissolved CO_2 ($\eta_{diffusion}$) [38,39]. Note that the ohmic drop (iR_s) across the electrolyte and ion exchange membrane is a potential loss governed by the system's ionic conductivity in the presence of current and should not be considered an overpotential.

2.3.4. Energy efficiency (EE)

EE is an indicator of the applied energy that is converted into chemically stored energy and serves as a measure of the net energy consumption for a target product. For any target product, the FE and overpotential can be combined with other losses, which can be defined as the ratio of the amount of energy used to produce the target product across the cell to the net energy supplied to the system.

$$EE_{product} = \frac{E^0 \times FE_{product}}{E^0 + \eta + iR_s} \tag{4}$$

where E^0 is the thermodynamic reaction voltage ($E^0_{cathode} - E^0_{anode}$) or the equilibrium cell potential for the desired product; η represents the sum of the overpotentials; and iR_s is the ohmic loss across the cell. EE is one of the most important metrics, and it provides operational cost analysis. Higher FE and voltage are key requirements to achieve good EE.

2.3.5. Reactor stability

System stability is crucial for industrialization and is influenced by workload characteristics and operating conditions. The stability and lifetime of the electrochemical cell in eCOR, including catalyst, electrode, electrolyte, ion exchange membrane, and the cell itself, is an underexplored aspect. Performance can be altered by contaminants in the electrolyte. Chronopotentiometry helps assess stability by monitoring the potential difference. A reliable system maintains a steady potential for hours and stable product selectivity for efficient reactions [40]. Enhancing catalytic process stability minimizes maintenance and expenses, which are crucial for scaling up the reactor.

2.3.6. Tafel plot

A Tafel plot links the rate of an electrochemical reaction and the overpotential used to produce that rate. The overpotential is typically plotted against the logarithm of the CD in the Tafel plot, which is useful for measuring the catalyst activity and investigating the reaction mechanism. The lower the Tafel slope, the better the charge transfer and electrocatalyst performance. A sharp change in the slope indicates a change in the reaction process because of the reaction environment, such as reactant concentration, electrolyte concentration, and surface morphology of the catalyst. The Tafel relation is given by [41,42].

$$\eta = a + blog(i) = -2.303\frac{RT}{\alpha F}\log(i_0) + 2.303\frac{RT}{\alpha F}\log(i) \quad (5)$$

where, η is the overpotential, i is the current density, a and b are the empirical Tafel constants. The charge transfer coefficient α, is reversely proportional to b, which is the slope of the Tafel plot. R represents the universal gas constant, F is the Faraday's constant, T denotes the absolute temperature. The exchange current density, or the current density at equilibrium, is represented by i_0 measured from the intercept of the plot, indicates the reaction kinetics and catalytic properties [42]. Since different products are formed in these various reactions processes, the exchange current and Tafel slopes for these products obtained from the CO_2R must be accurately differentiated. Thus, instead of using the total CD, which necessitates precise product measurement at lower concentrations, employing the partial CD is the conventional approach for plotting the Tafel slope of a specific CO_2R product. In contrast, if the overall CD is used to calculate the Tafel slope, the obtained values will include contributions from the CO_2 reduction (CO_2R) reaction and the hydrogen evolution reaction (HER). Ultimately, the Tafel slope is an essential metric derived from electrochemical measurements. It is valuable for investigating the reaction process and enables faster research advancement and enhanced reaction control in the industrial field.

3. Electrolyzer configuration: cell design and architectures for eCO_2R

The overall catalytic activity and selectivity in CO_2R are greatly influenced by electrolyzer system design, which can be divided into two categories: aqueous-fed (liquid-phase reactors) and gas-fed reactors. Liquid-phase electrolyzer feed CO_2 to the catalyst as CO_2 dissolved in the electrolyte. Early CO_2R catalyst studies used aqueous-fed reactors, which experience mass transfer limitations due to CO_2's low solubility (34 mM) [43]. Gas-fed electrolyzers overcome this problem by introducing gaseous CO_2 using gas diffusion electrodes (GDEs). An ideal CO_2 electrolyzer must have a high CD (fast CO_2-to-product conversion) and high FE (selectivity for a certain CO_2 derivative) for a specific CO_2 derivative to be commercially feasible.

A well-designed CO_2 electrochemical conversion process is as crucial as an efficient electrocatalyst for the system's performance. While much research has focused on improving catalytic performance, fewer studies have investigated eCO_2R reactor design and engineering [44–47]. However, recent studies have investigated electrolyzers [48,49], which are essential for commercial-scale applications. Key variables in designing an electrochemical reactor include the catalyst surface type, transporting reactants and products, and selecting the electrolyte. Various CO_2 electrolyzer geometries (H-type, flow, and microfluidic reactors) have been developed, along with key components (gas diffusion electrode and membrane electrode assembly). The electrochemical cell's reaction depends on the applied external voltage and open-circuit potential.

3.1. Liquid-phase electrolyzer

Several research groups have employed liquid-phase reactors to study CO_2R in aqueous solutions, with significant work done since Hori et al.'s pioneering studies in the 1980 s [50–53]. These studies have explored the effects of catalyst structure, composition, surface tailoring, electrolyte concentration, pH, ion and mass transport, temperature, and pressure on CO_2R activity and selectivity. Flow cells can address some diffusion limitations in batch liquid-phase electrolyzers, but low CO_2 solubility in aqueous electrolytes still hinders mass transfer and conversion rates [54]. Higher pressures and lower temperatures [55] can increase dissolved CO_2 but do not always result in higher CDs and are not commercially viable. In a diffusion-limited regime, only the outermost part of the catalyst interacts with CO_2, using only a few microns of electrode porosity depths.

Techno-economic studies show that significant improvements in electrochemical performance are needed for cost-competitive liquid-phase eCO_2R technologies, including high current density (>200 mA cm^{-2}), good selectivity, low overpotential (1 V), and prolonged operation (>8000 h or one year) [56]. However, aqueous-fed electrolyzers struggle to meet these requirements due to mass transport limitations, resulting in CDs around 35 mA cm^{-2} (for two-electron reduction processes) [57]. Low CO_2 solubility in the aqueous phase constrains catalytic CD and product selectivity, making this cell architecture commercially unviable. Limited solubility and diffusivity of CO_2 in electrolyte, as well as the limited mass transport of OH^- near the electrode, further limit conversion rates and energy efficiency, reducing CO_2R productivity [58].

Although liquid-phase reactors have limitations in practical applications, they remain relevant for understanding factors affecting catalytic activity. Their design enables simple product separation and various catalyst electrode configurations, making them useful for evaluating CO_2R catalysts and advancing CO_2R research. Adjusting the design parameters or settings of a liquid-phase electrolyzer could potentially increase CO_2 conversion yield.

3.2. Gas/vapor-fed electrolyzers

Recently, gas-phase cell systems have demonstrated better performance than liquid-phase reactors. Gas-fed electrolyzers have no mass transfer limitations and can achieve CDs greater than 200 mA/cm^{-2} [59]. The close interface proximity creates a significant CO_2 concentration gradient at the CO_2/electrolyte boundary, enabling rapid CO_2 transfer to the catalyst (short diffusion path of approximately 50 nm) and achieving a high electrochemically active surface area. Additionally, gaseous products quickly diffuse towards the gas flow chamber before nucleation occurs on the catalyst surface, preventing active sites disturbance. Gaseous CO_2R products are obtained on the gas side of the GDE, while liquid products remain in the electrolyte solution. This results in higher geometric CDs and lower overpotential compared to liquid-fed electrolyzers [60]. Two major configurations for gas-phase electrolyzers are flow-by and flow-through (Fig. 6). In flow-by mode, CO_2 gas reaches the GDE but does not fully cross it, while in flow-through mode, CO_2 gas enters, passes the GDE, and exits as bubbles in the catholyte.

In gas-phase CO_2R, two representative techniques with distinct reactor configurations. Microfluidic and MEA types are compared for continuous CO_2 reactant supply. Efficiency can be further improved with ionic liquids and bipolar membranes [62–66]. However, most gas-fed electrolyzers lack durability and degrade after several hours of operation [67]. Commercial applications require stability for up to 30, 000 h and selectivity at CDs greater than 250 mA/cm^{-2} [40,68,69]. Although current performance shows high feasibility, more well-established technologies still need to be developed.

3.3. H-type cell: batch/semi-batch cell

The H-type cell, a liquid-phase electrolyzer, is widely used in fundamental eCO_2R research. In general, eCO_2R is performed in a three-

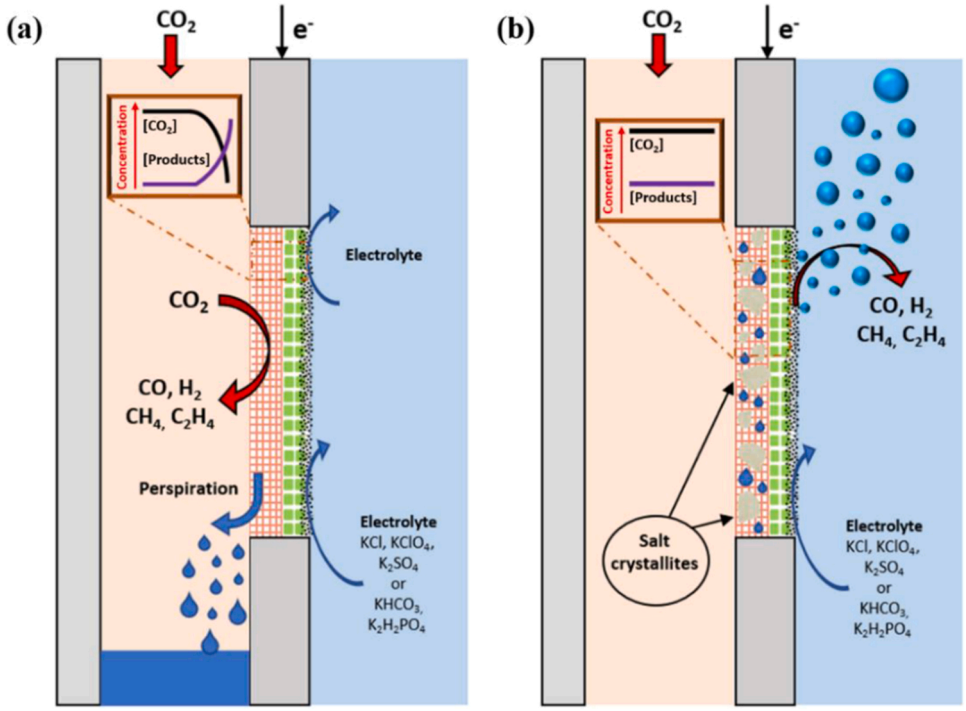

Fig. 6. Principle of the operation of gas-fed CO_2 electrolyzers: (a) flow-by and (b) flow-through configurations (Adapted from [61] Open access, MDPI).

compartment batch cell, i.e., an H-cell electrolyzer or H-cell reactor, as shown in Fig. 7**(a)** [70]. This cell type is cost-effective for screening various catalysts and quickly measuring catalytic activity. Cyclic voltammetry (CV) is a popular technique due to its ease of use and adaptability to different electrode materials and configurations. In an H-type cell, the working electrode (WE) and reference electrode (RE) are in the cathodic chamber, while the counter electrode (CE) is in the anodic chamber, with electrolyte pre-filled in both. A polymer-based porous diaphragm/membrane separates the two reaction chambers for ion exchange and prevents product re-oxidation and re-reduction. In lab-scale CO_2 electrolyzers (H-type cell reactors), the anode typically consists of graphite/platinum and the cathode is made of a simple carbon substrate (carbon paper/glassy carbon electrode). Catalysts can be applied to the cathode in various ways, such as drop-casting, electrodeposition, or spray-coating, as reduction occurs in this region. The anode in an H-type cell oxidizes water during OER, producing protons (H^+) and electrons (e^-), which balance the charge and complete the electrical circuit. The cathode converts CO_2 into value-added chemicals, such as C_1, C_2, or others, while a reference electrode measures potential. The electrolyte conducts ions and dissolves and transports CO_2 to the cathode's active area. A voltage source supplies the potential needed for electron transfer from the anode to the cathode. Gaseous CO_2 is purged into the cathode compartment from the top of the H-cell, dissolves in the liquid catholyte, and is transported to the electrolyte–cathode interface, where CO_2R occurs. Fig. 7**(b)** shows a modified polycarbonate electrochemical cell with a Teflon-coated silicon O-ring for CO_2 electrolysis experiments. The primary CO_2R steps are (1) CO_2 mass transfer from gas to bulk electrolyte, (2) dissolved CO_2 transport to the cathode/electrolyte interface, (3) CO_2 adsorption at the cathode, (4) decomposition of adsorbed CO_2 into intermediates, like *COOH, *CO, *CHO, and *COH, (5) electron transfer from the cathode catalyst to intermediates, (6) product desorption from the electrode, and (7) product movement from the cathode/electrolyte interface to the bulk gas or liquid phase.

Though H-cells are cost-effective and successful in lab-scale studies, they are unsuitable for large-scale or commercial use due to CO_2 mass transfer limitation caused by the thick diffusion layer (> 50 μm) and low CO_2 solubility in aqueous electrolytes, leading to low CDs ($<$ 100 mA cm^{-2}) [59,71,72]. Consequently, practical applications should employ better configurations for higher CDs and EEs.

A pressurized H-cell variant has been developed, as shown in Fig. 7 **(c),** to evaluate CO_2 pressure's impact on product selectivity [74]. The CO_2R reaction took place in stainless steel autoclave, with the counter electrode in a cylindrical tube separated from the working electrode by a proton exchange membrane. This setup effectively demonstrated that high CO_2 pressures promoted C_2H_4 production over oxide-derived copper electrodes [27].

H-type cells are frequently used with lab-scale electrocatalyst screening for CO_2 reduction to various products because they facilitate the easy evaluation of catalyst effectiveness in solution-based systems. However, the system resistance increases during electrolysis, causing the cell voltage, which includes potentials for both anodic and cathodic processes, to rise up to the potentiostat's maximum. As a result, the solution may need changing during long-term stability tests. Furthermore, CO_2's low solubility in aqueous solutions and the system's low CD limit the maximum achievable CO_2R rate. Researchers suggest using H-type cells to assess different catalysts' performance, but efficient cells with reduced resistance and higher mass transfer efficiency are crucial for commercial applications.

3.4. *Continuous flow cell*

Continuous flow reactors provide advantages such as enhanced mass transfer and phase mixing, better temperature and heat transfer control, and more precise reaction mixture residence time [75]. Addressing mass transport issues requires a continuous flow system for eCO_2R, allowing reactants and products to be continuously recycled, increasing the CO_2 conversion rate to desired levels. The thermodynamics and kinetics of CO_2R in flow reactors differ substantially from those in H-cell batch reactors. Improved performance results from factors like high CO_2 concentration at the electrode surface interface, suitable gas diffusion layer substrate, small transmission channel, polymer electrolyte membrane in direct contact with the catalyst surface, and appropriate

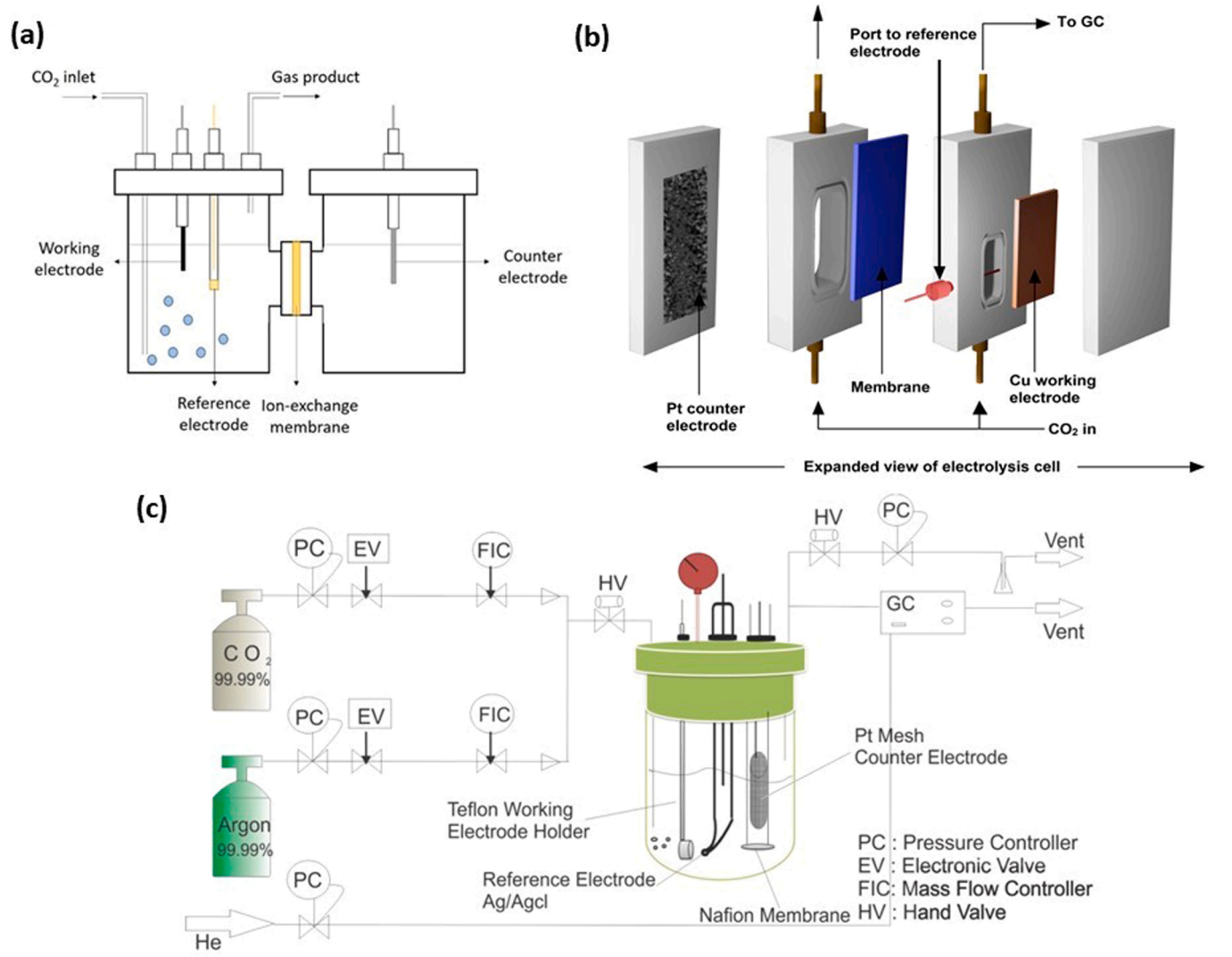

Fig. 7. (a) H-cell configuration of CO_2R electrolyzer. (b) Modified H-type electrochemical cell used for the CO_2R (c) Schematic of the pressurized reactor and additional equipment
(a) (Adapted from [27], Open access, MDPI). (b) (Redrawn, [73]) (c) (Adapted from [74], Copyright (2015) John Wiley and Sons).

electrocatalyst substrate.

To optimize CO_2R, a system-level approach has been used to modify flow reactor components. Electrolyzer design significantly influences catalytic activity and mechanism. Two key architectures are used: CO_2 electrolytic membrane-based flow reactors and microfluidic reactors. Electrocatalytic performance depends on the electrocatalyst properties and the selection and modification of specific components in microfluidic and/or membrane-based reactors. In both reactor designs, gaseous CO_2 is supplied to the cathode without being dissolved in the liquid electrolyte.

Fig. 8 **(a)** presents the typical architecture of a continuous flow cell, serving as the basis for all other configurations. An ion-exchange membrane separates the anolyte and catholyte flow channels. The cathode electrocatalyst is immobilized on the gas diffusion layer (GDL), which is in contact with the flowing catholyte on one side and directly supplies CO_2 gas on the other side [76]. Most components, such as GDLs and catalysts, are available and ready for scale-up, but no commercial equipment exists on an industrial scale. Pressure sensitivity is a significant challenge limiting the scalability of electrochemical flow cells [77]. The number of electrodes in a flow cell depends on the cell type and setup, as it determines the available surface area for electrochemical reactions. More electrodes in the flow cell lead to lower cell voltage, improving energy efficiency. Additionally, it reduces the pressure drop across the cell and ensures a more stable flow.

Some systems use only a working electrode and a counter electrode, allowing current control but not potential control. However, changes in working electrode surface properties, like copper oxide in an electrolyzer, can cause product distribution shifts over time [49]. In many cases, a reference electrode is incorporated into the cell near to the working electrode's surface in the electrolyzer setup to enable potential control. A four-electrode setup with two reference electrodes is feasible if the water oxidation stage is complex and both half-cells require monitoring.

Fig. 8**(b)–(d)** present classifications for various reactor architectures, including proposed CO_2 electrolyzer types based on feedstock requirements. The costs of an electrolyzer that removes CO_2 from a capture solution differ significantly from those requiring a pure gas-phase feedstock. Thus, comparing systems based on feedstock requirements is beneficial. The cathode GDE architecture and function in these electrolyzers, where reactants are introduced to the catalytic metals, are critical for their operation.

3.4.1. Technical benefits and critical parameters of flow cell systems

Transitioning from a batch-type study to a continuous flow cell

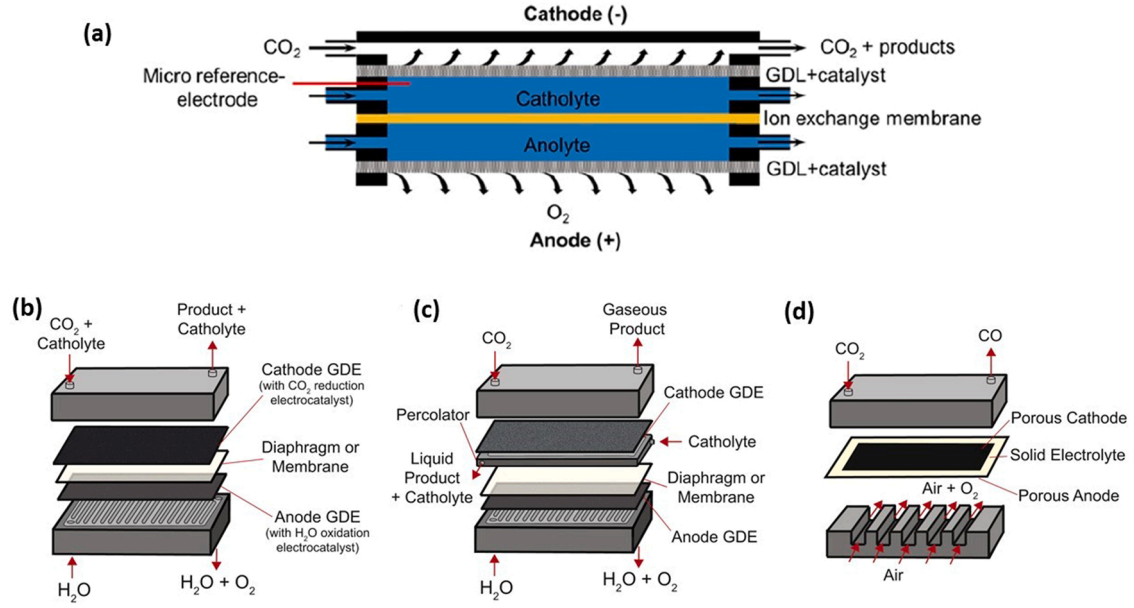

Fig. 8. (a) (a) Sketch of the cell configurations used in the continuous-flow electrochemical CO2 reduction reaction. (b) Continuous-flow CO2 electrolyzer, wherein (b) an ionic or dissolved form of CO2 in a feed solution to the cathode, (c) the anode is submerged in water and fed with gaseous CO2, each side is isolated from the other by a membrane, and (d) both the anode and cathode receive gaseous feeds, primarily from high-temperature solid-oxide electrolyzers (Adapted from [40], Open access, Elsevier). (Adapted with permission from [78], Copyright (2018) Elsevier).

requires precise identification of reactor architecture and design. This includes electrolyte type (liquid or gas), reactor material compatibility with the reaction mixture, temperature, flowrate, and reference electrode use. H-cells are commonly used for electrocatalyst screening, mainly to investigate reaction mechanisms, surface sites, material structures, and local pH environment effects. CO_2R kinetic and thermodynamic properties in flow reactors differ significantly from conventional H- cells due to factors like carbon accumulation on the electrode surface, direct interaction between the catalyst surface and polymer membrane, and the electrocatalyst substrate's accessible scope. Flow reactors offer higher eCO_2R efficiencies, high CDs, and compact structures, making them suitable for large-scale commercial applications [79,80].

Flow cells address H-cell mass transfer limitations by continuously circulating reactants and products across the electrodes, enabling higher CO_2 concentrations at the electrocatalyst surface. Gas-phase eCO_2R in flow cella alleviates limited CO_2 solubility in aqueous electrolyte solutions and complexities in recycling liquid-state products. A continuous flow electrolyzer setup overcomes issues associated with other setups, including (i) reference electrode placement, (ii) low CO_2 concentration at the electrode limiting current flow, iii) product crossover-diffusion into the anode, and (iv) H^+ crossover making the catholyte acidic. Flow reactors also offer more reagent delivery flexibility, including the option to supply gaseous CO_2 to the cathode. By minimizing H-cell mass transport issues, this configuration enables much larger CDs (J).

For large-scale implementation, systems require high catalytic activity, high production rates, low overpotential, and high CO_2 conversion efficiency, which are challenging to achieve using conventional H-cell reactors (partial CD of 250 – 300 mA cm^{-2} and ~ 70% FE for a single product). Although CO_2R flow electrolyzers are still under industrial development, recent advancements in membrane electrode assembly (MEA) electrolyzers show great potential for future commercialization. Understanding flow reactor types and optimizing their components is critical for selecting a flow cell type and providing key performance indicators for CD, selectivity, and energy conversion efficiency. This leads to the commercialization of advanced flow electrolyzers for eCO_2R. Both membrane-based flow cells and microfluidic reactors, which use distinct dynamic processes to transport gaseous CO_2 to electrocatalytic sites, have achieved large CDs ($J > 200$ mA cm^{-2}) for CO_2R.

Endrodi et al. reported the first multi-layered CO_2 electrolyzer stack for scaling up an electrolysis processes [53], effectively converting CO_2 into high-pressure gaseous products (Fig. 9). They employed a zero-gap electrolyzer cell that converts gaseous CO_2 into products without using liquid catholyte. The study illustrated two potential arrangements of the electrolyzer stack with multiple cells: parallel-connected electrolyzer layers with a gas supply, and layers connected in series, resulting in significantly higher conversion rates than a single-cell electrolyzer. These outcomes can advance this developing technology and bring it closer to commercialization. CO production with a partial CD of > 250 mA cm^{-2} was achieved by pressurizing the CO_2 inlet (up to 10 bar); this increased to 300 mA cm^{-2} with a 95% FE. The electrolyzer operates by distributing CO_2 gas uniformly between layers, equivalent to the sum of many single layer electrolyzer cells. CO_2 conversion efficiency increases when CO_2 gas passes through layers continuously. These electrolyzers exhibit a high partial CD, low cell voltage (3.0 V), good conversion efficiency of up to 40%, and high CO production selectivity.

A direct comparison between a batch (H-cell) and a flow cell was recently reported by Ahangari et al. [82], who analyzed the electrocatalytic reduction of CO_2 to CO at a gold cathode. They found that managing hydrodynamics at the electrolyte–electrode interface during eCO_2R is essential, and the electrolysis cell design significantly affects gold cathode performance. In their study, the flow cell had a higher local pH than the cathode immersed in a conventional batch cell, due to limited $KHCO_3$ transport through the porous cathode support. Using a gold cathode in a flow cell designed to restrict electrolyte species transport, the impact of $KHCO_3$ concentration on FE for CO generation was negligible. The batch cell's FE for CO production decreased from 75% to 35% as the $KHCO_3$ concentration increased from 0.05 to 0.5 mol L^{-1}, while the flow cell's FE remained at 80–90%, independent of $KHCO_3$ concentration (Fig. 10). CDs (~ 4 and ~ 10 mA cm^{-2} at 1.3 V vs. Ag/AgCl) were also independent of $KHCO_3$ concentration in both cells. They concluded that the cell or electrode design, rather than the electrocatalytic material, may influence product selectivity.

Membrane-based flow cells, with their efficient mass transfer,

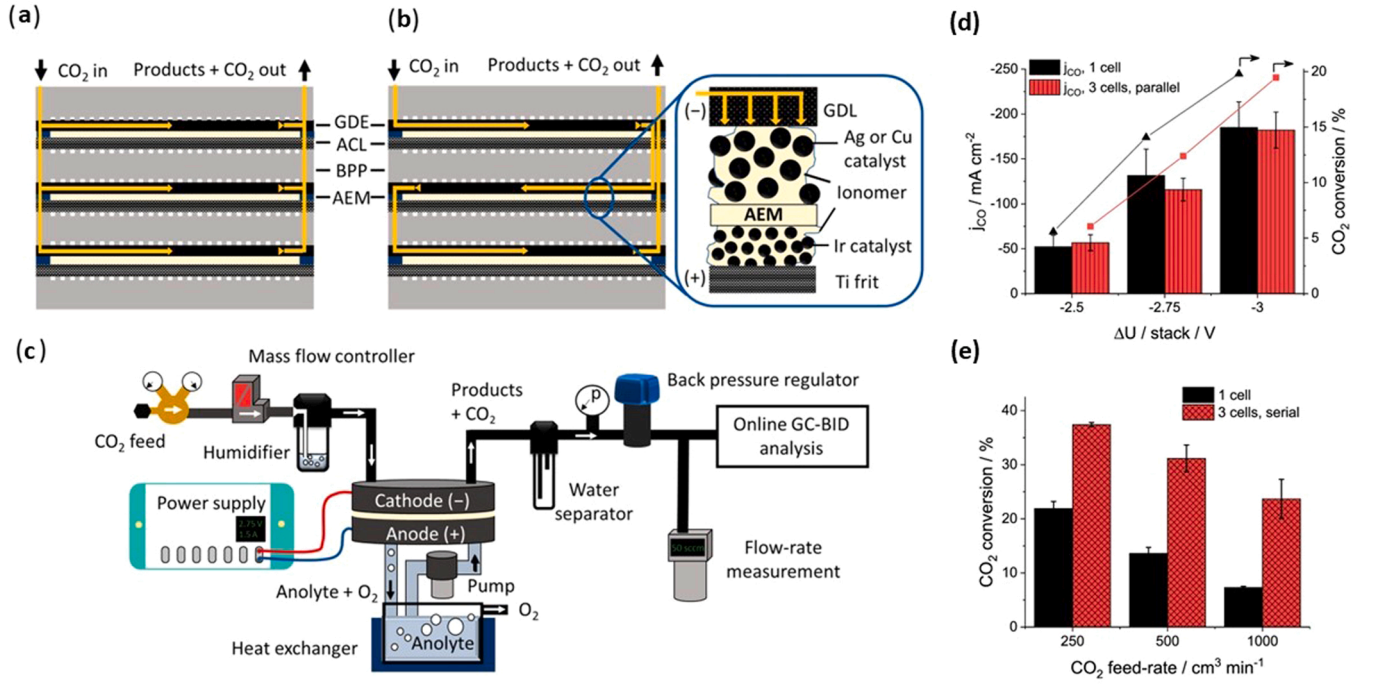

Fig. 9. CO_2 gas channel structure of an electrolyzer stack comprised of three layers in (a) parallel and (b) serial connection configuration. (c) Flow chart of the experimental setup. (d) One-cell electrolyzer and electrolyzer stack comprised of three cells, and the CO partial current density and CO_2 conversion observed for the parallel configuration [during electrolysis at different cell voltages with a 433 cm^3 min^{-1} CO_2 feed rate per cell at the cathode]. (e) CO_2 conversion for the serial configuration [at different CO_2 feed rates and $\Delta U = -2.75$ V/cell]
(Adapted with permission from [81] Copyright (2019) American Chemical Society).

compact structures, and high CDs (> 100 mA cm^{-2}), are ideal candidates for large-scale commercial implementations, having evolved from fuel cells and water electrolyzers. However, challenges remain for large-scale production, necessitating further studies on various factors, such as reactant phase, polymer membrane, electrode substrate, catalyst, and high overpotential reduction.

3.5. Microfluidic reactor (MFR)

Cook et al. first proposed a microfluidic reactor (MFR) consisting of an aqueous electrolyte, a gas diffusion zone, and Cu catalyst [83]. Membraneless electrolyzers with a GDL have been developed to reduce cell potential, overcome mass transport limitations, and commercialize CO_2R. A typical MFR, shown in Fig. 11**(a)** and **(b)**, operates without a membrane between the anode and cathode, relying instead on gaseous product diffusion to separate reduction and oxidation reaction products. MFRs minimize iR loss due to membrane deterioration during electrolysis. However, to ensure stability, the electrolyte must be prevented from penetrating the GDE's porous layer. Like fuel cells, MFRs for CO_2R operate in a continuous flow process to achieve high reaction rates [84]. Kenis et al. developed a microfluidic cell-based configuration for eCO_2R to produce formic acid [85]. The design featured an ultra-thin flowing electrolyte channel (< 1 mm thick) separating the anode and cathode, with CO_2 reduction and oxygen evolution catalysts coated on two GDEs [86]. A gaseous CO_2 stream was introduced on the cathode side, diffusing through the porous cathodic GDL, making direct contact with the GDE, while oxygen was released from the anode side. The electrolyte stream transported the products from the cathode and excess protons from the anode. CO_2R occurred when CO_2 interacted with the catalyst/electrolyte interface, producing catalytic products. To monitor individual electrode potentials independently, an Ag/AgCl reference electrode is typically placed in the electrolyte flow stream or effluent.

An MFR can continuously produce organic fuels, such as formic acid, while consuming CO_2. Understanding the reactor's microscopic processes and their impact on performance is crucial. Wang et al. [86] developed one of the first numerical models to analyze mass transport and electrochemical properties on the cathode side of the MFR for CO_2 reduction and fuel production using available experimental data. The model considers microfluidic flow, species transfer, charge transfer, and multiple competing electrode interactions. The main issues limiting electrode performance and efficiency were found to be (i) limited CO_2 diffusivity in the porous GDE, (ii) competitive HER at the cathode, and (iii) hydrogen dilution effects. Further investigation into parameters such as HER kinetics and CO_2 feed rate can lead to new strategies for optimizing reactor performance.

The results of investigations by Jhong, Dufek, and Delacourt at room temperature and ambient pressure are plotted in Fig. 11**(c)** for unbiased comparison based on the same kinetics [34,87,88]. Dufek et al. [89] reported better reactor performance at high temperatures and/or pressure. A key finding was that MFRs could achieve the same CDs and EEs at significantly lower cell potentials than conventional electrolyzers. This improvement is attributed to the superior catalyst layer structure of flow cell-based electrolyzers, showing that the electrolyzer design, which significantly affects mass transport, does not limit CO_2 electrolyzer performance.

Jhong et al. [90] conducted a comparative study of MFRs and electrolyzers using flowing liquid electrolyte to separate electrodes and an external reference electrode to analyze each electrode's performance. When evaluating CO production performance for different systems (Fig. 11**(d)**), they found similarities.

Using tailored catalyst layers in reactors, as reported by Delacourt et al. and Dufek et al., is expected to result in much better performance. Increased CD in pressurized electrolyzers (e.g., 20 atm) has been previously reported [91]. Further enhancement of reactor performance and efficiency in CO_2 reduction can be achieved by modifying operating conditions, such as using electrolyzers operating at elevated pressure and temperature. For example, Furuya et al. demonstrated that a pressurized electrolyzer with GDEs coated with different metals (Pt, Ag, Cu,

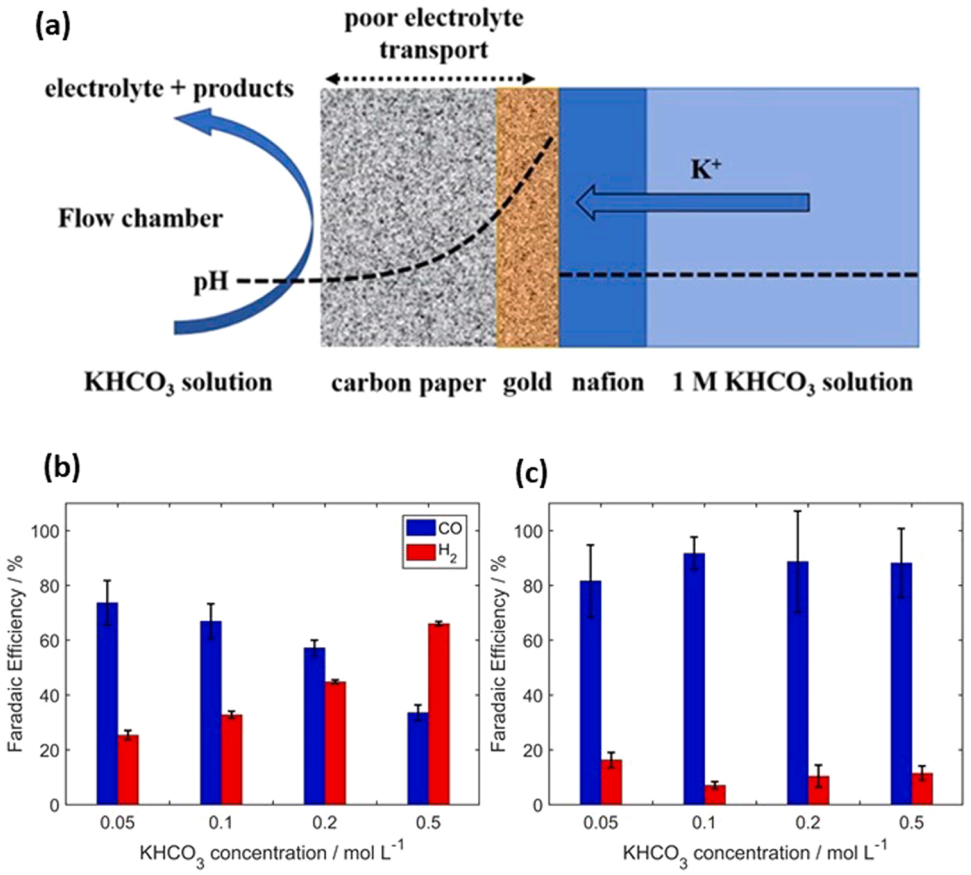

Fig. 10. Proposed transport phenomenon in the flow cell for enhanced CO_2 reduction. Faradaic efficiency for CO and H_2 production upon varying the $KHCO_3$ concentration (at −1.3 V vs. AgCl) in the (a) batch cell and (b) flow cell
(Adapted with permission from [82], Copyright (2019) Elsevier).

Ni, Co, Pd) can achieve a total CD in the range of 300–900 mA cm^{-2} at 20 atm [92].

The compact size and high surface area-to-volume ratio of microfluidic electrolyzer allow faster CO_2 mass transfer to the cathode surface and high CD for CO_2R [85]. However, MFRs are prone to product crossover, where cathodic products diffuse to the anode and are re-oxidized, and oxygen diffuses to the cathode and is reduced, lowering overall energy efficiency and productivity. Unlike membrane-based flow cells, the intersection of reactants and products in this microfluidic flow design can be controlled under laminar flow conditions due to slow product diffusion. This enables MFRs with a flowing stream to reduce water management issues, such as electrode overflow, without needing expensive membranes [85]. Additionally, the electrolyte composition and pH can be easily adjusted. Effectively controlling MFR operating conditions increases the CD of CO_2R and links it to various factors, such as electrode layer deposition type, diffusion layer composition, and electrolyte pH [34,84,85,93,94]. The MFR design overcomes challenges caused by water molecules permeability resistance and proton transport through the membrane, such as anode drying and cathode flooding, at high CDs.

3.6. Gas diffusion electrode (GDE)

GDEs can achieve higher CDs than conventional electrodes due to the strong CO_2 mass transfer and shortened diffusion lengths within the catalyst layer [95]. In early work by Cook et al. in 1990 [83], high CO_2 reduction rates and FEs of 71.3% were observed for gaseous CO_2 reduction reaction to form gaseous hydrocarbons at CDs of > 0.5 A/cm^2 using electrolytic GDEs. GDEs already show impressive performance in electrochemical energy conversion devices like fuel cells [96]. Since only physically dissolved CO_2 is electrochemically active, the CD is limited to saturated electrolyte electrolysis under mild conditions ($p < 10$ bar) due to reduced solubility [97]. Several studies report high eCO_2R rates using metal electrodes under extreme operating pressure conditions [98,99].

However, the mass transport constraint of physically dissolved CO_2 from the bulk to the interfacial boundary can be circumvented using GDEs, making them the most promising route for high CDs [87,100]. GDEs are porous electrodes, with catalyst layers in contact with the electrolyte. Using GDEs allows for a relatively thin diffusion layer (approximately 50 nm) to overcome CO_2 mass transport difficulties, enhancing possible CD. In theory, GDEs can accommodate various catalysts, including metal-free, molecular, and enzyme-based catalysts [60,101,102].

A standard GDE consists of three components: a catalytic layer (CL), gas diffusion layer (GDL), and gas flow field, as shown in Fig. 12. The GDL has a porous structure sandwiched between the gas flow channel and the catalyst layer. It provides physical support to the catalyst and allows gas transport toward the CL. The GDL can be treated with hydrophobic additives, such as polytetrafluoroethylene (PTFE), polyvinylidene fluoride (PVDF), and fluorinated ethylene propylene (FEP) to prevent electrolyte clogging and facilitate gas delivery to the CL [61]. The dual-layer GDL, combining a microporous substrate (MPS) with a microporous layer (MPL), is widely used to prevent GDE electrolyte overflow, particularly in CO_2 electrolyzers. The gas flow field serves as a gas diffuser and current collector, interfacing directly with macroporous layer. The MPS is covered with a microporous layer containing carbon and hydrophobic agents to control catholyte overflow.

The appropriate catalyst selection (particularly the correct GDE) and the process conditions optimization enable the electrochemical

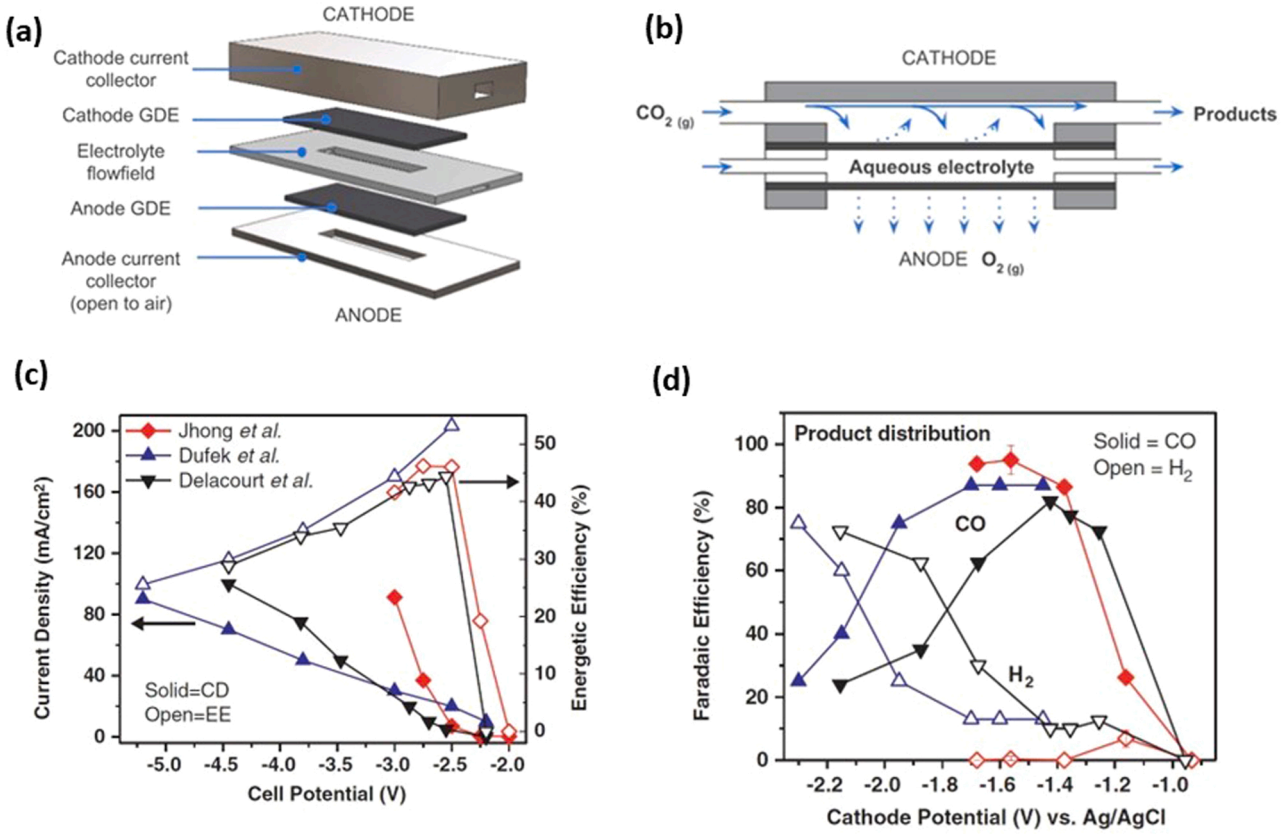

Fig. 11. a) (a & b) Magnified (left) and cross-sectional (right) diagram of a microfluidic reactor consisting of a liquid electrolyte flow channel between the anode and cathode GDE materials. (c & d) Comparison of the different electrolyzer configurations used for the electrochemical conversion of CO_2 to CO. Jhong et al.: A microfluidic flow cell; Dufek et al.: A traditional electrolyzer; Delacourt et al.: A modified alkaline fuel cell. (b) The data from the literature plotted here were all collected at room temperature and ambient pressure
(a & b) (Adapted with permission from [54], Copyright (2018) American Chemical Society). (Adapted with permission from [90], Copyright (2013) Elsevier).

conversion of CO_2 into value-added products. Jhong et al. [90] showed that using a GDE with an improved catalyst layer deposition procedure significantly enhances electrode performance for CO_2R. GDEs can host various catalysts, such as metal, metal-free, and molecular catalysts, as well as enzymes and microorganisms [60,101,102]. In eCO_2R, GDEs can be widely applied using conductive composite-coated porous frameworks, forming a stable and extended three-phase boundary at the gas–liquid–solid interface, reduce the gas diffusion pathway, and improving mass transfer [91,104].

3.7. Membrane electrode assembly (MEA) electrolyzers

A MEA is a gas-phase electrolyzer consisting of an ion exchange membrane attached to a catalyst-deposited cathode. Unlike other electrolyzers, it does not require a liquid electrolyte, making it crucial for improved GDE operation. The key feature of the MEA design is direct contact between the cathode, anode, and PEM, facilitating ionic charge transfer and allowing stable and continuous charge transfer in the circuit. The cathode CO_2 feed must be humidified, or an aqueous anolyte must be present to provide water to the cathode catalyst and enable CO_2 reduction. Addressing membrane degradation and controlling the delivered CO_2 phase in the MEA system are significant challenges for increasing CO_2R activity [49]. The MEA system, shown in Fig. 13, addresses issues of conventional membrane-based flow reactors by having the cathodic GDE and PEM's catalyst are in direct contact with zero-gap distance. Using a GDE improves the CO_2R rate and CD due to higher local CO_2 concentrations and reduced mass transport resistance. In the MEA system, cell voltage or current regulation is used instead of working electrode potential, as a reference electrode is not employed. Diffusion through the membrane into the catholyte is minimized, allowing gaseous and liquid products to exit the cathode flow plate, and producing a highly concentrated liquid phase product. The catalytic activity and selectivity of eCO_2R are significantly enhanced upto the level required for commercialization through the use of a flow-cell reactor and MEA (Fig. 13**(a)** and **(b)**),

3.8. Liquid-to-gas phase electrolyzers and performance parameters for CO_2R

According to the gross-margin model by Verma et al., achieving a high CD of at least 200 mA cm^{-2} and long-term durability are essential for the economic viability of CO_2R technology [40]. In the aqueous phase, water tends to adsorb on the catalyst surface, leading to less CO_2 enrichment. To address this issue, gas-phase CO_2R can be employed, as it can mitigate CO_2's low solubility in water under conventional conditions [105]. Generally, gas-phase cell systems show higher CDs for target chemical products than liquid-phase reactors due to the absence of reactant mass transfer limitations [80, 106–111]. Fig. 14**(a)** and **(b)** depict the CO_2 reduction schematic in liquid and gas-phase reactors, respectively. Fig. 14**(c)** shows the common trend in the reported CDs for CO_2R ($j_{CO2\ Reduction}$), indicating that gas-phase reactors can achieve a larger CD of approximately 100 mA cm^{-2}, while liquid-phase reactors typically report a $j_{CO2\ Reduction}$ value of < 100 mA cm^{-2}. GDEs can enhance mass transfer and maintain high gas concentrations near the catalyst, resulting in high CDs.

Fig. 14**(d)** illustrates the FEs and their respective partial CDs obtained using aqueous-fed (empty symbols) and gas-fed (full symbols) electrolyzers for various catalytic systems that reduce CO_2 into carbon

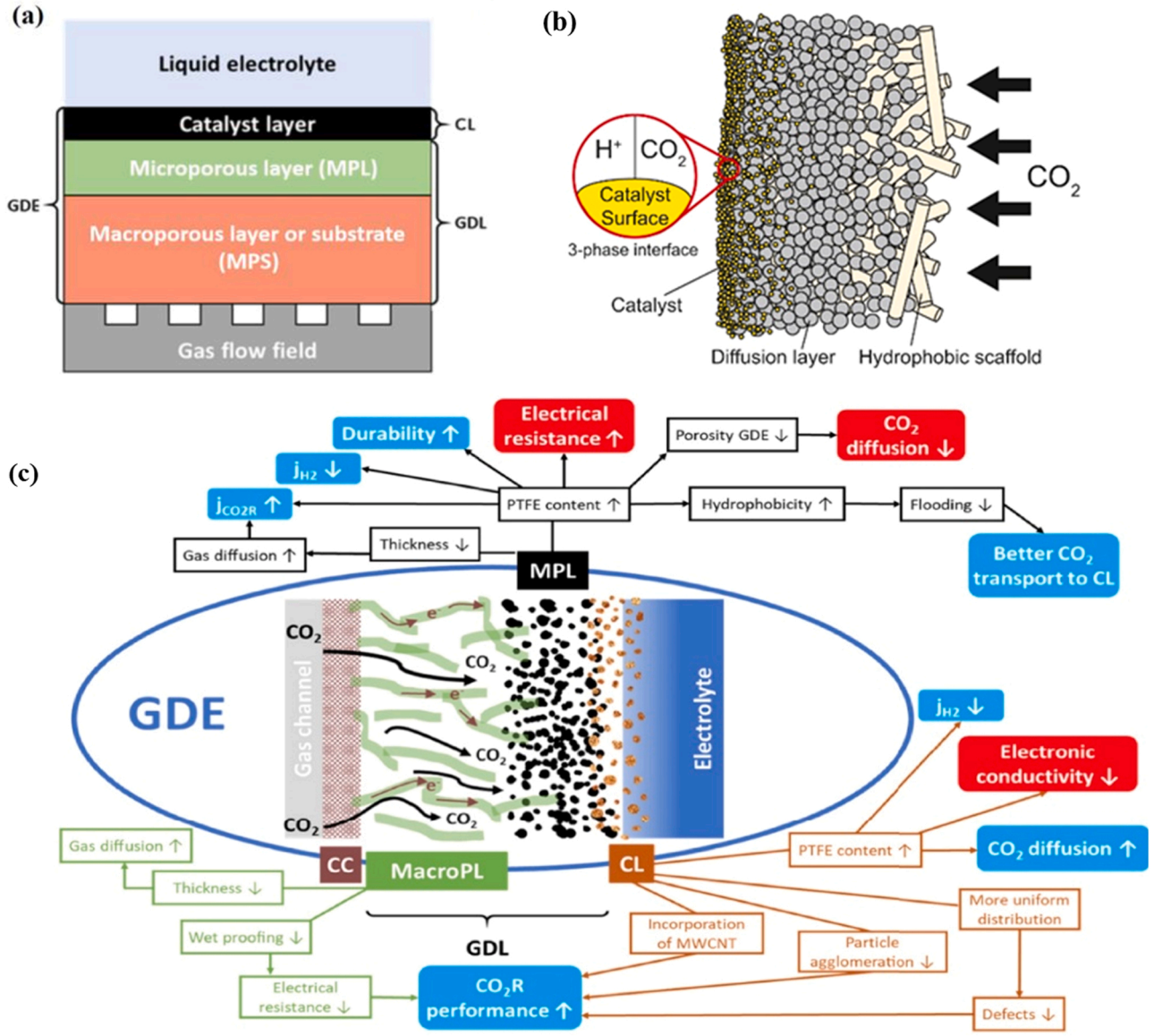

Fig. 12. Simplified schematic of a gas diffusion electrode (GDE). (a) Stacked structure of the GDE installed between the gas flow field and liquid electrolyte as typically found in the cathodic compartment of a CO_2 electrolyzer. (b) Example of the GDE design depicting one approach for incorporating a catalyst into an electrolyzer that generates CO or HCOOH. (c) Schematic of a GDE including the interrelated effects of the GDL and CL design parameters. (c) The parameters shown in black, brown, and green boxes refer to the microporous layer, catalyst layer, and macroporous layer, respectively
(a) (Adapted from [61] Open access, MDPI). (b) (Adapted with permission from [78], Copyright (2018) Elsevier). (c) (Adapted with permission from [103] Copyright (2019) Elsevier).

monoxide, ethylene, ethanol, or formate. The data show that gas-fed electrolyzers consistently outperform liquid-fed electrolyzers. Despite variations in cell and catalyst designs, this comparison highlights the advantage of using a gas-fed electrolyzer to increase CD while maintaining similar product selectivity. Notably, GDEs have been shown to achieve high CO_2 reduction rates in the literature [83,112]. Recently, Cu oxide/ZnO-based GDEs used in a gas-phase PEM flow cell achieved an ethylene formation rate of 487.9 mol m^2s^1 and an FE of 91.1%, greatly surpassing previous records for ethylene formation using Cu-based electrocatalysts. These results demonstrate the effectiveness of combining a gaseous reactant with a GDE to attain high reaction rates and efficiencies [113]. By utilizing a gas-phase electrolysis method in tandem with CO_2 surface enrichment, a highly efficient and selective CO_2R can be achieved.

Gas-phase electrolyzers have several advantages over liquid-phase electrolyzers in the absence of a flowing catholyte, such as higher partial CDs, improved stabilities, and better control over liquid product concentration for formate synthesis [114]. They are also more selectivity in generating CO [62] and can even produce alcohols [115] and other multi-carbon compounds [116,117] using membrane-coated electrodes or MEAs at low CDs.

However, using gaseous CO_2 to increase CD (J) has been challenging due to difficulties in monitoring and controlling electroless electrochemical reactions at a solid-gas interface in dynamic flow cell systems [106,118]. Li et al. [63] compared a PEM flow cell fed with a humidified gaseous CO_2 cathode stream to a liquid electrolyte to demonstrate the benefits of using gaseous CO_2 in a flow reactor. In their study, they introduced humidified CO_2 gas to the cathode upon contact with porous carbon paper in the gas-phase cell and utilized 0.5 M $NaHCO_3$ saturated with CO_2 as an electrolyte for liquid-phase cell. CV study was performed using a nickel-foam anode, silver nanoparticles on a carbon-cloth cathode, and an anode electrolyte comprising 1 M NaOH. As shown in

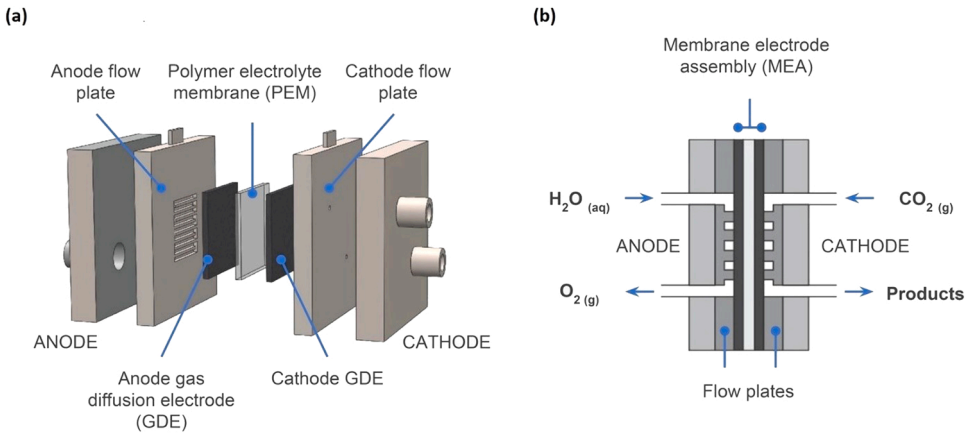

Fig. 13. (a) Membrane-based reactor containing a membrane electrode assembly (MEA) comprising the anode and cathode gas diffusion electrodes (GDEs) on either side of the polymer electrolyte membrane (PEM). (b) MEA is assembled between the anode and cathode current collectors and flow field plate; it separates the respective OER and CO_2R
(Adapted with permission from [54] Copyright (2018) American Chemical Society).

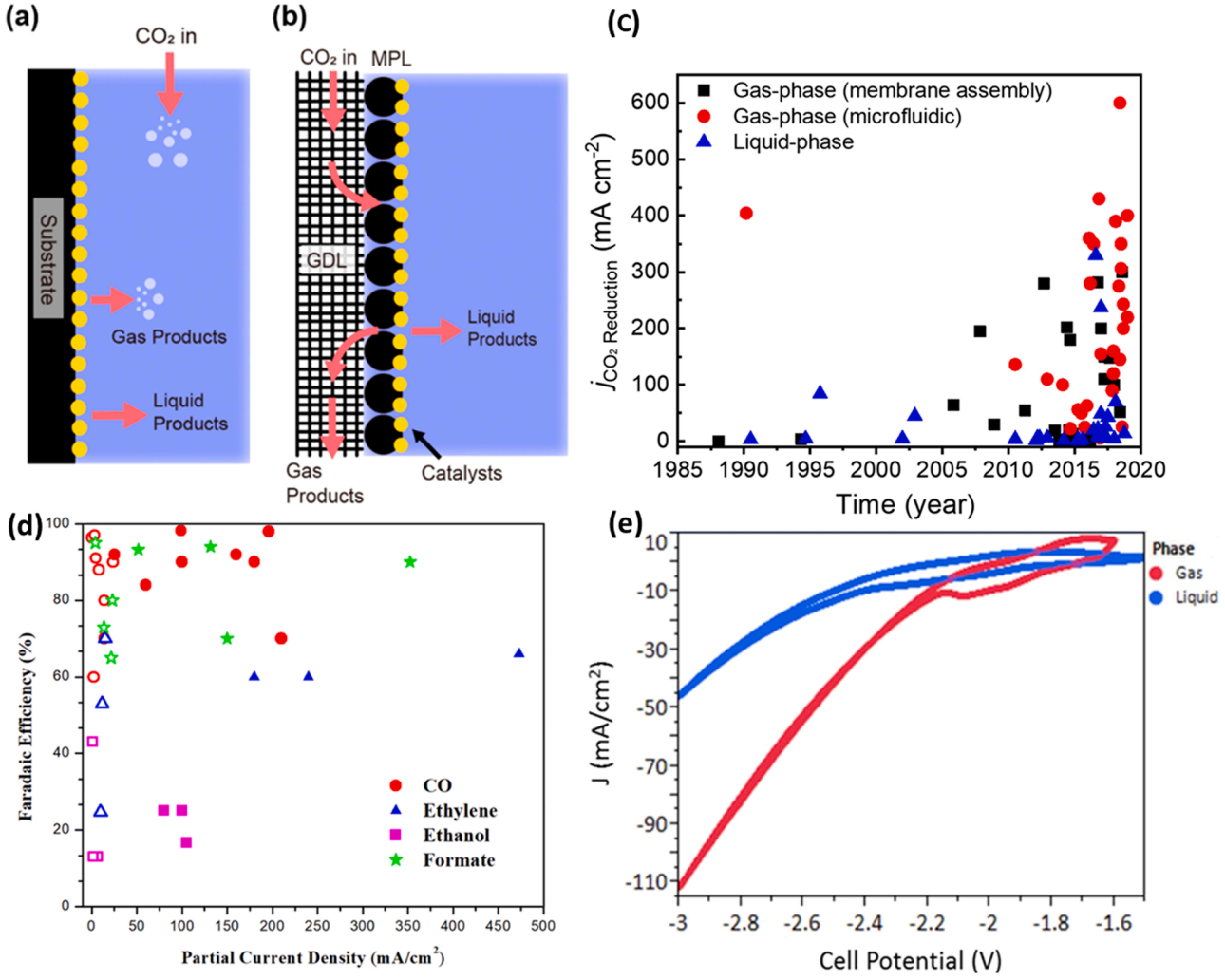

Fig. 14. (a) Comparison of the concepts of the (a) liquid-phase and (b) gas-phase CO2 reduction processes (c) Trends in the partial current density were observed for the reduction of CO2 (jCO2 Reduction) using liquid- and gas-phase reactors $_2$ reduction processes (c) Trends in the partial current density were observed for the reduction of CO_2 ($j_{CO2\ Reduction}$(b) (d) Summary of previous reports of the CO_2R performance observed using an aqueous-fed (empty symbols) and gas-fed (full symbols) electrolyzer. (c) (e) Comparison of the J–V curves observed for gas-phase and liquid-phase cathodes (using a bicarbonate electrolyte in the cathode compartment)-based bipolar membrane (BPM) cells
(Adapted from [119] Open access, MDPI). (Adapted from [61] Open access, MDPI). (Adapted with permission from [63], Copyright (2016) American Chemical Society).

Fig. 14**(e)**, the shape of the *J–V* curve at high driving voltages kinetically limited the current in both cases, with the free energy loss associated with acid-base neutralization at the BPM/catholyte interface. At a scan rate of 100 mV/s, the resulting CVs produced J values between –1.5 and −3.0 V higher for the gas-fed flow cell (using 100 sccm humidified gaseous CO_2) than for the liquid-fed flow cell (using 1.0 M CO_2-saturated $NaHCO_3$).

These results have inspired the development of a gas-phase CO_2-to-CO flow cell utilizing a silver catalyst supported by a GDL, bipolar membrane, and a solid-supported aqueous layer, which can achieve a J value of $>$ 200 mA cm^{-2} (with an FE of approximately 50%) and prolonged stability ($>$ 24 h) at 100 mA cm^{-2} (with a stable FE of 65% for CO). Recent research on GDE CO_2R have shown promising signs for the scale-up and commercialization of CO_2 electrolysis. However, most gas-fed electrolyzers have a limited lifespan, resulting in performance degradation after a relatively short operating time [67].

Optimizing the design parameters and architecture of gas-phase reactors is crucial to efficiently produce desired target products, such as formate, carbon monoxide, and hydrocarbons, which have been previously generated using various catalysts in liquid-phase reactors. Although gas-phase reactor systems have demonstrated the potential to produce target products at high CDs, several challenges remain before they can be effectively utilized for industrial applications. Addressing issues related to reactor architecture and electrocatalysts, which determine overpotential and final product selectivity, is critical for the successful implementation of gas-phase reactors in practical applications.

4. Choice of separator membrane and design

The performance of a gas-phase CO_2 electrolyzer largely depends on the quality of its PEM membrane [106,120,121]. PEMs function as ion exchange membranes, enabling ion exchange while preventing product crossover during electrolysis. These membranes can be classified as cation exchange membrane (CEM) (e.g., Nafion), anion exchange membrane (AEM) (e.g., Sustainion), or bipolar membrane (BPM) [122, 123]. The chosen membrane type affects ion transport channels kinetics and optimal electrolyte conditions for efficient eCO_2R. A CEM transports protons from the anolyte to cathode catalytic sites, while an AEM transports hydroxide (OH^-) (generated during water electrolysis) and anions (CO_3^{2-}) from the cathode to the anode. A BPM combines two distinct membrane types, supplying OH^- and H^+ to the anode and cathode, respectively. Despite maintaining a constant pH on both sides of the cell, BPM reduces the EE of the entire reactor due to its significant membrane potential [106].

Enhancing CO_2 electrolyzer's efficiency can be achieved by modifying the membrane. In 2016, Kutz et al. reported the fabrication and testing of novel anion-conductive membranes (Sustainion) for CO_2 electrolysis [106]. The membrane's effectiveness as a co-catalyst is attributed to the imidazolium cationic functional groups, rather than adding amine groups or doping with strong acids or bases. Incorporating an imidazolium group to the styrene side chain [polystyrene methyl methylimidazolium chloride (PSMIM)], as shown in Fig. 15 **(a)**, increased reaction selectivity from approximately 25% to over 95%. At 3 V, the current increased 14-fold. By adjusting these parameters, stable cells with CDs exceeding 100 mA cm^{-2} and CO product selectivity above 98% at a cell potential of 3 V can be achieved. Moreover, stable performance was observed over 6 months of continuous operation. This membrane significantly outperformed commercially available membranes in terms of CD and product selectivity standards, as shown in Fig. 15**(b)** and **(c)**. These results suggest that imidazolium-based polymers are excellent candidates for CO_2 electrolysis membranes. However, fabricating durable membranes for CO_2 electrolyzers requires a careful balance between mechanical and catalytic properties, achievable by adjusting polymer components and cross-linking agent properties. These membranes enable CO_2 electrolyzer operation with an MEA design using widely available fuel cell hardware in the market.

5. Electrolyte selection

Selecting an appropriate electrolyte is crucial in electrochemistry, as its primary function is to conduct ionic charges between electrodes. An electrolyte typically comprises three components: electroactive species, solvent (e.g., water), and inert electrolyte or salt. For CO_2R processes, an inert electrolyte with high ion conductivity and easy dissociation into cations and anions is preferred [124]. Ideal electrolytes for efficient eCO_2R should have a stable pH, high electrochemical stability, moderate to high CO_2 solubility, lower viscosity, good ionic conductivity, and good chemical compatibility with electrode materials. These properties promote efficient CO_2 mass transfer from the bulk electrolyte solution to the electrode surface, as well as ease of use, storage, and safety. Water, a common solvent for CO_2R electrolytes, meets these criteria and can act as both a proton donor and acceptor, enabling diverse electroactive species synthesis. The electrolyte's role is crucial, as the interaction between the electrocatalyst surface and electrolyte determines CO_2R progression. Thus, choosing the right electrolyte is essential for selective and efficient electrochemical CO_2 conversion into desired products [121,125].

Inert electrolytes do not directly participate in redox reactions. However, in CO_2R, they serve as charge carriers and influence the reaction through their interaction with ions and radicals generated during

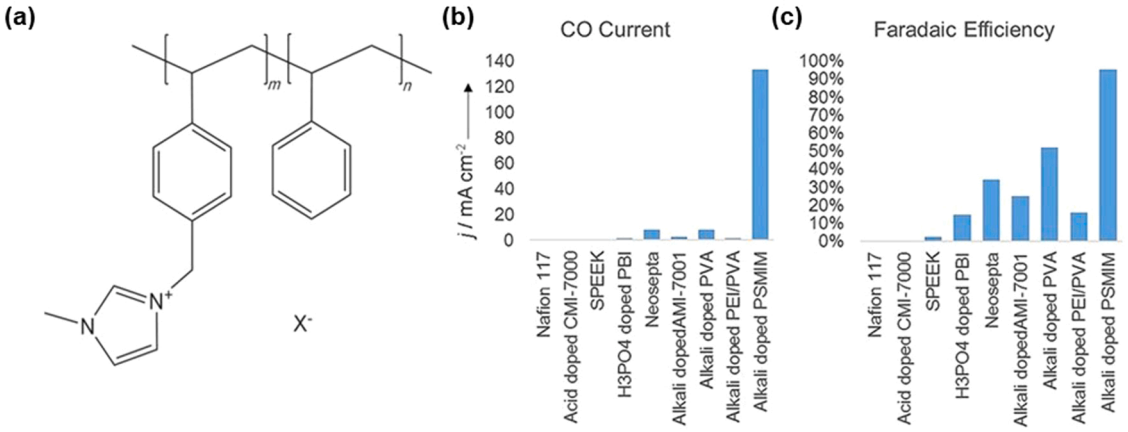

Fig. 15. (a) General structure of the PSMIM membrane. (b) Comparison of the total CO current density and (c) Faradaic efficiency of cells that run the CO_2R with some of the commercial membranes versus the Sustainion membrane [Measurement conditions: 23 °C and 3 V applied cell potential]
(Adapted with permission from [106] Copyright (2017) John Wiley and Sons).

the reaction [126]. Contaminants in the electrolyte can affect the cathode catalyst, necessitating high-purity inert electrolytes or pre-electrolysis purification. Trace metal impurities electrodeposited on the cathode during CO_2R process may lead to a loss of selectivity due to an increased HER rate [127]. Impurity effects on the electrolyte can be mitigated using chelating agents such as ethylenediaminetetraacetic acid (EDTA) or solid-supported iminodiacetate resin [128].

5.1. Aqueous electrolytes

One of the most widely used liquid electrolyte systems for real-world applications is an aqueous salt solution, such as potassium bicarbonate ($KHCO_3$), despite its lower CO_2 solubility compared to other CO_2 capture solvents like aqueous amine solutions [129,130]. Aqueous salt solutions are easy to prepare, handle, and store in large quantities, inexpensive, and have stable ionic conductivity. However, liquid-electrolyte systems have inherent limitations, such as flooding and high ohmic resistance. The electrocatalytic conversion efficiency of CO_2 can be affected by the pH and concentration of cations, anions, and aqueous electrolytes [131,132]. Aqueous solutions can also function as proton acceptors and donors, promoting the production of specific electroactive compounds.

Typically, CO_2R is conducted using a bicarbonate electrolyte due to its near-neutral bulk pH (approximately 7) and buffering capability. Compared to other conductive salts like sulfides, sulfates, and halides, carbonates exhibit better chemical compatibility with most electrode materials [133,134]. The most prevalent aqueous electrolytes are 0.1–0.5 M $NaHCO_3$ or $KHCO_3$ solutions with a pH of ~7 after CO_2 saturation [124,134]. Bicarbonate (HCO_3^-) can reversibly bind a free hydrogen ion, providing a buffer against pH fluctuations. However, CO_2 solubility in a bicarbonate electrolyte is relatively low compared to organic electrolytes, hindering CO_2 transport within the electrolyte and catalyst. As CO_2R and HER occur simultaneously in an aqueous electrolyte, CO_2R's FE decreases. Understanding the experimental parameters, such as pH, electrolyte species concentration, and mass transport, which govern the competition between CO_2R and HER, is essential for enhancing CO_2R FE and developing an ideal CO_2 conversion system [107].

Marcandalli et al. conducted a comprehensive quantitative analysis [135] examining the impact of electrolyte composition on FE during the CO_2-to-CO conversion on a gold electrode under well-defined mass transport conditions via rotating ring-disk electrode voltammetry. By altering the electrolyte cation and bicarbonate concentrations at various rotation rates, they assessed the influence of these parameters on FE. Two distinct potential regimes were identified for electrolyte effects, each affected by cation and bicarbonate concentrations differently. This study provided in-depth insights into the role of electrolyte composition and mass transport (CO) in determining optimal electrolyte conditions for high FE. An illustration of various proton donors (PDs) used for HER in a bicarbonate electrolyte and how FE (CO) varies with electrolyte parameters is shown in the bell-shaped curve obtained for FE (CO) plotted as a function of the applied potential in Fig. 16.

Another method to enhance CO_2 solubility in an aqueous electrolyte is increasing cell pressure. Dufek et al. designed a pressurized electrochemical cell for CO_2 electrolysis [89]. However, achieving high CD and CO selectivity simultaneously in CO_2 electrolysis requires further engineering of cell components for robustness under high-pressure conditions. Aqueous solutions tend to favor $HCOO^-$ synthesis, while solvents with low proton availability, such as N,N-dimethylformamide (DMF), promote oxalate and CO production [136].

5.2. Non-aqueous electrolytes

Non-aqueous electrolytes are generally preferred over aqueous solutions, as they address low CO_2 solubility and eliminate the need for high-pressure conditions. For instance, N,N-dimethylformamide (DMF),

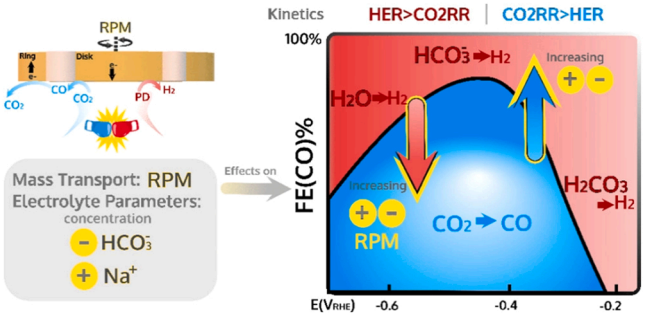

Fig. 16. Schematic of the bell-shaped curve of Faradaic efficiency (CO) with respect to the applied potential showing different PDs for the HER in a bicarbonate electrolyte and the Faradaic efficiency (CO) shift with the electrolyte parameters
(Adapted from [135] Open access (2021) American Chemical Society).

Propylene Carbonate (PC), and CH_3OH can dissolve up to 20, 8, and 5 times more CO_2 than equal amounts of aqueous solutions, respectively [136,137]. A lower H^+ ion concentration in methanol solutions can potentially reduce HER [138], making the selection of an appropriate methanol-based electrolyte beneficial for CO_2R. Saeki et al. investigated CO_2 conversion using various metal electrodes [139] finding formate production in methanol more effective for most metals than in aqueous systems. However, low proton concentration limits eCO_2R selectivity in many organic solvents, including methanol [140]. Ikeda et al. observed a similar example in 0.1 M TEAP/H_2O (tetraethylammonium perchlorate, TEAP), where formate production significantly decreased during CO_2 proton reactions [141]. The influence of anionic species on eCO_2R in a methanol/aqueous electrolyte using a Cu electrode remains under investigation. Kaneco et al. found that ethylene production was more selective than methane in the order of bromide > iodide > chloride > thiocyanate > acetate [142]. They achieved an FE of > 80% for hydrocarbons at a Cu electrode using methanol as the electrolyte under the same experimental conditions as eCO_2R performed in an aqueous solution (30% FE) [138]. Notably, adding a secondary electrolyte can considerably alter mass transfer and selectivity of reduction targets. Direct CO_2 reduction at p-type silicon (p-Si) in a highly pressurized non-aqueous electrolyte exhibited high FE [143]. The interaction between the solvent and CO_2 molecules acts as a catalyst, lowering the activation energy for CO_2 conversion, making a non-aqueous solvent system for CO_2 conversion analogous to molecular catalysis [144].

Ionic liquids (ILs) are recognized as effective promoters for electrocatalytic CO_2 reduction into valuable chemicals. IL-based electrolytes are proposed as alternatives to conventional aqueous and organic electrolytes, such as methanol/alcohol, as well as non-conventional aqueous electrolytes like bicarbonate [145,146]. ILs can enhance eCO_2R by promoting CO_2 adsorption on the catalyst surface compared to conventional electrolytes. Fig. 17 **(a)** illustrates the impact of IL molecular weight on CO_2 solubility [147]. However, ILs are less commonly used in practical CO_2 electrolyzers due to their lower cost-effectiveness and CD compared to aqueous electrolytes, as well as inconsistent stability in the presence of water [148]. Despite these limitations, ILs possess advantages for eCO_2R, including higher CO_2 solubility, reduced overpotential, wider electrochemical potential window, greater absorption capacity of CO_2, and higher intrinsic ionic conductivity compared to aqueous electrolytes [149,150]. Examples of ILs include 1-butyl-3-methylimidazolium trifluoromethanesulfonate (EMIM-OTf) [151], 1-ethyl-3-methylimidazolium tetrafluoroborate (EMIM-BF_4) [144], and 1-butyl-3-methylimidazolium tetrafluoroborate (BMIM-BF_4) [145].

DiMeglio et al. developed a rosebud-shaped Bi thin film on a glassy carbon electrode (GCE) and investigated its CO_2 conversion activity in an IL-containing electrolyte [152]. Bi, a well-known formate selective catalyst in aqueous electrolytes, demonstrated a significant shift to CO-selectivity in the IL-containing electrolyte. A marked increase in

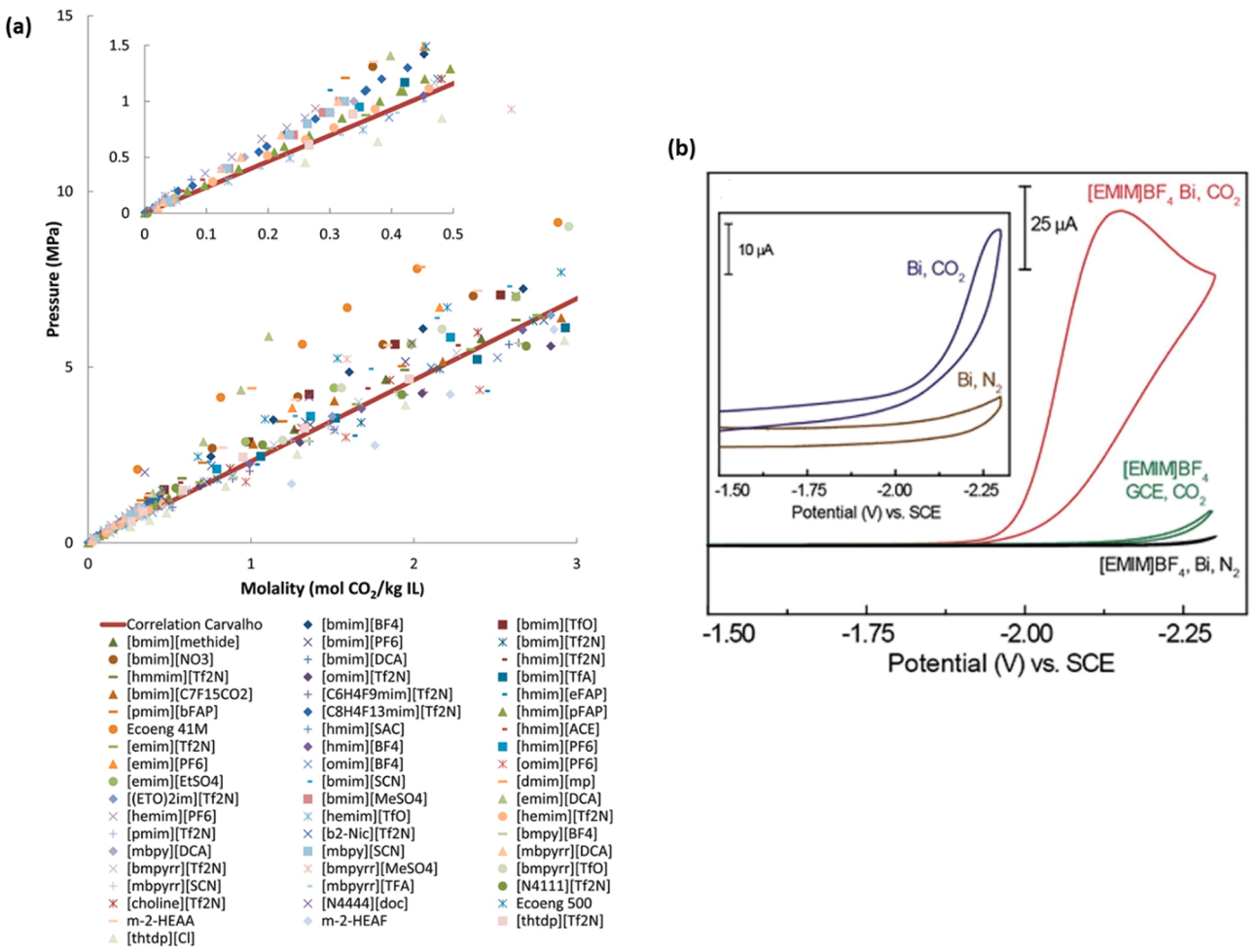

Fig. 17. (a) Solubility of carbon dioxide expressed as molality in different ionic liquids. (b) CV traces were recorded for Bi-deposited and bare GCEs in MeCN containing 20 mM [EMIM]BF_4. (b) Inset: Bi-deposited GCE in MeCN without the ionic liquid
(a) (Adapted with permission from [147] Copyright (2012) American Chemical Society (Adapted with permission from [152] Copyright (2013) American Chemical Society).

activity was observed upon IL introduction. At −1.95 V vs. SCE, the IL-containing electrolyte generated a CD of around 4 mA cm^{-2} with a FE of about 93% for CO (Fig. 17**(b)**).

5.3. Solid-state electrolyte (SSE)

In eCO_2R with solution-phase electrolytes, liquid products mix with dissolved salts, requiring costly separation and concentration processes to obtain pure liquid fuel for practical applications [153]. Wang's team at Rice University developed a CO_2 conversion cell using a solid-state electrolyte (SSE) instead of a conventional liquid electrolytes [154]. They combined electrochemically produced cations (H^+) and anions ($HCOO^-$) to prepare a pure HCOOH solution with the aid of a solid ion conductor. Employing an HCOOH-selective (FE > 90%) and scalable Bi catalyst as the cathode, they demonstrated production of up to 12 M HCOOH. They also reported continuous eCO_2C (100 h) for pure liquid product generation (steady formation of 0.1 M HCOOH with minimal selectivity and activity degradation), free of undesirable salts and avoiding energy-intensive downstream separation. Furthermore, they utilized a Cu catalyst to produce various electroless C2 liquid oxygenate solutions, such as ethanol and n-propanol acetic acid. This CO_2R cell with SSE can be tailored for more complex practical applications.

Fig. 18**(a)** shows that the SSE can function as either an anion or cation conductor, facilitating HCOOH formation via ion recombination of the crossover ions at the left (H^+-conductor) or right ($HCOO^-$-conductor) interface between the middle channel and the membrane. The product then diffuses through the liquid water, depending on the type of solid ion-conducting electrolyte used. In another study, Fan et al. [155] developed an SSE reactor addressing challenges in producing and separating CO_2 reduction products, as shown in Fig. 18**(b)**. This approach allows continuous generation of high-purity, high-concentration formic acid vapor and solutions. A GDL was used for both the cathode and anode to enhance CO_2 and H_2 mass transfer, while an inert gas stream (N_2) carried away formic acid vapor, yielding a highly concentrated product. The porous solid electrolyte (PSE) layer facilitated the recombination of protons with the electrochemically generated formate to produce molecular formic acid. Employing a grain boundary-enriched bismuth catalyst resulted in high activity (partial CD of 450 mA cm^{-2} for formate), selectivity (97% FE), and stability (100 h) compared to prior literature, as depicted in Fig. 18**(c)**. Inductively coupled plasma atomic emission spectroscopy (ICP-OES) measurements showed an extremely pure formic acid solution, with iron, bismuth, and platinum levels below 0.01 ppm and low levels of other impurities. This high purity level is economically promising, and the product can be condensed from the vapor through flexible tuning of the carrier gas stream.

6. Electrocatalysts

As CO_2 molecules are fully oxidized and thermodynamically stable,

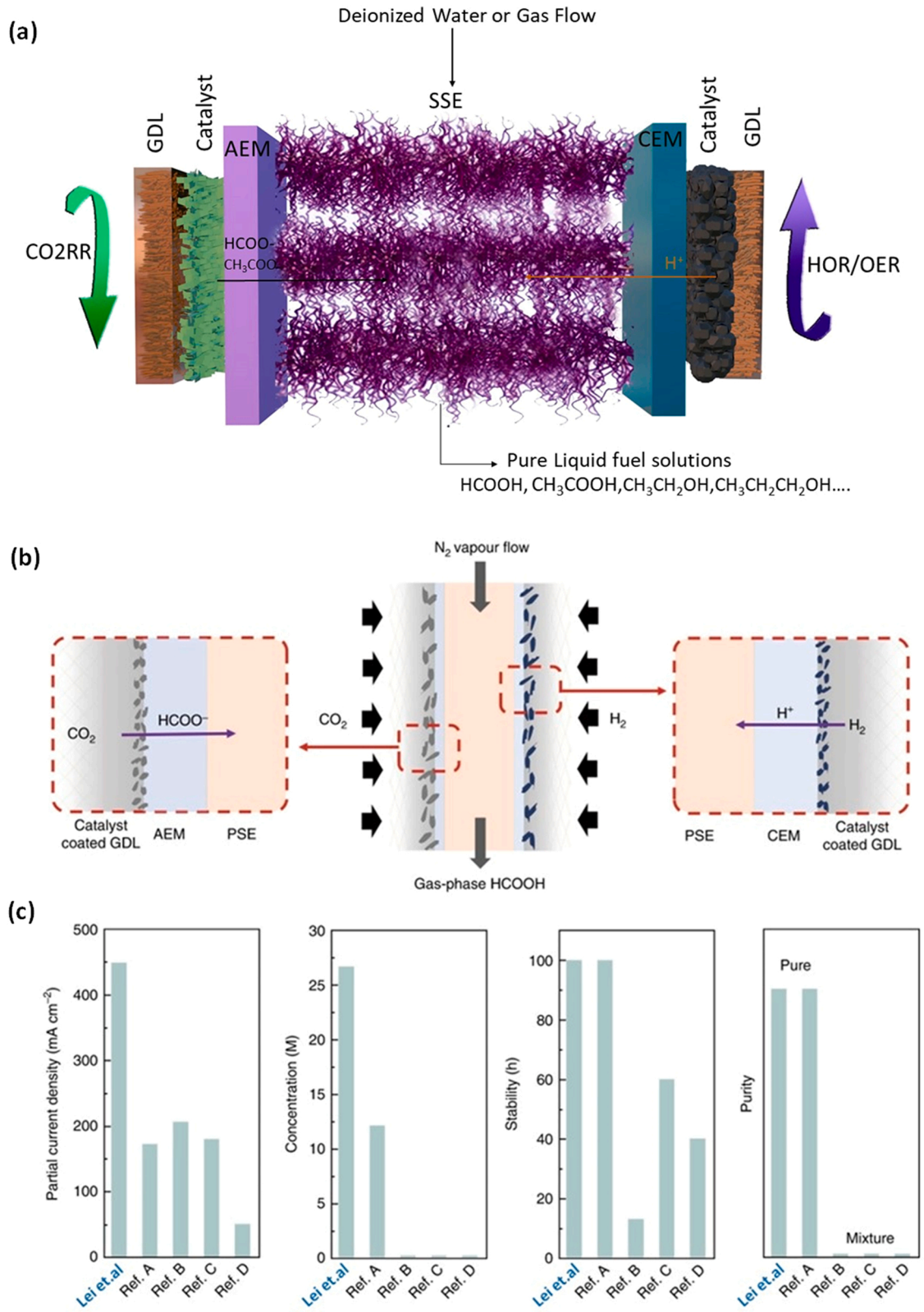

Fig. 18. (a) Schematic of the CO_2 reduction cell with a solid electrolyte. (b) Illustration of the all-solid-state electrochemical CO_2R reactor used to produce formic acid. AEM: Anion exchange membrane; CEM: Cation exchange membrane; GDL: Gas diffusion layer; PSE: porous solid electrolyte.(c) Electrochemical performance of the all-solid-state CO_2R reactor [155] compared with those previously reported in the literature
(a) (Redrawn from [143]). (A: [154]; B: [156]; C: [157]; D: [158]) (Adapted from [155] Open access, Springer Nature).

an electrocatalyst must bind and activate CO_2 to minimize overpotential during chemical reactions and enable conversion. An efficient electrocatalyst design can selectively promote desired product formation and control reaction pathways. To achieve optimal CO_2R performance, electrocatalysts must exhibit high activity, low overpotential, and high product selectivity. The chosen catalyst directly influences reaction channels and intermediate energy stages. Various micro/nanoscale catalysts have been studied for eCO_2R since the 1980 s. During CO_2 transport, *CO intermediate species typically form, interacting with *H or other *CO to produce *CHO/C-C species at the CO_2-electrocatalyst interface. Homogeneous catalysts display high CO_2 conversion selectivity, but the most active ones are often unstable and degrade during continuous reactions [159]. Alternative solvents like ionic liquids can reduce the overpotential, but lower-overpotentials catalysts are required for practical applications.

Efficient and selective heterogeneous electrocatalysts are being developed for CO_2 conversion to CO. Although CO_2 to CO is a simple two-electron reduction at ambient temperatures, efficient and selective electrocatalysts are still in development. Noble metals are considered prime candidates, with gold catalysts in an aqueous solution recognized for strong CO selectivity decades ago [160].

Catalyst selection is crucial in determining product categories resulting from CO_2R. Both homogeneous and heterogeneous catalysts have been extensively studied for CO_2R, with Fig. 19 illustrating various eCO_2R catalyst types. To comprehend the correlation between electrocatalysts and mass transfer effects during eCO_2R, numerous electrocatalysts must be thoroughly examined and summarized.

Initial eCO_2R studies focused on metal catalysts (monometallic, alloys, and multi-metallic) due to their ease of production, enhanced stability, and straightforward morphology, making them ideal for fundamental eCO_2R research. Monometallic catalysts can be classified into subgroups based on selectivity for the desired product. Noble metal catalysts like gold (Au) and silver (Ag), along with metal Zn, excel at electroproducing CO_2 to CO [160]. Sn, In, and Pb are formic acid-selective metals, while Fe, Ni, and Pt favor hydrogen. Copper-based electrocatalysts have garnered significant attention for their unique catalytic activity, generating various CO_2 reduction products with high FE [97,162].

Recently, zeolitic imidazolate frameworks (ZIFs), a metal-organic frameworks (MOFs) subclass, have received interest as heterogenous catalysts due to their multifunctionality, unimodal micropores, rapid electron transfer, and remarkable chemical and thermal stabilities. ZIF materials' metal centers influence electrocatalyst performance, and high-conductivity ZIF-based catalysts can enhance eCO_2C [163,164]. Ongoing efforts aim to design novel catalysts to improve stability, catalytic activity, and selectivity, including fabricating nanostructured metals to increase active site proportion [165,166], ion-modified materials [167,168], bimetallics for selectivity tuning [169,170], and non-metallic materials, which show promise as CO_2 reduction catalysts. Hori et al. investigated various transition-based metal electrodes to determine their selectivity and catalytic activity for CO_2 reduction products [97,171]. Nitrogen-doped carbon-based compounds also exhibit remarkable catalytic properties, presenting new eCO_2C opportunities. An efficient catalyst must facilitate multiple electrons and proton transfer to CO_2 without high overpotentials, reduce CO_2 in the presence of H_2O, and selectively form suitable products. Challenges associated CO_2R catalysts include low energy efficiency, poor product selectivity, and rapid deactivation.

6.1. *Recent developments in the field of heterogeneous catalysts for the target products*

Recently, numerous novel and modified CO_2 conversion catalysts have been developed for improved performance. Catalyst selectivity significantly impacts the economics of the CO_2 conversion process, potentially lowering capital and operating costs by reducing extreme or challenging operating conditions, such as temperature and pressure [172]. CO_2R can produce various products, including carbon monoxide (CO), formic acid (HCOOH), ethylene (C_2H_4), ethanol (CH_3CH_2OH), and n-propanol ($CH_3CH_2CH_2OH$), using a suitable electrocatalyst. Among these products, CO and HCOOH are particularly profitable due to their high yield and selectivity. This review primarily focuses on heterogeneous catalysts that generate CO, formic acid, and C_2 products.

6.1.1. *Selective formation of CO*

CO is considered the most promising CO_2R product commercially due to its high efficiency and cost-effectiveness. Its gaseous form also reduces costs associated with aqueous electrolyte separation during production. The eCO_2R to CO is a two-proton/electron process, resulting in the simplest gaseous product from CO_2 reduction. Understanding this mechanism can aid in designing modified catalysts with improved performance using surface engineering, particle size control, morphology, grain boundary, and GDE. Various catalysts, including noble and non-noble metals, transition metal chalcogenides, carbon materials, and molecular catalysts, have been developed for effective CO_2 to CO conversion. Despite the potential of non-precious metals like Pb, Bi, Sn, and

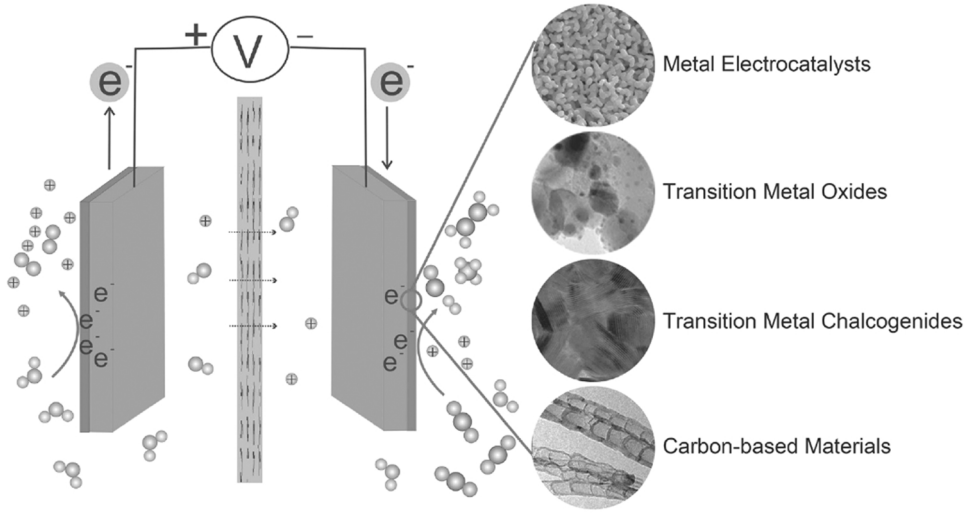

Fig. 19. Diagram of the reaction unit used for the CO_2R and four types of electrochemical CO_2 reduction catalysts (Adapted with permission from [161] Copyright (2016) John Wiley and Sons).

Ni for CO production via eCO_2R, silver, and gold have demonstrated the most promising results [173,174].

Metallic catalysts (or electrodes), particularly *sp* group metals such as In or Pb, generally promote CO formation in aqueous solutions at pH < 4 [175]. Metal cathodes like Ag, Au, and Zn in aqueous solutions (e.g., $KHCO_3$) exhibit high selectivity for CO production with excellent current efficiency [176–179]. Kim et al. explored the morphology and characteristics of Au nanostructures that displayed superior CO selectivity at low overpotentials compared to untreated Au film in the eCO_2R reaction [180].

Silver is recognized for its high selectivity and CD in electroreducing CO_2 to CO [181]. Various methods can be employed to fabricate Ag-based catalysts or electrode materials for CO production. By switching from conventional carbon support to TiO_2 support, Ag nanoparticles can achieve an FE of 90% and a CD of 101 mA cm^{-2} [182]. Fig. 20 suggests that the enhanced adsorption and stability of CO_2^- on TiO_2 may contribute to improved performance at low CDs. In this study, four different cathode catalysts, namely 40 wt% Ag/TiO_2, 40 wt% Ag/C, AgNP, and TiO_2, were immobilized on a GDE with the same total cathodic catalyst loading of 1 mg cm^{-2}. Pure TiO_2 did not exhibit any CO generation activity when used as the GDE's cathode catalyst, confirming that CO production in subsequent tests results from Ag's presence.

Tornow et al. examined nitrogen-based organometallic silver catalysts supported on carbon in an electrochemical flow reactor for CO_2R [183]. They found that these catalysts demonstrated a similar performance to Ag catalysts in selectively producing CO, even with a relatively low silver loading. The organometallic catalyst exhibited a FE of $> 90\%$. Moreover, the addition of an amine ligand to Ag/C led to a significant increase in the partial CD for CO, suggesting a potential co-catalyst mechanism. To enhance activity and selectivity, a better understanding of CO_2R mechanism and the assembly of these complexes on the carbon support is desired. The electrochemical reduction of CO_2 to CO, particularly using Ag-based materials in membrane electrode assembly (MEA) design, has attracted considerable attention. Ag-GDE-embedded MEA systems rely on factors such as pH, pressure, and temperature for optimal performance. Tables 2 and 3.

Verma et al. successfully achieved high-performance levels, approaching economic feasibility, for eCO_2R by utilizing a supported gold catalyst in an alkaline flow electrolyzer [186]. Fig. 21 demonstrates that higher pH values result in a smaller cathodic overpotential, indicating the pH-dependence of the entire CO_2R process. The low overpotential required for CO production in alkaline media is attributed to the pH-independent rate-determining step of electron transfer, in contrast to the overall pH-dependent process observed through onset cathode potentials, kinetic isotope effect, and Tafel slopes. Essentially, the utilization of a high-pH electrolyte facilitates the CO_2R process.

6.1.2. Selective formation of formic acid

Formic acid (HCOOH) fuel stands out as the most profitable product in terms of moles of electrons among the various products obtained from eCO_2R [78]. Metal oxides [194], alloys [2], and MOFs [195] are generally effective catalysts for HCOOH production. Bismuth (Bi), among the commonly used *p*-block elements for formic acid formation, has garnered significant attention due to its low toxicity, widespread availability, and strong selectivity towards formate. Transition metals such as Pd and Cu also promote HCOOH formation in aqueous solutions [175]. Notably, ultra-thin bismuth nanosheets have demonstrated high efficiency as electrocatalysts for selective formate production in a two-compartment electrochemical cell, separated by a Nafion membrane, employing a three-electrode system at − 1.0 V. These Bi nanosheets exhibit excellent stability and selectivity towards formate over a 5-h electrolysis period [196]. According to Greeley's study, the higher free energy of hydrogen adsorption on the Bi electrode surface leads to reduced HER catalytic activity and increased selectivity towards $CHOO^-$ [197].

In microfluidic reactor (MFR) systems, several studies have utilized diverse catalysts for CO_2 reduction. Liang employed cryo-exfoliation to fabricate highly crystalline SnO_2 nanoparticles with significantly smaller sizes (5 nm) [198]. The prepared SnO_2 nanoparticles exhibited 2 – 3 times higher CD compared to SnS_2 sheets and bulk SnO_2. The predominant product ratio of $CO/HCOO^-$, which is linked to variations in the SnOx/Sn ratio, depended on the applied potential. Interestingly, this Sn-based catalyst also displayed a 10% FE for CH_4 and C_2H_4OH production. This can be attributed to the unique structure of interconnected SnO_2 nanoparticles, characterized by numerous grain boundaries that serve as active sites for oxygenates and hydrocarbons.

García et al. reported 2D metal catalysts based on bismuth oxyhalides for formate synthesis [157]. The BiOBr-template catalyst was obtained by electroreduction of precursor in a CO_2-saturated $KHCO_3$ solution. The CO_2R activity was evaluated in an H-type electrochemical cell for liquid-phase reactions before employing the BiOBr catalysts in a GDE setup. Fig. 22 demonstrates that formate was produced with an FE of approximately 1 at a high CD of 80 mA cm^{-2} and exhibited remarkable stability over 65 h, despite mass transport limitations. These properties enabled a CD of 200 mA cm^{-2} in a microfluidic cell (MFC) utilizing a 2.0 M $KHCO_3$ electrolyte. Hence, the assessment of liquid and gas-phase reactors indicates the advantages and importance of gas-phase reactors for high productivity.

For formate production, MEA reactors have been extensively used, particularly with Sn electrocatalysts. Ma et al. investigated the electroreduction of CO_2 in proton exchange membrane reactors (PEMRs) with a buffer layer to examine key factors affecting cell performance [199]. One effective approach to increase the current efficiency of HCOOH formation is to incorporate a buffer layer between the cathode and the proton exchange membrane. In traditional cell architectures, significant potential drop occurs across the membrane, and the buffer layer plays a crucial role in ensuring the catalyst surface maintains an adequate potential for CO_2 reduction. Moreover, the buffer layer exhibits strong

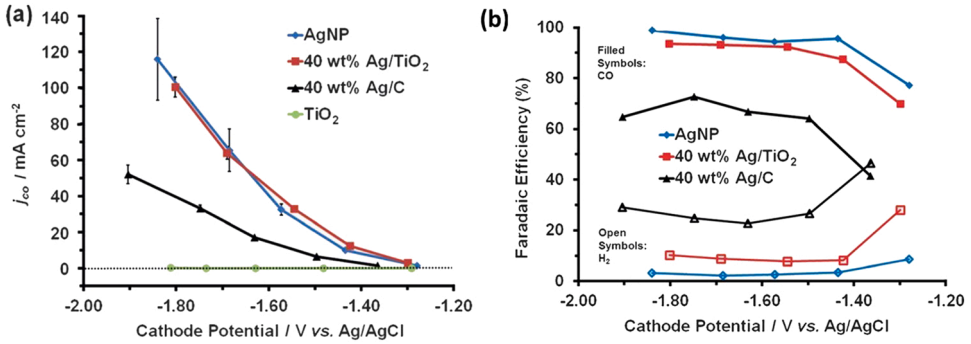

Fig. 20. (a) Partial current density for CO generation with four catalysts: 40 wt% Ag/TiO_2, 40 wt% Ag/C, AgNP, and TiO_2. (b) Faradaic efficiencies of 40 wt% Ag/TiO_2, 40 wt% Ag/C, and AgNP
(Adapted with permission from [182] Copyright (2−014) John Wiley and Sons).

Table 2
Electrochemical reduction of CO_2 to CO using various electrolyzers.

Cell Type	Catalyst	Electrolyte	FE %	Current density (mA/cm^2)	Potential	Remarks	Ref
H-Cell	Monodisperse Au Nanoparticles	0.5 M $KHCO_3$ at 25 °C	90	-	− 0.67 V vs RHE	More edge sites (active for CO evolution) than corner sites (active for the competitive H_2 evolution reaction) on the Au NP surface facilitate the stabilization of the reduction intermediates, such as COOH* , and the formation of CO	[178]
H-Cell	Mn–C_3N_4/ CNT	0.5 M $KHCO_3$ Bmim][BF_4]/ CH_3CN–H_2O	98.8 98.3	14 18.6	− 0.55 V vs. RHE − 2.1 V vs. Ag/ Ag	the Mn–N_3 site is the active center, on which CO_2 is more easily adsorbed and the free energy barrier of key intermediate formation is greatly decreased.	[184]
H-Type	Ni/Fe–N–C	0.5 M $NaHCO_3$	98	5	0.50 V vs. RHE	The optimized Ni/Fe–N–C catalyst shows an exclusive selectivity (a maximum FE(CO) of 98%) at a low overpotential of 390 mV vs. RHE, which is superior to both the single metal counterparts (Ni–N–C and Fe–N–C catalysts) and other state-of-the-art M–N–C catalysts	[185]
Flow cell	Ag/TiO_2	1 M KOH	90	100	1.8 V vs. Ag/ AgCl	TiO_2 is superior support for Ag catalysts (1) TiO_2 improves the stability of these Ag particles (minimizes agglomeration during the synthesis); (2) TiO_2 improves CO_2 reduction kinetics,	[182]
Flow cell	MWNT/PyPBI/ Au coated GDL	2.0 M KOH	> 49.4%	158	− 0.04 V vs RHE	Uses IrO_2 anode. the onset cell potential of − 1.50 V, The electrochemical system exhibits durability over 8 h	[186]
Flow cell based on GDE	Uniform mixture of AgNPs and MWCNTs deposited on a GDL	3 M KOH	> 95%	350	− 0.77 V v s.RHE	Energy efficiency of 45% achieved, The cell potential of the electrolyzer is − 3 V, High performance ascribed to decrease in charge transfer resistance of mixed catalyst layer, Reduces noble metal catalyst loading.	[187]
Flow cell	silver coordination polymer (Ag-CP)	0.1 M $KHCO_3$	> 96%	300	− 1.0 V vs RHE	Stable operation over a 4 h run. MOF-mediated methods omit inappropriate deposition processes (such as drop-casting)	[188]
Flow cell	silver (Ag)-based system	1 M KOH	84	300	-0.109 V vs. RHE	lower overpotential 300 mV operating at high current densities, near unity selectivity. Combined high alkalinity (decreases overpotentials) and pressurization (suppresses alternative product formation) enable efficient eCO_2R to CO.	[110]
GDE-type	Ni–N_4/C–NH_2	1 M KOH	90	450.0	− 1.0 V vs.RHE	Nearly 90% CO FE at a moderate overpotential of 0.89 V, particularly CO FE, can be maintained over 85% in a wide operating potential range from − 0.5 V to − 1.0 V. From DFT calculations and experimental research demonstrate that the superior activity is attributed to enhanced adsorption energies of CO_2 * and COOH* intermediates caused by the regulation of the electronic structure of the aminated catalysts.	[189]
GDE-type	CoTMAPc@CNT	1 M KOH	95.6	239	− 0.7 V vs. RHE	In a flow cell, the covalently immobilized structure delivers an industrially relevant current density and CO selectivity at 590 mV overpotential and very low molecular loading of 0.069 mg cm^2. Provides mechanistic insight and a design strategy for charged molecular catalysts for high-performance and stable heterogeneous electrolysis.	[190]
GDE-type	Ni–N–C	1 M KOH	90	726.0	− 1.18 V vs. RHE	DFT calculations reveal that the shortening Ni–N bonds in compressively strained NiN4 sites could intrinsically enhance the CO_2RR activity and selectivity of the Ni–N–C catalyst.	[191]
MEA	The carbonate-derived Ag/PTFE	1 M $KHCO_3$, 1 M KOH electrolyte	> 90	> 150	− 1 V vs RHE in 1 M $KHCO_3$ electrolyte − 0.7 V vs RHE in 1 M KOH electrolyte	Selective and stable electroreduction to produce CO at high CDs, High-performance metrics obtained in both $KHCO_3$ and KOH electrolytes. Over 100 h operation	[192]
MEA	Ag & Imidazolium-based ILs as co-catalysts	10 mM $KHCO_3$	95%	200	3 V	For 1000 h duration, the cell is stable enough to operate at or under 3 V. CO selectivity is maintained at above 90%	[106]
MEA	Au/CN catalyst	0.5 M KHCO3	90.6%	Partial current density (196.8)	-	The total cell voltage of 2.2 V low total cell potential of 2.2 V, a high mass activity for CO production of 985 A/g_{Au} was achieved at room temperature. 60.4% energy efficiency	[193]

control over HER. With the presence of the buffer layer, the Sn-based GDE achieved a CD of approximately 150 mA cm^{-2}; with a 60% selectivity towards HCOOH, whereas without the buffer layer, only about 5% selectivity towards HCOOH was obtained.

7. Commercial aspects of eCO_2R reaction and major challenges

Commercializing lab-scale eCO_2R is vital for reducing CO_2 emissions and mitigating climate change. Masel et al. conducted a study on the industry's perspective and identified CO and formate as the most

Table 3
Some recent results obtained for the CO_2 electrochemical reduction into formic acid/formate using various CO_2 electrolyzers.

Cell Type	Catalyst	Electrolyte	FE %	Current density (mA/cm^2)	Potential	Remarks	Ref
H-Tpye	PbO_2	[BZMIM]BF_4: CH_3CN: H_2O 14.7:73.6:11.7 (wt%)	95.5	40.8	2.3 V vs. Ag/Ag^+	[Bzmim]BF_4 - best performance over a series of ILs. CO_2 obtaining one electron to form CO_2^- intermediate on the surface of PbO_2 was the rate-determining step.	[200]
H-Tpye	PbSn alloy sheets	EMIM][OTf]:CH_3CN:H_2O 81:14:5 (wt%)	91	7.7	1.95 V vs.Ag/AgC	Inexpensive and easily Prepared Post-Transition Metal Alloy Catalysts Tin and lead and their alloys (PbSn) are excellent cathode materials to reduce CO_2 in an IL/water/acetonitrile electrolyte media.	[201]
H-Tpye	Ultrathin Bi	0.1 M $KHCO_3$	86	16.5	− 1.10 V vs. RHE	Significant potential of 2D nanostructured metals for highly efficient and long-life electrocatalytic CO_2 conversion. Ultrathin Bi nanosheets reached much superior activity, selectivity and stability for formate production to bulk Bi.	[202]
H-Tpye	urchin-like nanostructured SnO_2	0.5 M $KHCO_3$	62	-	− 1.0 V vs SHE	This nanocatalyst exhibited the best eCO_2R reaction performance in terms of the onset potential, electron transfer, CD and a very low overpotential of 0.39 V, essentially representing one among the lowest overpotentials reported for Sn(SnOx)-based catalysts	[203]
H-Tpye	Reduced BiNs	0.5 M $NaHCO_3$	> 90	11	− 1.5 V vs SCE	High selectivity (~100%) and large current density are measured over a broad potential, as well as excellent durability for > 10 h.	[204]
H-Tpye	N-doped graphene monolayer-coated Sn foil	0.5 M $KHCO_3$	92	21.3	− 1.00 V vs. RHE	Renewable and flexible SL-NG@Sn foil is designed to boost formate production. The SL-NG@Sn foil outperforms most of the reported Sn nanoparticles-based catalysts.	[205]
Flow cell	boron-doped diamond (BDD)	1.0 m KOH	94.7%.	2	− 2.5 V vs. Ag/AgCl	The production rate was increased to 473μmol m^{-2} s^{-1} at a current density of 15 mA cm^{-2} with a FE of 61%. The stability of the BDD electrodes was confirmed by 24 h operation, indicating that the BDD electrode can replace the metal electrode in formic acid production.	[206]
Flow cell	Chain like mesoporous SnO_2	0.1 M $KHCO_3$	95	13.6	-1.06 V vs. RHE	Crystallographically interconnected SnO_2 nanocrystals with abundant grain boundaries, high specific surface area, and easily accessible porosity The synthesized SnO_2-based gas diffusion electrode allows efficient diffusion of CO_2 even at high kinetics because of the highly open porous structure.	[207]
Flow cell	Sn nanoparticles (commercial)	1 M KOH Anolyte	93.3	51.7	-0.2 V vs. RHE	Proposed to avoid a solubility limitation in an aqueous electrolyte. CF-CO_2R method provides a sufficient dissolved CO_2 for the cathodic reaction with extremely reduced water amount, result in high CO_2R performances	[114]
MEA	BiO_x/C	0.5 M NaCl	96	12.5	-0.17 V vs. Ag/AgCl	pH dependence for $HCOO^-$ production at higher potentials suggests that the formation of the CO_2^- anion is the RDS because BiOx/C is reduced to form a Bi^0-rich surface	[208]
MEA	SnO_2 catalyst carbon black	1 M KOH	80	251	-1.43 V vs. RHE	Optimum SnO_2/C mass ratio was obtained to build an appropriate three-phase reaction interface with efficient charge and mass transfer leading to higher selectivity of formate production.	[209]
MR	SnO_2 nanoparticles	1 M KOH	97	147	-0.95 V vs. RHE	The distinctive grain boundary and exposed corner/step sites in the interconnected SnO_2 nanoparticles contribute to the high FE of CO_2 reduction and unique selectivity.	[198]
MR	Sn nanocatalyst/graphite rod	0.5 M $KHCO_3$	84.25	19.5	2.5 V vs. RHE	HCOOH concentration in the batch reactor was continuously decreasing with time, whereas it was almost constant in the continuous semi-micro reactor.	[210]

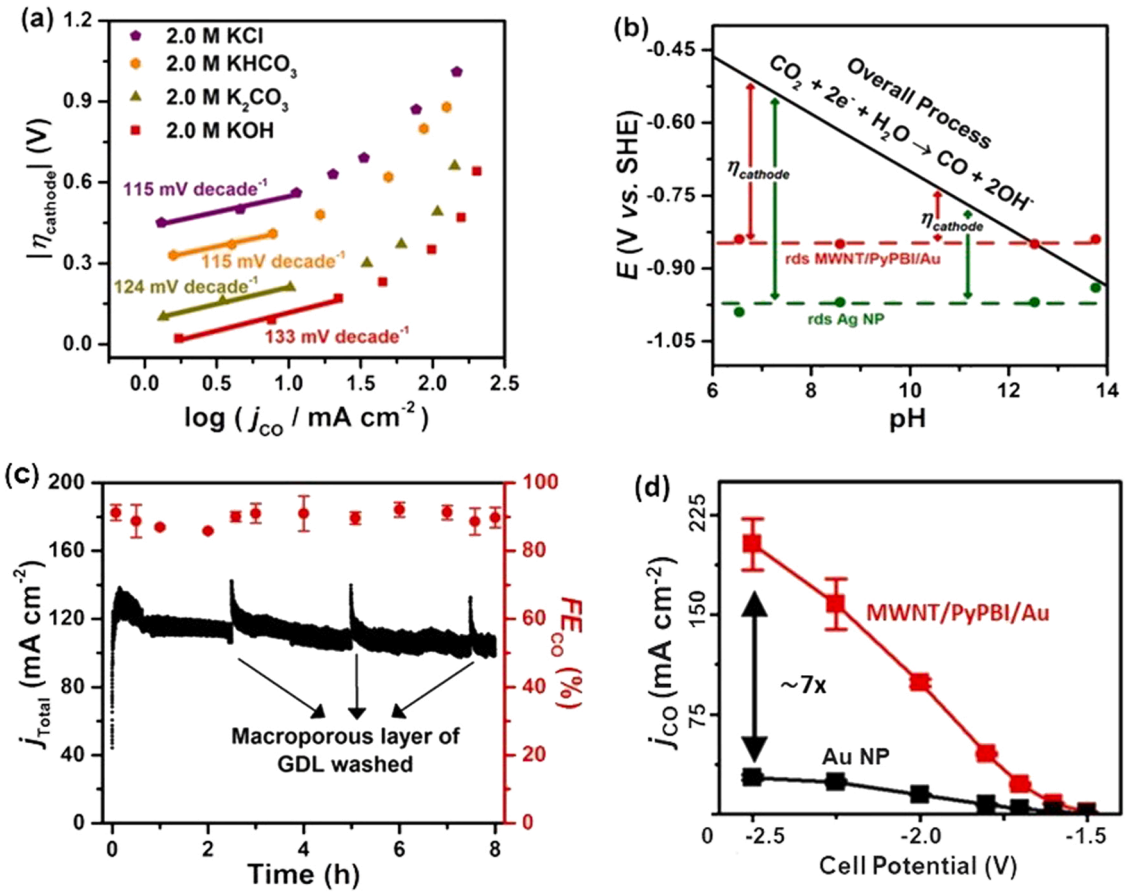

Fig. 21. (a) Tafel slopes obtained for the electroreduction of CO_2 to form CO with various electrolytes. Cathode: MWNT/PyPBI/Au; anode: IrO_2. (b) E – pH (Pourbaix) diagram for the electroreduction of CO_2 to form CO depicting the pH independence of the onset cathode potentials [hence, rate-determining step (rds)] vs. pH dependence of the overall process. (c) Variation in the total current density (j_{Total}) and Faradaic efficiency for CO with time at a constant cathode potential of − 0.44 V vs. RHE. Electrolyte: 2.0 M KOH. (d) Diagram with seven-fold enhancement in the current density with MWNT/PyPBI/Au compared with Au NPs (Adapted with permission from [186] Copyright (2018) American Chemical Society).

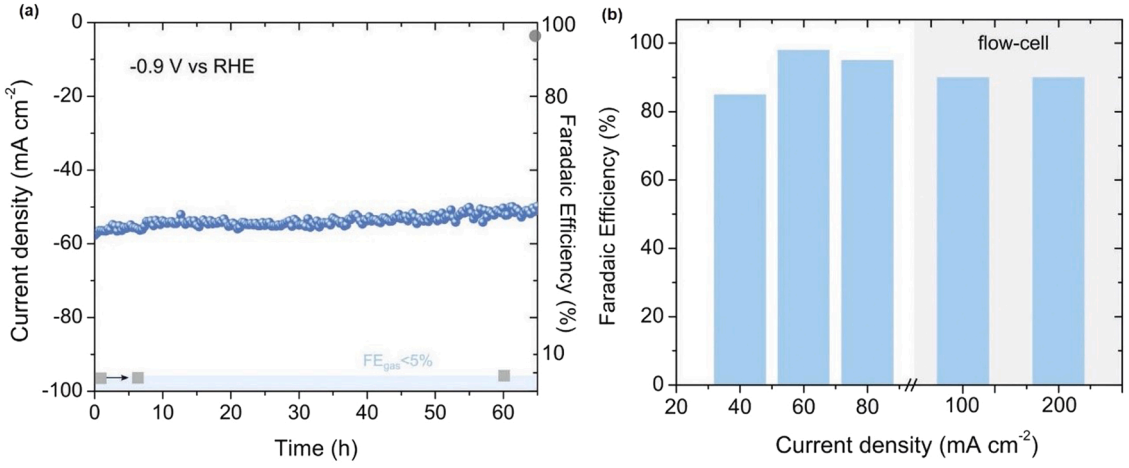

Fig. 22. BiOBr-templated catalysts used for the efficient and stable electroreduction of CO_2: (a) Current density trace obtained at − 0.9 V versus RHE. Faradaic efficiency for H_2 throughout the run is < 4%, and the cumulative Faradaic efficiency for formate approaches 1. (b) Faradaic efficiency as a function of current in the H-cell and flow-cell configurations. A Faradaic efficiency of 90% is sustained at up to 200 mA cm^{-2}
(Adapted with permission from [157] Copyright (2018) John Wiley and Sons).

economically viable products (Tables 4 and 5) [211]. These electrochemical processes compete with traditional methods and, for industrial use, require 30,000-h stability and selectivity at CDs > 250 mA cm^{-2} [40,68,69].

Scaling up eCO_2R is essential for industrial feasibility, but it requires long-term stability and selectivity at higher CDs. The main goal is to increase energy efficiency by reducing overpotential, which poses challenges in electrolytic cell design (i.e., mass and electron transfer

Table 4
Performance of the state-of-the-art electrolyzers used for converting CO_2 and water to HCOOH (data adapted from [211]).

CO_2 → HCOOH	
Electrolyzer current density	> 200 mA cm^{-2}
Catalyst activity	> 50 A g^{-1}
Initial Faradaic efficiency in an electrolyzer producing 2 M formic acid	> 80%
Faradaic efficiency loss at a constant current of 200 mA cm^{-2} in an electrolyzer producing 2 M formic acid	~10^{-4} h^{-1}
Initial Faradaic efficiency in an electrolyzer producing < 0.5 M formic acid	> 90%
Turnovers demonstrated	> 15,000,000
Single-pass HCOOH concentration	2–5 mol l^{-1}

Table 5
Industrial benchmarks for electrolyzers used to convert CO_2 into CO (data adapted from [211]).

CO_2→CO	
Electrolyzer current density	200–500 mA cm^{-2}
Catalyst activity	> 100 A g^{-1}
Faradaic efficiency	> 95%
Voltage increase at constant current	< 10 μV h^{-1}
Turnovers demonstrated	> 70,000,000
Turnover target	> 500,000,000

resistance), electrocatalyst design (i.e., selectivity), and GDEs (i.e., hydrophobicity and flooding). Achieving consistent benchmarking of catalysts is challenging, but the technology readiness level (TRL) could improve in the future [37,212].

CO is a vital product of CO_2 electroreduction for commercialization (industrial requirement: CD of 200 mA cm^{-2}). One of the main issues causing operational failures in eCO_2R electrolyzers is salt precipitation, which reduces the catalyst surface's active area and hampers gas transport. The limitation impacts the long-term durability and industrial applicability of the technology. When CO_2 and electrochemically generated hydroxide interact in cathode compartments, salt crystals, along with significant amounts of carbonate, are formed. The solubility limits of these species are reached when a sufficient number of electrolyte cations are present, leading to "salting out" conditions. This phenomena is often observed in zero-gap membrane electrode assemblies, particularly at high current densities, and can have detrimental effects [213].

Low-temperature CO_2 electrolyzers show promise for dynamic operation, but managing thermal conditions in large-scale high-temperature systems poses challenges [49]. Developing stable electrolyte systems for long-term eCO_2R remains a hurdle and is still in the lab phase [121]. Microfluidic flow cells (MFCs) offer potential for enhancing the electrochemical production of multi-carbon compounds, but they face scale-up limitations due to pressure sensitivity [48]. On the other hand, MEAs, utilizing solid ion-conducting polymer electrolytes and gaseous feeds, can address key challenges and enable industrial-scale electrolysis.

8. Merits - Electrochemical CO_2 conversion approach

Direct electrochemical conversion of CO_2 into valuable products offers a promising way to reduce atmospheric CO_2 while utilizing renewable energy sources. The eCO_2R process has gained considerable interest due to its advantages, including (1) controllable operation at ambient conditions; (2) production of fuels and valuable chemicals with electrolyte recycling; (3) good control over corrosion and degradation; (4) adjustable selectivity via external parameters (e.g., applied potentials); (5) renewable energy-powered operation of eCO_2R electrolyzers without additional CO_2 generation; (6) scalability due to modularity; and (7) compact, adaptable, economical, and easy-to-operate design for expansion to meet demand [2,214].

9. Strategies for efficient electrochemical CO_2 reduction (eCO_2R)

Efficient and selective eCO_2R poses challenging due to obstacles like low efficiency, poor selectivity, and catalyst instability [37,215]. Strategies include optimizing catalyst composition, structure, morphology, and surface state, while controlling reaction conditions such as voltage, temperature, and pressure. Crucial for improving eCO_2R efficiency is the design of a suitable reactor that determines CD, FE, and operational stability. By reducing mass transport limitations, minimizing ohmic resistance, and lowering cell potential, the reactor design can enhance energy efficiency (EE) and conversion rates. The role of the electrolyte in eCO_2R is essential, but research on modified systems incorporating novel catalysts is limited. High-performing and durable electrocatalysts are crucial for the cathode (CO_2R) and anode (OER), alongside a conductive electrolyte with efficient mass transport. Advanced materials like 3D-printed flow-through electrodes, tailored gas diffusion layers, and composite membranes with high ionic conductivity show promise in enhancing eCO_2R efficiency and durability by addressing CO_2 mass transport limitations. Ultimately, identifying optimal operating conditions and developing reliable electrocatalysts with high EE (low overpotential) are crucial for a sustainable and cost-effective eCO_2R process.

Mi-Young et al. [38] conducted a comprehensive evaluation of eCO_2R over a span for 15 years, assessing its large-scale applicability. Fig. 23 **(a)-(f)** summarize the figure of merit parameters for eCO_2R in liquid and gas phases, while Fig. 23 **(g)** illustrates a schematic comparison. Notably, gas-phase electrolysis of CO_2 has shown remarkable results when compared to liquid-phase eCO_2R benchmarks. Techno-economic analysis for large-scale applications reveals that gas-phase reaction performance parameters exceeded the base value, excluding operational expenses and electrode costs.

Liquid-fed electrolyzers possess advantages such as operation simplicity, ease of scaling up, low operational costs, high selectivity, and reasonable energy requirements, but they must overcome hurdles to compete with gas-fed electrolyzers. Liquid-fed electrolyzers are useful for gas-liquid-solid multiphase reactions and can reduce emissions, control chemistry, and increase efficiency [216]. Modifying surface roughness is a common method to decrease overpotential and increase catalyst selectivity [217]. Zero-gap electrolyzers minimize ohmic losses, facilitating the future application of industrial systems for CO_2 reduction to value-added products. By utilizing electrolyzers with continuous liquid feed and intermittent flow, the electrolyte flow can be regulated at a desired frequencies, allowing for effective reduction of CO_2 gas molecules into products [218].

Various methods have been proposed to prevent carbonate formation, including performing eCO_2R in an acidic environment, coupling membrane engineering with electrode structure, or altering the local microenvironment with an electric field [219]. In an acidic environment, eCO_2R offers a solution to address salt precipitation issues [220]. Mark et al. summarized research on eliminating salt precipitation through approaches such as passive modification of the MEA [213]. However, theoretical predictions like density functional theory (DFT) have limitations as they do not consider electrochemical conditions, cross-over effects among various active centers, or catalyst nano-structuring. Therefore, experimental validation is crucial for scaling up [221].

10. Summary and future perspectives

This review outlines the core components of eCO_2R and gas/liquid electrolyzer systems, highlighting their respective advantages, disadvantages, and key considerations. It emphasizes the need for effective coordination among all electrolyzer components in eCO_2R and discusses methods to address mass transfer limitations in liquid-phase CO_2 electrolyzers. The advantages and challenges of gas-phase electrolyzers are

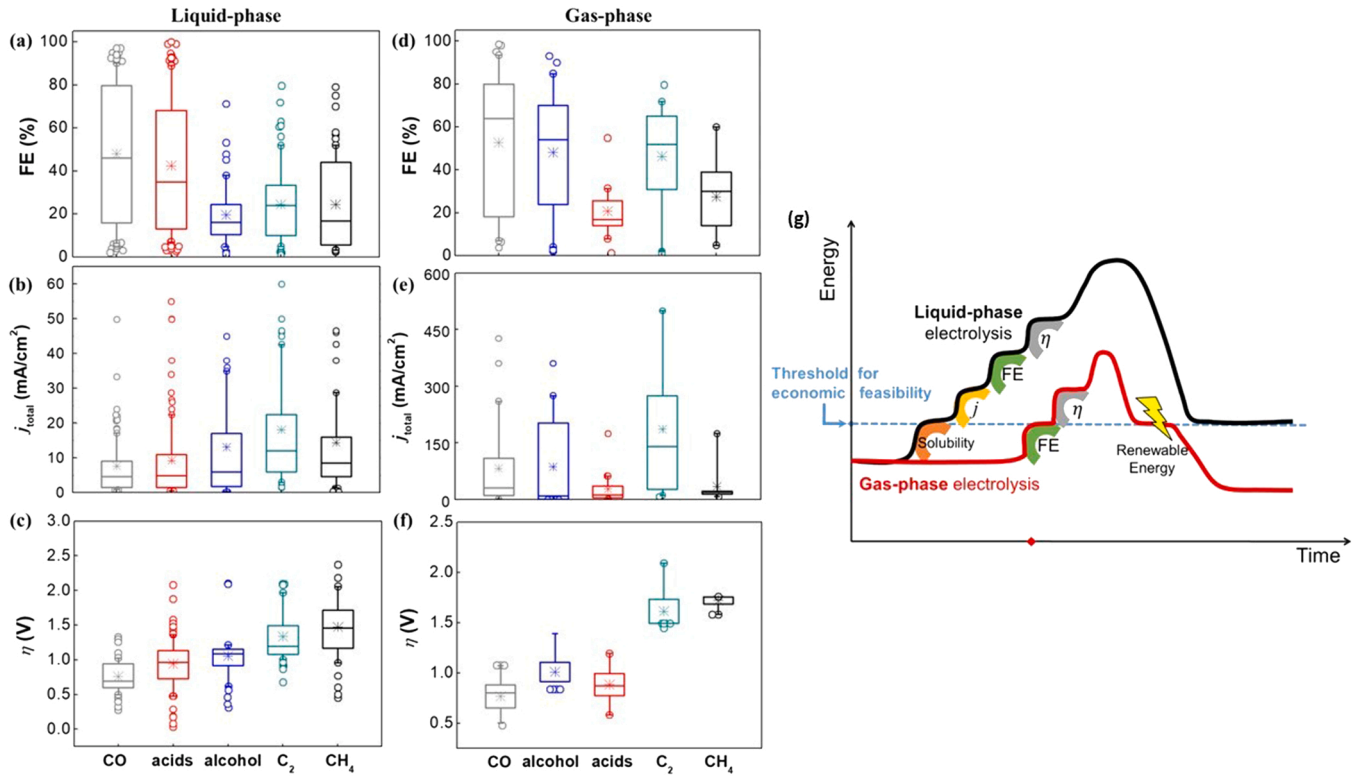

Fig. 23. Summary of figure of merit parameters of electrochemical CO_2 reduction (a, b, c) in liquid-phase, and (d, e, f) in gas-phase CO_2 electrolysis.; (g) Schematic illustration for comparison of liquid-phase and gas-phase electrochemical CO_2 reduction
(Adapted with permission from [38] Copyright (2020) Taylor & Francis)

examined, along with recent corrective approaches. Additionally, the review addresses key challenges for the economic and commercial viability of CO_2 electrolysis, focusing on the development of highly selective electrocatalysts and their CO_2 reduction mechanisms.

Future eCO_2R sresearch should prioritize the design of efficient and long-lasting electrolyzers, development of high-performance and stable catalysts, and enhancement of selectivity and CD [219]. Comprehensive understanding and improved performance of CO_2 electrolyzer systems necessitate optimization of electrode morphology, surface structure, reaction conditions, transport phenomena, catalyst stability, and electrode/electrolyte interface, alongside studying electrolyte/solvent effects. A primary concern is long-term stability, as current electrocatalysts' lifetimes range are limited to several hours. Aiming for thousands of hours at high current densities (400–500 $mAcm^{-2}$) is a key target. Electrolyzer design should also consider engineering strategies for multi-carbon products. While surface engineering and morphological control have proven effective in increasing FE and reducing overpotential [128], additional stability tests and life cycle analysis (LCA) under appropriate conditions are necessary. Therefore, future studies should focus on catalyst surface design and management for target product synthesis, emphasizing solvent-molecular interface interaction under high currents. Understanding the influence of various eCO_2R conditions is crucial. Further research should compare acidic and alkaline conditions for eCO_2R, to determine the optimal approach for achieving long-lasting, selective electrolyzers operating at industrially relevant current densities with high energy efficiency.

In the context of CO_2R for elecrofuel production, it is essential to consider the coordinated impact of all relative factors rather tahn merely prioitizing highly active or selective electrocatalysts. Electrofuels, as a carbon-neutral alternative to fossil fuels, warrant multifaceted research focus. MEAs have shown promise in CO_2 reduction to gas products, with reduced swelling and durability concerns compared to liquid products like alcohol. However, further research is needed to address MEA hydration management and product/CO_2 crossover in various reactions [222]. A key strategy involves optimizing the microenvironment of GDEs to enhance CO_2 mass transport and lower catalytic energy barriers for key intermediates, thereby addressing salt precipitation caused by carbonate production, a significant stability challenge in eCO_2R [219]. Future CO_2 electrolyzers may benefit from intermittent operation to adapt to renewable power supply fluctuations, thus ensuring an environmentally friendly and sustainable process [223]. Integration of electrofuel production with renewable energy systems should be maximized for efficiency and grid balancing, facilitating energy storage in chemical fuels. Research should target efficient, cost-effective materials, nanostructures, and hybrid catalyst systems for enhanced electrocatalysis to boost CO_2 conversion to electrofuels.

Efforts should be made to increase energy efficiency by minimizing losses during electrocatalysis, optimizing reaction conditions, and innovating electrode materials and structures for improved CO_2 capture and conversion, thereby bolstering the sustainability of electrofuel production. Exploring new electrocatalytic pathways can unveil efficient routes to desired electrofuels. Furthermore, investigating alternative pathways beyond methane and dimethyl ether (DME) could expand the range of liquid fuels suitable for transportation.

Future CO_2 electrolyzer designs can leverage advanced materials and innovative configurations to enhance efficiency and reduce costs. One promising approach entails the use of solid oxide electrolytes (SOEs), which operate at high temperatures, fostering higher conversion rates and reducing reliance on costly, corrosive liquid electrolytes. Innovative electrode materials such as carbon nanotubes or MOFs may enhance CO_2 reduction kinetics and selectivity. Unconventional electrolyzer designs, like flow-through or stacked cell configurations, could increase the reaction surface area and improve mass transport, resulting in higher conversion rates and less energy consumption. Scaling CO_2 conversion methods necessitates the enhancement of reactor designs, investigation of continuous flow systems, manufacturing of durable electrodes,

improvement of process effectiveness, and the commercial viability analysis. To successfully transition from R&D to competitive implementation, early-stage techno-economic feasibility studies are important in system development and process design.

CRediT authorship contribution statement

Sajna Shamsudeen: Conceptualization, Writing – original draft preparation. **Sifani Zavahir:** Methodology. **Anton Popelka:** Writing – review & editing **Peter Kasak:** Writing-Review & Editing **Ali Al-Sharshani:** Writing – review & editing. **Udeogu Onwusogh:** Writing – review & editing. **Miao Wang:** Data curation Hyunwoong Park: Writing – review & editing. **Dong Suk Han:** Conceptualization, Writing – review & editing, Supervision, Funding acqusition.

Declaration of Competing Interest

The authors declare that they have no known competing financial interests or personal relationships that could have appeared to influence the work reported in this paper.

Data Availability

Data will be made available on request.

Acknowledgments

This publication was made possible by the Qatar National Research Fund (a member of Qatar Foundation) under NPRP grant (NPRP13S-0202-200228). H.P. is grateful to the National Research Foundation of Korea (RS-2023-00254645, 2018R1A6A1A03024962, and 2021K1A4A7A02102598) and the Korea Evaluation Institute of Industrial Technology (Alchemist Project 20018904, NTIS-1415180111) through the Ministry of Trade, Industry, and Energy, Korea.

References

[1] P.Z.V. Masson-Delmotte, A. Pirani, S.L. Connors, C. Péan, S. Berger, Y.C.N. Caud, L. Goldfarb, M.I. Gomis, M. Huang, K. Leitzell, E. Lonnoy, J.B.R. Matthews, T. K. Maycock, T. Waterfield, O. Yelekçi, R. Yu, B. Zhou, IPCC, Summary for Policymakers, in: Climate Change 2021: The Physical Science Basis. Contribution of Working Group I to the Sixth Assessment Report of the Intergovernmental Panel on Climate Change, 2021, Cambridge University Press, United Kingdom and New York, NY, USA, 2021, pp. 3–32.

[2] A.S. Agarwal, Y. Zhai, D. Hill, N. Sridhar, The electrochemical reduction of carbon dioxide to formate/formic acid: engineering and economic feasibility, ChemSusChem 4 (2011) 1301–1310, https://doi.org/10.1002/cssc.201100220.

[3] M. Freer, C. Gough, A. Welfle, A. Lea-Langton, Carbon optimal bioenergy with carbon capture and storage supply chain modelling: how far is too far? Sustain. Energy Technol. Assess. 47 (2021), 101406 https://doi.org/10.1016/j.seta.2021.101406.

[4] T. Iglina, P. Iglin, D. Pashchenko, Industrial CO_2 capture by algae: a review and recent advances, Sustainability (2022), https://doi.org/10.3390/su14073801.

[5] A. Gulzar, A. Gulzar, M.B. Ansari, F. He, S. Gai, P. Yang, Carbon dioxide utilization: a paradigm shift with CO_2 economy, Chem. Eng. J. Adv. 3 (2020), 100013, https://doi.org/10.1016/j.ceja.2020.100013.

[6] C. Xiang, Y. Wang, H. Liu, A scientometrics review on nonpoint source pollution research, Ecol. Eng. 99 (2017) 400–408, https://doi.org/10.1016/j.ecoleng.2016.11.028.

[7] N.J. van Eck, L. Waltman, Software survey: VOSviewer, a computer program for bibliometric mapping, Scientometrics 84 (2010) 523–538, https://doi.org/10.1007/s11192-009-0146-3.

[8] W.J. Lee, C. Li, H. Prajitno, J. Yoo, J. Patel, Y. Yang, S. Lim, Recent trend in thermal catalytic low temperature CO_2 methanation: a critical review, Catal. Today 368 (2021) 2–19, https://doi.org/10.1016/j.cattod.2020.02.017.

[9] X. Zhang, M. Cibian, A. Call, K. Yamauchi, K. Sakai, Photochemical CO_2 reduction driven by water-soluble copper(I) photosensitizer with the catalysis accelerated by multi-electron chargeable cobalt porphyrin, ACS Catal. 9 (2019) 11263–11273, https://doi.org/10.1021/acscatal.9b04023.

[10] W. Wang, R. Snoeckx, X. Zhang, M.S. Cha, A. Bogaerts, Modeling PLASMA-BASEd CO_2 and CH_4 conversion in mixtures with N_2, O2, and H_2O: the bigger plasma chemistry picture, J. Phys. Chem. C 122 (2018) 8704–8723, https://doi.org/10.1021/acs.jpcc.7b10619.

[11] H.S. Shafaat, J.Y. Yang, Uniting biological and chemical strategies for selective CO_2 reduction, Nat. Catal. 4 (2021) 928–933, https://doi.org/10.1038/s41929-021-00683-1.

[12] J. Albero, Y. Peng, H. García, Photocatalytic CO_2 reduction to C_{2+} Products, ACS Catal. 10 (2020) 5734–5749, https://doi.org/10.1021/acscatal.0c00478.

[13] J. Shi, Y. Jiang, Z. Jiang, X. Wang, X. Wang, S. Zhang, P. Han, C. Yang, Enzymatic conversion of carbon dioxide, Chem. Soc. Rev. 44 (2015) 5981–6000, https://doi.org/10.1039/C5CS00182J.

[14] V. Kumaravel, J. Bartlett, S.C. Pillai, Photoelectrochemical conversion of carbon dioxide (CO_2) into fuels and value-added products, ACS Energy Lett. 5 (2020) 486–519, https://doi.org/10.1021/acsenergylett.9b02585.

[15] S.R. Hui, P.De Luna, How increasing proton and electron conduction benefits electrocatalytic CO_2 reduction, Matter 4 (2021) 1555–1577, https://doi.org/10.1016/j.matt.2021.02.021.

[16] F. Pan, X. Yang, T. O'Carroll, H. Li, K.-J. Chen, G. Wu, Carbon catalysts for electrochemical CO_2 reduction toward multicarbon products, Adv. Energy Mater. 12 (2022) 2200586, https://doi.org/10.1002/aenm.202200586.

[17] S. Popović, M. Smiljanić, P. Jovanovič, J. Vavra, R. Buonsanti, N. Hodnik, Stability and degradation mechanisms of copper-based catalysts for electrochemical CO_2 reduction, Angew. Chem. Int. Ed. 59 (2020) 14736–14746, https://doi.org/10.1002/anie.202000617.

[18] B. Deng, M. Huang, X. Zhao, S. Mou, F. Dong, Interfacial electrolyte effects on electrocatalytic CO_2 reduction, ACS Catal. 12 (2022) 331–362, https://doi.org/10.1021/acscatal.1c03501.

[19] S. Overa, B.H. Ko, Y. Zhao, F. Jiao, Electrochemical approaches for CO_2 conversion to chemicals: a journey toward practical applications, Acc. Chem. Res. 55 (2022) 638–648, https://doi.org/10.1021/acs.accounts.1c00674.

[20] L.M. Alsarhan, A.S. Alayyar, N.B. Alqahtani, N.H. Khdary, Circular carbon economy (CCE): a way to invest CO_2 and protect the environment, a review, Sustainability (2021), https://doi.org/10.3390/su132111625.

[21] D.A. Bulushev, J.R.H. Ross, Towards sustainable production of formic acid, ChemSusChem 11 (2018) 821–836, https://doi.org/10.1002/cssc.201702075.

[22] C. Rice, S. Ha, R.I. Masel, P. Waszczuk, A. Wieckowski, T. Barnard, Direct formic acid fuel cells, J. Power Sources 111 (2002) 83–89, https://doi.org/10.1016/S0378-7753(02)00271-9.

[23] F. Joó, Breakthroughs in hydrogen storage—formic acid as a sustainable storage material for hydrogen, ChemSusChem 1 (2008) 805–808, https://doi.org/10.1002/cssc.200800133.

[24] O. Yishai, S.N. Lindner, J. Gonzalez de la Cruz, H. Tenenboim, A. Bar-Even, The formate bio-economy, Curr. Opin. Chem. Biol. 35 (2016) 1–9, https://doi.org/10.1016/j.cbpa.2016.07.005.

[25] J. Zhang, PEM Fuel Cell Electrocatalysts and Catalyst Layers: Fundamentals and Applications, Springer Science & Business Media, 2008.

[26] J. Qiao, Y. Liu, J. Zhang, Electrochemical Reduction of Carbon Dioxide: Fundamentals and Technologies, CRC Press, 2016.

[27] R. Lin, J. Guo, X. Li, P. Patel, A. Seifitokaldani, Electrochemical reactors for CO_2 conversion, Catalysts (2020), https://doi.org/10.3390/catal10050473.

[28] J. Wu, Y. Huang, W. Ye, Y. Li, CO_2 reduction: from the electrochemical to photochemical approach, Adv. Sci. 4 (2017) 1700194, https://doi.org/10.1002/advs.201700194.

[29] S. Valluri, V. Claremboux, S. Kawatra, Opportunities and challenges in CO_2 utilization, J. Environ. Sci. 113 (2022) 322–344, https://doi.org/10.1016/j.jes.2021.05.043.

[30] X. Zhu, Y. Li, Review of two-dimensional materials for electrochemical CO_2 reduction from a theoretical perspective, WIREs Comput. Mol. Sci. 9 (2019), e1416, https://doi.org/10.1002/wcms.1416.

[31] M. Jouny, W. Luc, F. Jiao, General techno-economic analysis of CO_2 electrolysis systems, Ind. Eng. Chem. Res. 57 (2018) 2165–2177, https://doi.org/10.1021/acs.iecr.7b03514.

[32] S. Nitopi, E. Bertheussen, S.B. Scott, X. Liu, A.K. Engstfeld, S. Horch, B. Seger, I.E. L. Stephens, K. Chan, C. Hahn, J.K. Nørskov, T.F. Jaramillo, I. Chorkendorff, Progress and perspectives of electrochemical CO_2 reduction on copper in aqueous electrolyte, Chem. Rev. 119 (2019) 7610–7672, https://doi.org/10.1021/acs.chemrev.8b00705.

[33] G.H. Han, J. Bang, G. Park, S. Choe, Y.J. Jang, H.W. Jang, S.Y. Kim, S.H. Ahn, Recent advances in electrochemical, photochemical, and photoelectrochemical reduction of CO_2 to C_{2+} products, Small (2023) 2205765, https://doi.org/10.1002/smll.202205765.

[34] H.-R.M. Jhong, F.R. Brushett, P.J.A. Kenis, The effects of catalyst layer deposition methodology on electrode performance, Adv. Energy Mater. 3 (2013) 589–599, https://doi.org/10.1002/aenm.201200759.

[35] A.J. Martín, G.O. Larrazábal, J. Pérez-Ramírez, Towards sustainable fuels and chemicals through the electrochemical reduction of CO_2: lessons from water electrolysis, Green Chem. 17 (2015) 5114–5130, https://doi.org/10.1039/C5GC01893E.

[36] C.S. Chen, A.D. Handoko, J.H. Wan, L. Ma, D. Ren, B.S. Yeo, Technology Stable Sel, Electrochem. Reduct. Carbon Dioxide Ethyl. Copp. mesocrystals 5 (2015) 161–168, https://doi.org/10.1039/C4CY00906A.

[37] D.T. Whipple, P.J.A. Kenis, Prospects of CO_2 utilization via direct heterogeneous electrochemical reduction, J. Phys. Chem. Lett. 1 (2010) 3451–3458, https://doi.org/10.1021/jz1012627.

[38] M.-Y. Lee, K.T. Park, W. Lee, H. Lim, Y. Kwon, S. Kang, Current achievements and the future direction of electrochemical CO_2 reduction: a short review, Crit. Rev. Environ. Sci. Technol. 50 (2020) 769–815, https://doi.org/10.1080/10643389.2019.1631991.

[39] D. Salvatore, C.P. Berlinguette, Voltage matters when reducing CO_2 in an electrochemical flow cell, ACS Energy Lett. 5 (2020) 215–220, https://doi.org/10.1021/acsenergylett.9b02356.

[40] S. Verma, B. Kim, H.-R.M. Jhong, S. Ma, P.J.A. Kenis, A gross-margin model for defining technoeconomic benchmarks in the electroreduction of CO_2, ChemSusChem 9 (2016) 1972–1979, https://doi.org/10.1002/cssc.201600394.

[41] Y.-H. Fang, Z.-P. Liu, Tafel kinetics of electrocatalytic reactions: from experiment to first-principles, ACS Catal. 4 (2014) 4364–4376, https://doi.org/10.1021/cs501312v.

[42] T. Shinagawa, A.T. Garcia-Esparza, K. Takanabe, Insight on Tafel slopes from a microkinetic analysis of aqueous electrocatalysis for energy conversion, Sci. Rep. 5 (2015) 13801, https://doi.org/10.1038/srep13801.

[43] E. Wilhelm, R. Battino, R.J. Wilcock, Low-pressure solubility of gases in liquid water, Chem. Rev. 77 (1977) 219–262, https://doi.org/10.1021/cr60306a003.

[44] M. Ma, K. Liu, J. Shen, R. Kas, W.A. Smith, In situ fabrication and reactivation of highly selective and stable Ag catalysts for electrochemical CO_2 conversion, ACS Energy Lett. 3 (2018) 1301–1306, https://doi.org/10.1021/acsenergylett.8b00472.

[45] K.J.P. Schouten, Z. Qin, E. Pérez Gallent, M.T.M. Koper, Two pathways for the formation of ethylene in CO reduction on single-crystal copper electrodes, J. Am. Chem. Soc. 134 (2012) 9864–9867, https://doi.org/10.1021/ja302668n.

[46] H. Mistry, A.S. Varela, C.S. Bonifacio, I. Zegkinoglou, I. Sinev, Y.-W. Choi, K. Kisslinger, E.A. Stach, J.C. Yang, P. Strasser, B.R. Cuenya, Highly selective plasma-activated copper catalysts for carbon dioxide reduction to ethylene, Nat. Commun. 7 (2016) 12123, https://doi.org/10.1038/ncomms12123.

[47] M. Ma, H.A. Hansen, M. Valenti, Z. Wang, A. Cao, M. Dong, W.A. Smith, Electrochemical reduction of CO_2 on compositionally variant Au-Pt bimetallic thin films, Nano Energy 42 (2017) 51–57, https://doi.org/10.1016/j.nanoen.2017.09.043.

[48] S. Liang, N. Altaf, L. Huang, Y. Gao, Q. Wang, Electrolytic cell design for electrochemical CO_2 reduction, J. CO_2 Util. 35 (2020) 90–105, https://doi.org/10.1016/j.jcou.2019.09.007.

[49] B. Endrődi, G. Bencsik, F. Darvas, R. Jones, K. Rajeshwar, C. Janáky, Continuous-flow electroreduction of carbon dioxide, Prog. Energy Combust. Sci. 62 (2017) 133–154, https://doi.org/10.1016/j.pecs.2017.05.005.

[50] Y. Hori, A. Murata, R. Takahashi, S. Suzuki, Enhanced formation of ethylene and alcohols at ambient temperature and pressure in electrochemical reduction of carbon dioxide at a copper electrode, J. Chem. Soc. Chem. Commun. (1988) 17–19, https://doi.org/10.1039/C39880000017.

[51] Y. Hori, R. Takahashi, Y. Yoshinami, A. Murata, Electrochemical reduction of CO at a copper electrode, J. Phys. Chem. B 101 (1997) 7075–7081, https://doi.org/10.1021/jp970284i.

[52] Y. Hori, I. Takahashi, O. Koga, N. Hoshi, Electrochemical reduction of carbon dioxide at various series of copper single crystal electrodes, J. Mol. Catal. A: Chem. 199 (2003) 39–47, https://doi.org/10.1016/S1381-1169(03)00016-5.

[53] Y. Hori, K. Kikuchi, A. Murata, S. Suzuki, Production of methane and ethylene in electrochemical reduction of carbon dioxide at copper electrode in aqueous hydrogencarbonate solution, Chem. Lett. 15 (1986) 897–898, https://doi.org/10.1246/cl.1986.897.

[54] D.M. Weekes, D.A. Salvatore, A. Reyes, A. Huang, C.P. Berlinguette, Electrolytic CO_2 reduction in a flow cell, Acc. Chem. Res. 51 (2018) 910–918, https://doi.org/10.1021/acs.accounts.8b00010.

[55] F. Lucile, P. Cézac, F. Contamine, J.-P. Serin, D. Houssin, P. Arpentinier, Solubility of carbon dioxide in water and aqueous solution containing sodium hydroxide at temperatures from (293.15 to 393.15) K and pressure up to 5 MPa: experimental measurements, J. Chem. Eng. Data 57 (2012) 784–789, https://doi.org/10.1021/je200991x.

[56] J. Lin, S. Yan, C. Zhang, Q. Hu, Z. Cheng, Electroreduction of CO_2 toward high current density, Processes 10 (2022) 826, https://doi.org/10.3390/pr10050826.

[57] M. Li, S. Garg, X. Chang, L. Ge, L. Li, M. Konarova, T.E. Rufford, V. Rudolph, G. Wang, Toward excellence of transition metal-based catalysts for CO_2 electrochemical reduction: an overview of strategies and rationales, Small Methods 4 (2020) 2000033, https://doi.org/10.1002/smtd.202000033.

[58] M.R. Singh, E.L. Clark, A.T. Bell, Effects of electrolyte, catalyst, and membrane composition and operating conditions on the performance of solar-driven electrochemical reduction of carbon dioxide, Phys. Chem. Chem. Phys. 17 (2015) 18924–18936, https://doi.org/10.1039/C5CP03283K.

[59] T. Burdyny, W.A. Smith, CO_2 reduction on gas-diffusion electrodes and why catalytic performance must be assessed at commercially-relevant conditions, Energy Environ. Sci. 12 (2019) 1442–1453, https://doi.org/10.1039/C8EE03134G.

[60] D. Higgins, C. Hahn, C. Xiang, T.F. Jaramillo, A.Z. Weber, Gas-diffusion electrodes for carbon dioxide reduction: a new paradigm, ACS Energy Lett. 4 (2019) 317–324, https://doi.org/10.1021/acsenergylett.8b02035.

[61] S. Hernandez-Aldave, E. Andreoli, Fundamentals of gas diffusion electrodes and electrolysers for carbon dioxide utilisation: challenges and opportunities, Catalysts (2020), https://doi.org/10.3390/catal10060713.

[62] D.A. Salvatore, D.M. Weekes, J. He, K.E. Dettelbach, Y.C. Li, T.E. Mallouk, C. P. Berlinguette, Electrolysis of gaseous CO_2 to CO in a flow cell with a bipolar membrane, ACS Energy Lett. 3 (2018) 149–154, https://doi.org/10.1021/acsenergylett.7b01017.

[63] Y.C. Li, D. Zhou, Z. Yan, R.H. Gonçalves, D.A. Salvatore, C.P. Berlinguette, T. E. Mallouk, Electrolysis of CO_2 to syngas in bipolar membrane-based electrochemical cells, ACS Energy Lett. 1 (2016) 1149–1153, https://doi.org/10.1021/acsenergylett.6b00475.

[64] X. Lu, D.Y.C. Leung, H. Wang, J. Xuan, A high performance dual electrolyte microfluidic reactor for the utilization of CO_2, Appl. Energy 194 (2017) 549–559, https://doi.org/10.1016/j.apenergy.2016.05.091.

[65] B. Kim, S. Ma, H.-R. Molly Jhong, P.J.A. Kenis, Influence of dilute feed and pH on electrochemical reduction of CO_2 to CO on Ag in a continuous flow electrolyzer, Electrochim. Acta 166 (2015) 271–276, https://doi.org/10.1016/j.electacta.2015.03.064.

[66] A. Nakada, O. Ishitani, Selective electrocatalysis of a water-soluble rhenium(I) complex for CO_2 reduction using water as an electron donor, ACS Catal. 8 (2018) 354–363, https://doi.org/10.1021/acscatal.7b03275.

[67] Y.Y. Birdja, E. Pérez-Gallent, M.C. Figueiredo, A.J. Göttle, F. Calle-Vallejo, M.T. M. Koper, Advances and challenges in understanding the electrocatalytic conversion of carbon dioxide to fuels, Nat. Energy 4 (2019) 732–745, https://doi.org/10.1038/s41560-019-0450-y.

[68] X. Li, P. Anderson, H.-R.M. Jhong, M. Paster, J.F. Stubbins, P.J.A. Kenis, Greenhouse gas emissions, energy efficiency, and cost of synthetic fuel production using electrochemical CO_2 conversion and the fischer–tropsch process, Energy Fuels 30 (2016) 5980–5989, https://doi.org/10.1021/acs.energyfuels.6b00665.

[69] J.M. Spurgeon, B. Kumar, A comparative technoeconomic analysis of pathways for commercial electrochemical CO_2 reduction to liquid products, Energy Environ. Sci. 11 (2018) 1536–1551, https://doi.org/10.1039/C8EE00097B.

[70] J. Lee, Y. Tak, Electrocatalytic activity of Cu electrode in electroreduction of CO_2, Electrochim. Acta 46 (2001) 3015–3022, https://doi.org/10.1016/S0013-4686(01)00527-8.

[71] P. Sebastián-Pascual, S. Mezzavilla, I.E.L. Stephens, M. Escudero-Escribano, Structure-sensitivity and electrolyte effects in CO_2 electroreduction: from model studies to applications, ChemCatChem 11 (2019) 3626–3645, https://doi.org/10.1002/cctc.201900552.

[72] Y. Pang, T. Burdyny, C.-T. Dinh, M.G. Kibria, J.Z. Fan, M. Liu, E.H. Sargent, D. Sinton, Joint tuning of nanostructured Cu-oxide morphology and local electrolyte programs high-rate CO_2 reduction to C_2H_4, Green Chem. 19 (2017) 4023–4030, https://doi.org/10.1039/C7GC01677H.

[73] K.P. Kuhl, E.R. Cave, D.N. Abram, T.F.J.E. Jaramillo, E. Science, N. Insights into Electrochem. Reduct. Carbon Dioxide Met. Copp. Surf. 5 2012 7050 7059 doi: 10.1039/C2EE21234J.

[74] R. Kas, R. Kortlever, H. Yılmaz, M.T.M. Koper, G. Mul, Manipulating the hydrocarbon selectivity of copper nanoparticles in CO_2 electroreduction by process conditions, ChemElectroChem 2 (2015) 354–358, https://doi.org/10.1002/celc.201402373.

[75] A. Adamo, N. Aiichiro, L. Anghileri, M. Baumann, D. Blanco-Ania, T.G. Bloemberg, C. Bracken, M. Cattoen, Y. Chen, B.J. Deadman, Flow chemistry–fundamentals Walter De. Gruyter GmbH Co. KG 2021.

[76] S. Ma, M. Sadakiyo, R. Luo, M. Heima, M. Yamauchi, P.J.A. Kenis, One-step electrosynthesis of ethylene and ethanol from CO_2 in an alkaline electrolyzer, J. Power Sources 301 (2016) 219–228, https://doi.org/10.1016/j.jpowsour.2015.09.124.

[77] J. Hereijgers, H. Ottevaere, T. Breugelmans, W. De Malsche, Membrane deflection in a flat membrane microcontactor: experimental study of spacer features, J. Membr. Sci. 504 (2016) 153–161, https://doi.org/10.1016/j.memsci.2016.01.015.

[78] C. Chen, J.F. Khosrowabadi Kotyk, S.W. Sheehan, Progress toward commercial application of electrochemical carbon dioxide reduction, Chem 4 (2018) 2571–2586, https://doi.org/10.1016/j.chempr.2018.08.019.

[79] P. Wang, H. Yang, Y. Xu, X. Huang, J. Wang, M. Zhong, T. Cheng, Q. Shao, Synergized Cu/Pb core/shell electrocatalyst for high-efficiency CO_2 reduction to C2+ liquids, ACS Nano 15 (2021) 1039–1047, https://doi.org/10.1021/acsnano.0c07869.

[80] T.-T. Zhuang, Z.-Q. Liang, A. Seifitokaldani, Y. Li, P. De Luna, T. Burdyny, F. Che, F. Meng, Y. Min, R. Quintero-Bermudez, C.T. Dinh, Y. Pang, M. Zhong, B. Zhang, J. Li, P.-N. Chen, X.-L. Zheng, H. Liang, W.-N. Ge, B.-J. Ye, D. Sinton, S.-H. Yu, E. H. Sargent, Steering post-C–C coupling selectivity enables high efficiency electroreduction of carbon dioxide to multi-carbon alcohols, Nat. Catal. 1 (2018) 421–428, https://doi.org/10.1038/s41929-018-0084-7.

[81] B. Endrődi, E. Kecsenovity, A. Samu, F. Darvas, R.V. Jones, V. Török, A. Danyi, C. Janáky, Multilayer Electrolyzer Stack Converts Carbon Dioxide to Gas Products at High Pressure with High Efficiency, ACS Energy Lett. 4 (2019) 1770–1777, https://doi.org/10.1021/acsenergylett.9b01142.

[82] H.T. Ahangari, T. Portail, A.T. Marshall, Comparing the electrocatalytic reduction of CO_2 to CO on gold cathodes in batch and continuous flow electrochemical cells, Electrochem. Commun. 101 (2019) 78–81, https://doi.org/10.1016/j.elecom.2019.03.005.

[83] R.L. Cook, R.C. MacDuff, A.F. Sammells, High Rate Gas Phase CO 2 Reduction to Ethylene and Methane Using Gas Diffusion Electrodes, J. Electrochem. Soc. 137 (1990) 607, https://doi.org/10.1149/1.2086515.

[84] R.S. Jayashree, S.K. Yoon, F.R. Brushett, P.O. Lopez-Montesinos, D. Natarajan, L. J. Markoski, P.J.A. Kenis, On the performance of membraneless laminar flow-based fuel cells, J. Power Sources 195 (2010) 3569–3578, https://doi.org/10.1016/j.jpowsour.2009.12.029.

[85] D.T. Whipple, E.C. Finke, P.J.A. Kenis, Microfluidic reactor for the electrochemical reduction of carbon dioxide: the effect of pH, Electrochem. Solid-State Lett. 13 (2010) B109, https://doi.org/10.1149/1.3456590.

[86] H. Wang, D.Y.C. Leung, J. Xuan, Modeling of a microfluidic electrochemical cell for CO_2 utilization and fuel production, Appl. Energy 102 (2013) 1057–1062, https://doi.org/10.1016/j.apenergy.2012.06.020.

[87] E.J. Dufek, T.E. Lister, M.E. McIlwain, Bench-scale electrochemical system for generation of CO and syn-gas, J. Appl. Electrochem. 41 (2011) 623–631, https://doi.org/10.1007/s10800-011-0271-6.

[88] C. Delacourt, P.L. Ridgway, J.B. Kerr, J. Newman, Design of an Electrochemical Cell Making Syngas ($CO + H_2$) from CO_2 and H_2O Reduction at Room Temperature, J. Electrochem. Soc. 155 (2008) B42, https://doi.org/10.1149/1.2801871.

[89] E.J. Dufek, T.E. Lister, S.G. Stone, M.E. McIlwain, Operation of a Pressurized System for Continuous Reduction of CO_2, J. Electrochem. Soc. 159 (2012) F514, https://doi.org/10.1149/2.011209jes.

[90] H.-R.M. Jhong, S. Ma, P.J.A. Kenis, Electrochemical conversion of CO_2 to useful chemicals: current status, remaining challenges, and future opportunities, Curr. Opin. Chem. Eng. 2 (2013) 191–199, https://doi.org/10.1016/j.coche.2013.03.005.

[91] N. Sonoyama, M. Kirii, T. Sakata, Electrochemical reduction of CO_2 at metal-porphyrin supported gas diffusion electrodes under high pressure CO_2, Electrochem. Commun. 1 (1999) 213–216, https://doi.org/10.1016/S1388-2481(99)00041-7.

[92] N. Furuya, T. Yamazaki, M. Shibata, High performance Ru-Pd catalysts for CO_2 reduction at gas-diffusion electrodes, J. Electroanal. Chem. 431 (1997) 39–41, https://doi.org/10.1016/S0022-0728(97)00159-9.

[93] B. Kim, F. Hillman, M. Ariyoshi, S. Fujikawa, P.J.A. Kenis, Effects of composition of the micro porous layer and the substrate on performance in the electrochemical reduction of CO_2 to CO, J. Power Sources 312 (2016) 192–198, https://doi.org/10.1016/j.jpowsour.2016.02.043.

[94] L.M. Aeshala, R. Uppaluri, A. Verma, Electrochemical conversion of CO_2 to fuels: tuning of the reaction zone using suitable functional groups in a solid polymer electrolyte, Phys. Chem. Chem. Phys. 16 (2014) 17588–17594, https://doi.org/10.1039/C4CP02389G.

[95] J. Durst, A. Rudnev, A. Dutta, Y. Fu, J. Herranz, V. Kaliginedi, A. Kuzume, A. A. Permyakova, Y. Paratcha, P. Broekmann, T.J. Schmidt, Electrochemical CO_2 reduction – a critical view on fundamentals, materials and applications, CHIMIA 69 (2015) 769, https://doi.org/10.2533/chimia.2015.769.

[96] M. Inaba, A.W. Jensen, G.W. Sievers, M. Escudero-Escribano, A. Zana, M. Arenz, Benchmarking high surface area electrocatalysts in a gas diffusion electrode: measurement of oxygen reduction activities under realistic conditions, Energy Environ. Sci. 11 (2018) 988–994, https://doi.org/10.1039/C8EE00019K.

[97] Y. Hori, Modern aspects of electrochemistry, in: C.G. Vayenas, R.E. White, M. E. Gamboa-Aldeco (Eds.), Electrochemical CO_2 Reduction on Metal Electrodes, Springer, New York, New York, NY, 2008, pp. 89–189, https://doi.org/10.1007/978-0-387-49489-0_3.

[98] M. Todoroki, K. Hara, A. Kudo, T. Sakata, Electrochemical reduction of high pressure CO_2 at Pb, Hg and In electrodes in an aqueous $KHCO_3$ solution, J. Electroanal. Chem. 394 (1995) 199–203, https://doi.org/10.1016/0022-0728(95)04010-L.

[99] K. Hara, A. Kudo, T. Sakata, Electrochemical reduction of carbon dioxide under high pressure on various electrodes in an aqueous electrolyte, J. Electroanal. Chem. 391 (1995) 141–147, https://doi.org/10.1016/0022-0728(95)03935-A.

[100] S. Verma, X. Lu, S. Ma, R.I. Masel, P.J.A. Kenis, The effect of electrolyte composition on the electroreduction of CO_2 to CO on Ag based gas diffusion electrodes, Phys. Chem. Chem. Phys. 18 (2016) 7075–7084, https://doi.org/10.1039/C5CP05665A.

[101] S. Bajracharya, K. Vanbroekhoven, C.J.N. Buisman, D. Pant, D.P.B.T.B. Strik, Application of gas diffusion biocathode in microbial electrosynthesis from carbon dioxide, Environ. Sci. Pollut. Res. 23 (2016) 22292–22308, https://doi.org/10.1007/s11356-016-7196-x.

[102] K. Murata, H. Tanaka, K. Ishii, Electrochemical reduction of CO_2 by a gas-diffusion electrode composed of fac-Re(diimine)(CO)3Cl and carbon nanotubes, J. Phys. Chem. C 123 (2019) 12073–12080, https://doi.org/10.1021/acs.jpcc.8b12505.

[103] O.G. Sánchez, Y.Y. Birdja, M. Bulut, J. Vaes, T. Breugelmans, D. Pant, Recent advances in industrial CO_2 electroreduction, Curr. Opin. Green Sustain. Chem. 16 (2019) 47–56, https://doi.org/10.1016/j.cogsc.2019.01.005.

[104] P. Yue, Q. Fu, J. Li, L. Zhang, L. Xing, Z. Kang, Q. Liao, X. Zhu, Triple-phase electrocatalysis for the enhanced CO_2 reduction to HCOOH on a hydrophobic surface, Chem. Eng. J. 405 (2021), 126975, https://doi.org/10.1016/j.cej.2020.126975.

[105] P. Hou, X. Wang, Z. Wang, P. Kang, Gas phase electrolysis of carbon dioxide to carbon monoxide using nickel nitride as the carbon enrichment catalyst, ACS Appl. Mater. Interfaces 10 (2018) 38024–38031, https://doi.org/10.1021/acsami.8b11942.

[106] R.B. Kutz, Q. Chen, H. Yang, S.D. Sajjad, Z. Liu, I.R. Masel, Sustainion imidazolium-functionalized polymers for carbon dioxide electrolysis, Energy Technol. 5 (2017) 929–936, https://doi.org/10.1002/ente.201600636.

[107] E.J. Dufek, T.E. Lister, S.G. Stone, Sampling dynamics for pressurized electrochemical cells, J. Appl. Electrochem. 44 (2014) 849–855, https://doi.org/10.1007/s10800-014-0693-z.

[108] D.-H. Nam, O.S. Bushuyev, J. Li, P. De Luna, A. Seifitokaldani, C.-T. Dinh, F. P. García de Arquer, Y. Wang, Z. Liang, A.H. Proppe, C.S. Tan, P. Todorović, O. Shekhah, C.M. Gabardo, J.W. Jo, J. Choi, M.-J. Choi, S.-W. Baek, J. Kim, D. Sinton, S.O. Kelley, M. Eddaoudi, E.H. Sargent, Metal–organic frameworks mediate Cu coordination for selective CO_2 electroreduction, J. Am. Chem. Soc. 140 (2018) 11378–11386, https://doi.org/10.1021/jacs.8b06407.

[109] S.D. Sajjad, Y. Gao, Z. Liu, H. Yang, R. Masel, Tunable-high performance sustainion™ anion exchange membranes for electrochemical applications, ECS Trans. 77 (2017) 1653, https://doi.org/10.1149/07711.1653ecst.

[110] C.M. Gabardo, A. Seifitokaldani, J.P. Edwards, C.-T. Dinh, T. Burdyny, M. G. Kibria, C.P. O'Brien, E.H. Sargent, D. Sinton, Combined high alkalinity and pressurization enable efficient CO_2 electroreduction to CO, Energy Environ. Sci. 11 (2018) 2531–2539, https://doi.org/10.1039/C8EE01684D.

[111] D. Kopljar, A. Inan, P. Vindayer, N. Wagner, E. Klemm, Electrochemical reduction of CO_2 to formate at high current density using gas diffusion electrodes, J. Appl. Electrochem. 44 (2014) 1107–1116, https://doi.org/10.1007/s10800-014-0731-x.

[112] C.-T. Dinh, T. Burdyny, M.G. Kibria, A. Seifitokaldani, C.M. Gabardo, F.P. García de Arquer, A. Kiani, J.P. Edwards, P. De Luna, O.S. Bushuyev, C. Zou, R. Quintero-Bermudez, Y. Pang, D. Sinton, E.H. Sargent, CO_2 electroreduction to ethylene via hydroxide-mediated copper catalysis at an abrupt interface, Science 360 (2018) 783–787, https://doi.org/10.1126/science.aas9100.

[113] I. Merino-Garcia, J. Albo, J. Solla-Gullón, V. Montiel, A. Irabien, Cu oxide/ZnO-based surfaces for a selective ethylene production from gas-phase CO_2 electroconversion, J. CO_2 Util. 31 (2019) 135–142, https://doi.org/10.1016/j.jcou.2019.03.002.

[114] W. Lee, Y.E. Kim, M.H. Youn, S.K. Jeong, K.T. Park, Catholyte-free electrocatalytic CO_2 reduction to formate, Angew. Chem. Int. Ed. 57 (2018) 6883–6887, https://doi.org/10.1002/anie.201803501.

[115] A. Marcos-Madrazo, C. Casado-Coterillo, Á. Irabien, Sustainable membrane-coated electrodes for CO_2 electroreduction to methanol in alkaline media, ChemElectroChem 6 (2019) 5273–5282, https://doi.org/10.1002/celc.201901535.

[116] D. Sebastián, A. Palella, V. Baglio, L. Spadaro, S. Siracusano, P. Negro, F. Niccoli, A.S. Aricò, CO_2 reduction to alcohols in a polymer electrolyte membrane co-electrolysis cell operating at low potentials, Electrochim. Acta 241 (2017) 28–40, https://doi.org/10.1016/j.electacta.2017.04.119.

[117] B.C. Marepally, C. Ampelli, C. Genovese, T. Saboo, S. Perathoner, F.M. Wisser, L. Veyre, J. Canivet, E.A. Quadrelli, G. Centi, Enhanced formation of >C1 products in electroreduction of CO_2 by adding a CO_2 adsorption component to a gas-diffusion layer-type catalytic electrode, ChemSusChem 10 (2017) 4442–4446, https://doi.org/10.1002/cssc.201701506.

[118] I. Merino-Garcia, J. Albo, A. Irabien, Productivity and selectivity of gas-phase CO_2 electroreduction to methane at copper nanoparticle-based electrodes, Energy Technol. 5 (2017) 922–928, https://doi.org/10.1002/ente.201600616.

[119] J.T. Song, H. Song, B. Kim, J. Oh, Towards higher rate electrochemical CO_2 conversion: from liquid-phase to gas-phase systems, Catalysts (2019), https://doi.org/10.3390/catal9030224.

[120] S. Komatsu, M. Tanaka, A. Okumura, A. Kungi, Preparation of cu-solid polymer electrolyte composite electrodes and application to gas-phase electrochemical reduction of CO_2, Electrochim. Acta 40 (1995) 745–753, https://doi.org/10.1016/0013-4686(94)00325-U.

[121] J.-B. Vennekötter, T. Scheuermann, R. Sengpiel, M. Wessling, The electrolyte matters: Stable systems for high rate electrochemical CO_2 reduction, J. CO_2 Util. 32 (2019) 202–213, https://doi.org/10.1016/j.jcou.2019.04.007.

[122] H. Yang, J.J. Kaczur, S.D. Sajjad, R.I. Masel, Electrochemical conversion of CO_2 to formic acid utilizing Sustainion™ membranes, J. CO_2 Util. 20 (2017) 208–217, https://doi.org/10.1016/j.jcou.2017.04.011.

[123] N.M. Vargas-Barbosa, G.M. Geise, M.A. Hickner, T.E. Mallouk, Assessing the utility of bipolar membranes for use in photoelectrochemical water-splitting cells, ChemSusChem 7 (2014) 3017–3020, https://doi.org/10.1002/cssc.201402535.

[124] W. Plieth, Electrochemistry for Materials Science, Elsevier Science, 2008.

[125] S. Garg, M. Li, A.Z. Weber, L. Ge, L. Li, V. Rudolph, G. Wang, T.E. Rufford, Advances and challenges in electrochemical CO_2 reduction processes: an engineering and design perspective looking beyond new catalyst materials, J. Mater. Chem. A 8 (2020) 1511–1544, https://doi.org/10.1039/C9TA13298H.

[126] B.M. Setterfield-Price, R.A.W. Dryfe, The influence of electrolyte identity upon the electro-reduction of CO_2, J. Electroanal. Chem. 730 (2014) 48–58, https://doi.org/10.1016/j.jelechem.2014.07.009.

[127] Y. Hori, H. Konishi, T. Futamura, A. Murata, O. Koga, H. Sakurai, K. Oguma, "Deactivation of copper electrode" in electrochemical reduction of CO_2, Electrochim. Acta 50 (2005) 5354–5369, https://doi.org/10.1016/j.electacta.2005.03.015.

[128] A. Wuttig, Y. Surendranath, Impurity Ion complexation enhances carbon dioxide reduction catalysis, ACS Catal. 5 (2015) 4479–4484, https://doi.org/10.1021/acscatal.5b00808.

[129] Y. Liu, M. Hou, G. Yang, B. Han, Solubility of CO_2 in aqueous solutions of NaCl, KCl, $CaCl_2$ and their mixed salts at different temperatures and pressures, J. Supercrit. Fluids 56 (2011) 125–129, https://doi.org/10.1016/j.supflu.2010.12.003.

[130] M. Wagner, I. von Harbou, J. Kim, I. Ermatchkova, G. Maurer, H. Hasse, Solubility of carbon dioxide in aqueous solutions of monoethanolamine in the low and high gas loading regions, J. Chem. Eng. Data 58 (2013) 883–895, https://doi.org/10.1021/je301030z.

[131] A.S. Varela, M. Kroschel, N.D. Leonard, W. Ju, J. Steinberg, A. Bagger, J. Rossmeisl, P. Strasser, pH effects on the selectivity of the electrocatalytic CO_2 reduction on graphene-embedded Fe–N–C motifs: bridging concepts between molecular homogeneous and solid-state heterogeneous catalysis, ACS Energy Lett. 3 (2018) 812–817, https://doi.org/10.1021/acsenergylett.8b00273.

[132] S. Zhu, B. Jiang, W.-B. Cai, M. Shao, Direct observation on reaction intermediates and the role of bicarbonate anions in CO_2 electrochemical reduction reaction on Cu surfaces, J. Am. Chem. Soc. 139 (2017) 15664–15667, https://doi.org/10.1021/jacs.7b10462.

[133] K. Hara, A. Tsuneto, A. Kudo, T. Sakata, Change in the product selectivity for the electrochemical CO_2 reduction by adsorption of sulfide ion on metal electrodes,

J. Electroanal. Chem. 434 (1997) 239–243, https://doi.org/10.1016/S0022-0728(97)00045-4.
[134] P. Dubé, G.M. Brisard, Influence of adsorption processes on the CO_2 electroreduction: An electrochemical mass spectrometry study, J. Electroanal. Chem. 582 (2005) 230–240, https://doi.org/10.1016/j.jelechem.2005.04.016.
[135] G. Marcandalli, A. Goyal, M.T.M. Koper, Electrolyte effects on the faradaic efficiency of CO_2 reduction to CO on a gold electrode, ACS Catal. 11 (2021) 4936–4945, https://doi.org/10.1021/acscatal.1c00272.
[136] C. Amatore, J.M. Saveant, Mechanism and kinetic characteristics of the electrochemical reduction of carbon dioxide in media of low proton availability, J. Am. Chem. Soc. 103 (1981) 5021–5023, https://doi.org/10.1021/ja00407a008.
[137] L. Zhang, Z.-J. Zhao, J. Gong, Nanostructured materials for heterogeneous electrocatalytic CO_2 reduction and their related reaction mechanisms, Angew. Chem. Int. Ed. 56 (2017) 11326–11353, https://doi.org/10.1002/anie.201612214.
[138] S. Kaneco, K. Iiba, H. Katsumata, T. Suzuki, K. Ohta, Effect of sodium cation on the electrochemical reduction of CO_2 at a copper electrode in methanol, J. Solid State Electrochem. 11 (2007) 490–495, https://doi.org/10.1007/s10008-006-0185-0.
[139] T. Saeki, K. Hashimoto, N. Kimura, K. Omata, A. Fujishima, Electrochemical reduction of CO_2 with high current density in a CO_2 + methanol medium at various metal electrodes, J. Electroanal. Chem. 404 (1996) 299–302, https://doi.org/10.1016/0022-0728(95)04374-8.
[140] B. Eneau-Innocent, D. Pasquier, F. Ropital, J.M. Léger, K.B. Kokoh, Electroreduction of carbon dioxide at a lead electrode in propylene carbonate: a spectroscopic study, Appl. Catal. B: Environ. 98 (2010) 65–71, https://doi.org/10.1016/j.apcatb.2010.05.003.
[141] S. Ikeda, T. Takagi, K. Ito, Selective formation of formic acid, oxalic acid, and carbon monoxide by electrochemical reduction of carbon dioxide, Bull. Chem. Soc. Jpn. 60 (1987) 2517–2522, https://doi.org/10.1246/bcsj.60.2517.
[142] S. Kaneco, K. Iiba, K. Ohta, T. Mizuno, Reduction of carbon dioxide to petrochemical intermediates, Energy Sources 22 (2000) 127–135, https://doi.org/10.1080/00908310050014108.
[143] K. Hirota, D.A. Tryk, T. Yamamoto, K. Hashimoto, M. Okawa, A. Fujishima, Photoelectrochemical reduction of CO_2 in a high-pressure CO_2 + methanol medium at p-type semiconductor electrodes, J. Phys. Chem. B 102 (1998) 9834–9843, https://doi.org/10.1021/jp9822945.
[144] B.A. Rosen, A. Salehi-Khojin, M.R. Thorson, W. Zhu, D.T. Whipple, P.J.A. Kenis, R.I. Masel, Ionic liquid–mediated selective conversion of CO_2 to CO at low overpotentials, Science 334 (2011) 643–644, https://doi.org/10.1126/science.1209786.
[145] J. Medina-Ramos, R.C. Pupillo, T.P. Keane, J.L. DiMeglio, J. Rosenthal, Efficient conversion of CO_2 to CO using tin and other inexpensive and easily prepared post-transition metal catalysts, J. Am. Chem. Soc. 137 (2015) 5021–5027, https://doi.org/10.1021/ja5121088.
[146] N. García Rey, D.D. Dlott, Structural transition in an ionic liquid controls CO_2 electrochemical reduction, J. Phys. Chem. C. 119 (2015) 20892–20899, https://doi.org/10.1021/acs.jpcc.5b03397.
[147] M. Ramdin, T.W. de Loos, T.J.H. Vlugt, State-of-the-art of CO_2 capture with ionic liquids, Ind. Eng. Chem. Res. 51 (2012) 8149–8177, https://doi.org/10.1021/ie3003705.
[148] J.-P. Jones, G.K.S. Prakash, G.A. Olah, Electrochemical CO_2 reduction: recent advances and current trends, Isr. J. Chem. 54 (2014) 1451–1466, https://doi.org/10.1002/ijch.201400081.
[149] M. Alvarez-Guerra, J. Albo, E. Alvarez-Guerra, A. Irabien, Ionic liquids in the electrochemical valorisation of CO_2, Energy Environ. Sci. 8 (2015) 2574–2599, https://doi.org/10.1039/C5EE01486G.
[150] M. Asadi, K. Kim, C. Liu, A.V. Addepalli, P. Abbasi, P. Yasaei, P. Phillips, A. Behranginia, J.M. Cerrato, R. Haasch, P. Zapol, B. Kumar, R.F. Klie, J. Abiade, L.A. Curtiss, A. Salehi-Khojin, Nanostructured transition metal dichalcogenide electrocatalysts for CO_2 reduction in ionic liquid, Science 353 (2016) 467–470, https://doi.org/10.1126/science.aaf4767.
[151] J. Medina-Ramos, J.L. DiMeglio, J. Rosenthal, Efficient reduction of CO_2 to CO with high current density using in situ or ex situ prepared Bi-based materials, J. Am. Chem. Soc. 136 (2014) 8361–8367, https://doi.org/10.1021/ja501923g.
[152] J.L. DiMeglio, J. Rosenthal, Selective conversion of CO_2 to CO with high efficiency using an inexpensive bismuth-based electrocatalyst, J. Am. Chem. Soc. 135 (2013) 8798–8801, https://doi.org/10.1021/ja4033549.
[153] O.S. Bushuyev, P. De Luna, C.T. Dinh, L. Tao, G. Saur, J. van de Lagemaat, S. O. Kelley, E.H. Sargent, What should we make with CO_2 and how can we make it? Joule 2 (2018) 825–832, https://doi.org/10.1016/j.joule.2017.09.003.
[154] C. Xia, P. Zhu, Q. Jiang, Y. Pan, W. Liang, E. Stavitski, H.N. Alshareef, H. Wang, Continuous production of pure liquid fuel solutions via electrocatalytic CO_2 reduction using solid-electrolyte devices, Nat. Energy 4 (2019) 776–785, https://doi.org/10.1038/s41560-019-0451-x.
[155] L. Fan, C. Xia, P. Zhu, Y. Lu, H. Wang, Electrochemical CO_2 reduction to high-concentration pure formic acid solutions in an all-solid-state reactor, Nat. Commun. 11 (2020) 3633, https://doi.org/10.1038/s41467-020-17403-1.
[156] Q. Gong, P. Ding, M. Xu, X. Zhu, M. Wang, J. Deng, Q. Ma, N. Han, Y. Zhu, J. Lu, Z. Feng, Y. Li, W. Zhou, Y. Li, Structural defects on converted bismuth oxide nanotubes enable highly active electrocatalysis of carbon dioxide reduction, Nat. Commun. 10 (2019) 2807, https://doi.org/10.1038/s41467-019-10819-4.
[157] F.P. García de Arquer, O.S. Bushuyev, P. De Luna, C.-T. Dinh, A. Seifitokaldani, M. I. Saidaminov, C.-S. Tan, L.N. Quan, A. Proppe, M.G. Kibria, S.O. Kelley, D. Sinton, E.H. Sargent, 2D metal oxyhalide-derived catalysts for efficient CO_2 electroreduction, Adv. Mater. 30 (2018) 1802858, https://doi.org/10.1002/adma.201802858.
[158] X. Zheng, P. De Luna, F.P. García de Arquer, B. Zhang, N. Becknell, M.B. Ross, Y. Li, M.N. Banis, Y. Li, M. Liu, O. Voznyy, C.T. Dinh, T. Zhuang, P. Stadler, Y. Cui, X. Du, P. Yang, E.H. Sargent, Sulfur-modulated tin sites enable highly selective electrochemical reduction of CO_2 to formate, Joule 1 (2017) 794–805, https://doi.org/10.1016/j.joule.2017.09.014.
[159] E.E. Benson, C.P. Kubiak, A.J. Sathrum, J.M. Smieja, Electrocatalytic and homogeneous approaches to conversion of CO_2 to liquid fuels, Chem. Soc. Rev. 38 (2009) 89–99, https://doi.org/10.1039/B804323J.
[160] Y. Hori, A. Murata, K. Kikuchi, S. Suzuki, Electrochemical reduction of carbon dioxides to carbon monoxide at a gold electrode in aqueous potassium hydrogen carbonate, J. Chem. Soc. Chem. Commun. (1987) 728–729, https://doi.org/10.1039/C39870000728.
[161] D.D. Zhu, J.L. Liu, S.Z. Qiao, Recent advances in inorganic heterogeneous electrocatalysts for reduction of carbon dioxide, Adv. Mater. 28 (2016) 3423–3452, https://doi.org/10.1002/adma.201504766.
[162] K.P. Kuhl, T. Hatsukade, E.R. Cave, D.N. Abram, J. Kibsgaard, T.F. Jaramillo, Electrocatalytic conversion of carbon dioxide to methane and methanol on transition metal surfaces, J. Am. Chem. Soc. 136 (2014) 14107–14113, https://doi.org/10.1021/ja505791r.
[163] Y. Liu, H. Cheng, M. Cheng, Z. Liu, D. Huang, G. Zhang, B. Shao, Q. Liang, S. Luo, T. Wu, S. Xiao, The application of Zeolitic imidazolate frameworks (ZIFs) and their derivatives based materials for photocatalytic hydrogen evolution and pollutants treatment, Chem. Eng. J. 417 (2021), 127914, https://doi.org/10.1016/j.cej.2020.127914.
[164] H.N. Abdelhamid, Removal of carbon dioxide using zeolitic imidazolate frameworks: adsorption and conversion via catalysis, Appl. Organomet. Chem. 36 (2022), e6753, https://doi.org/10.1002/aoc.6753.
[165] J. Rosen, G.S. Hutchings, Q. Lu, R.V. Forest, A. Moore, F. Jiao, Electrodeposited Zn dendrites with enhanced CO selectivity for electrocatalytic CO_2 reduction, ACS Catal. 5 (2015) 4586–4591, https://doi.org/10.1021/acscatal.5b00922.
[166] Q. Lu, J. Rosen, F. Jiao, Nanostructured metallic electrocatalysts for carbon dioxide reduction, ChemCatChem 7 (2015) 38–47, https://doi.org/10.1002/cctc.201402669.
[167] Y.-C. Hsieh, S.D. Senanayake, Y. Zhang, W. Xu, D.E. Polyansky, Effect of chloride anions on the synthesis and enhanced catalytic activity of silver nanocoral electrodes for CO_2 electroreduction, ACS Catal. 5 (2015) 5349–5356, https://doi.org/10.1021/acscatal.5b01235.
[168] P. Lobaccaro, M.R. Singh, E.L. Clark, Y. Kwon, A.T. Bell, J.W. Ager, Effects of temperature and gas–liquid mass transfer on the operation of small electrochemical cells for the quantitative evaluation of CO_2 reduction electrocatalysts, Phys. Chem. Chem. Phys. 18 (2016) 26777–26785, https://doi.org/10.1039/C6CP05287H.
[169] R. Kortlever, I. Peters, S. Koper, M.T.M. Koper, Electrochemical CO_2 reduction to formic acid at low overpotential and with high faradaic efficiency on carbon-supported bimetallic Pd–Pt nanoparticles, ACS Catal. 5 (2015) 3916–3923, https://doi.org/10.1021/acscatal.5b00602.
[170] D. Kim, J. Resasco, Y. Yu, A.M. Asiri, P. Yang, Synergistic geometric and electronic effects for electrochemical reduction of carbon dioxide using gold–copper bimetallic nanoparticles, Nat. Commun. 5 (2014) 4948, https://doi.org/10.1038/ncomms5948.
[171] Y. Hori, H. Wakebe, T. Tsukamoto, O. Koga, Electrocatalytic process of CO selectivity in electrochemical reduction of CO_2 at metal electrodes in aqueous media, Electrochim. Acta 39 (1994) 1833–1839, https://doi.org/10.1016/0013-4686(94)85172-7.
[172] N.R. Council, Catalysis looks to the future, National Academies Press 1992.
[173] T. Kunene, A. Atifi, J. Rosenthal, Selective CO_2 reduction over rose's metal in the presence of an imidazolium ionic liquid electrolyte, ACS Appl. Energy Mater. 3 (2020) 4193–4200, https://doi.org/10.1021/acsaem.9b01995.
[174] J.D. Froehlich, C.P. Kubiak, The homogeneous reduction of CO_2 by [Ni(cyclam)]+: increased catalytic rates with the addition of a CO scavenger, J. Am. Chem. Soc. 137 (2015) 3565–3573, https://doi.org/10.1021/ja512575v.
[175] R.P.S. Chaplin, A.A. Wragg, Effects of process conditions and electrode material on reaction pathways for carbon dioxide electroreduction with particular reference to formate formation, J. Appl. Electrochem. 33 (2003) 1107–1123, https://doi.org/10.1023/B:JACH.0000004018.57792.b8.
[176] H. Noda, S. Ikeda, Y. Oda, K. Imai, M. Maeda, K. Ito, Electrochemical reduction of carbon dioxide at various metal electrodes in aqueous potassium hydrogen carbonate solution, Bull. Chem. Soc. Jpn. 63 (1990) 2459–2462, https://doi.org/10.1246/bcsj.63.2459.
[177] S. Liu, H. Tao, L. Zeng, Q. Liu, Z. Xu, Q. Liu, J.-L. Luo, Shape-dependent electrocatalytic reduction of CO_2 to CO on triangular silver nanoplates, J. Am. Chem. Soc. 139 (2017) 2160–2163, https://doi.org/10.1021/jacs.6b12103.
[178] W. Zhu, R. Michalsky, Ö. Metin, H. Lv, S. Guo, C.J. Wright, X. Sun, A.A. Peterson, S. Sun, Monodisperse Au nanoparticles for selective electrocatalytic reduction of CO_2 to CO, J. Am. Chem. Soc. 135 (2013) 16833–16836, https://doi.org/10.1021/ja409445p.
[179] H. Won da, H. Shin, J. Koh, J. Chung, H.S. Lee, H. Kim, S.I. Woo, Highly efficient, selective, and stable CO_2 electroreduction on a hexagonal Zn catalyst, Angew. Chem. Int. Ed. Engl. 55 (2016) 9297–9300, https://doi.org/10.1002/anie.201602888.
[180] J. Kim, J.T. Song, H. Ryoo, J.-G. Kim, S.-Y. Chung, J. Oh, Morphology-controlled Au nanostructures for efficient and selective electrochemical CO_2 reduction, J. Mater. Chem. A 6 (2018) 5119–5128, https://doi.org/10.1039/C8TA01010B.

[181] T. Hatsukade, K.P. Kuhl, E.R. Cave, D.N. Abram, T.F. Jaramillo, Insights into the electrocatalytic reduction of CO_2 on metallic silver surfaces, Phys. Chem. Chem. Phys. 16 (2014) 13814–13819, https://doi.org/10.1039/C4CP00692E.
[182] S. Ma, Y. Lan, G.M.J. Perez, S. Moniri, P.J.A. Kenis, Silver supported on titania as an active catalyst for electrochemical carbon dioxide reduction, ChemSusChem 7 (2014) 866–874, https://doi.org/10.1002/cssc.201300934.
[183] C.E. Tornow, M.R. Thorson, S. Ma, A.A. Gewirth, P.J.A. Kenis, Nitrogen-based catalysts for the electrochemical reduction of CO_2 to CO, J. Am. Chem. Soc. 134 (2012) 19520–19523, https://doi.org/10.1021/ja308217w.
[184] J. Feng, H. Gao, L. Zheng, Z. Chen, S. Zeng, C. Jiang, H. Dong, L. Liu, S. Zhang, X. Zhang, A Mn-N3 single-atom catalyst embedded in graphitic carbon nitride for efficient CO_2 electroreduction, Nat. Commun. 11 (2020) 4341, https://doi.org/10.1038/s41467-020-18143-y.
[185] T. Zhang, X. Han, H. Liu, M. Biset-Peiró, X. Zhang, P. Tan, P. Tang, B. Yang, L. Zheng, J.R. Morante, J. Arbiol, Quasi-double-star nickel and iron active sites for high-efficiency carbon dioxide electroreduction, Energy Environ. Sci. 14 (2021) 4847–4857, https://doi.org/10.1039/D1EE01592C.
[186] S. Verma, Y. Hamasaki, C. Kim, W. Huang, S. Lu, H.-R.M. Jhong, A.A. Gewirth, T. Fujigaya, N. Nakashima, P.J.A. Kenis, Insights into the low overpotential electroreduction of CO_2 to CO on a supported gold catalyst in an alkaline flow electrolyzer, ACS Energy Lett. 3 (2018) 193–198, https://doi.org/10.1021/acsenergylett.7b01096.
[187] S. Ma, R. Luo, J.I. Gold, A.Z. Yu, B. Kim, P.J.A. Kenis, Carbon nanotube containing Ag catalyst layers for efficient and selective reduction of carbon dioxide, J. Mater. Chem. A 4 (2016) 8573–8578, https://doi.org/10.1039/C6TA00427J.
[188] R. Wang, H. Haspel, A. Pustovarenko, A. Dikhtiarenko, A. Russkikh, G. Shterk, D. Osadchii, S. Ould-Chikh, M. Ma, W.A. Smith, K. Takanabe, F. Kapteijn, J. Gascon, Maximizing Ag utilization in high-rate CO_2 electrochemical reduction with a coordination polymer-mediated gas diffusion electrode, ACS Energy Lett. 4 (2019) 2024–2031, https://doi.org/10.1021/acsenergylett.9b01509.
[189] Z. Chen, X. Zhang, W. Liu, M. Jiao, K. Mou, X. Zhang, L. Liu, Amination strategy to boost the CO_2 electroreduction current density of M–N/C single-atom catalysts to the industrial application level, Energy Environ. Sci. 14 (2021) 2349–2356, https://doi.org/10.1039/D0EE04052E.
[190] J. Su, J.-J. Zhang, J. Chen, Y. Song, L. Huang, M. Zhu, B.I. Yakobson, B.Z. Tang, R. Ye, Building a stable cationic molecule/electrode interface for highly efficient and durable CO_2 reduction at an industrially relevant current, Energy Environ. Sci. 14 (2021) 483–492, https://doi.org/10.1039/D0EE02535F.
[191] Y. Li, N.M. Adli, W. Shan, M. Wang, M.J. Zachman, S. Hwang, H. Tabassum, S. Karakalos, Z. Feng, G. Wang, Y.C. Li, G. Wu, Atomically dispersed single Ni site catalysts for high-efficiency CO_2 electroreduction at industrial-level current densities, Energy Environ. Sci. 15 (2022) 2108–2119, https://doi.org/10.1039/D2EE00318J.
[192] C.-T. Dinh, F.P. García de Arquer, D. Sinton, E.H. Sargent, High rate, selective, and stable electroreduction of CO_2 to CO in basic and neutral media, ACS Energy Lett. 3 (2018) 2835–2840, https://doi.org/10.1021/acsenergylett.8b01734.
[193] Y. Gu, J. Wei, X. Wu, X. Liu, A study on improving the current density performances of CO_2 electrolysers, Sci. Rep. 11 (2021) 11136, https://doi.org/10.1038/s41598-021-90581-0.
[194] Y. Chen, M.W. Kanan, Tin oxide dependence of the co2 reduction efficiency on tin electrodes and enhanced activity for tin/tin oxide thin-film catalysts, J. Am. Chem. Soc. 134 (2012) 1986–1989, https://doi.org/10.1021/ja2108799.
[195] R. Hinogami, S. Yotsuhashi, M. Deguchi, Y. Zenitani, H. Hashiba, Y. Yamada, Electrochemical reduction of carbon dioxide using a copper rubeanate metal organic framework, ECS Electrochem. Lett. 1 (2012) H17–H19, https://doi.org/10.1149/2.001204eel.
[196] P. Su, W. Xu, Y. Qiu, T. Zhang, X. Li, H. Zhang, Ultrathin bismuth nanosheets as a highly efficient CO_2 reduction electrocatalyst, ChemSusChem 11 (2018) 848–853, https://doi.org/10.1002/cssc.201702229.
[197] J. Greeley, T.F. Jaramillo, J. Bonde, I. Chorkendorff, J.K. Nørskov, Computational high-throughput screening of electrocatalytic materials for hydrogen evolution, Nat. Mater. 5 (2006) 909–913, https://doi.org/10.1038/nmat1752.
[198] C. Liang, B. Kim, S.-Z. Yang, Y. Liu, C. Woellner, Z. Li, R. Vajtai, W. Yang, J. Wu, P. Kenis, P. Ajayan, High efficiency electrochemical reduction of CO_2 beyond two-electron transfer pathway on grain boundary rich ultra-small SnO_2 nanoparticles, J. Mater. Chem. A 6 (2018), https://doi.org/10.1039/C8TA01367E.
[199] L. Ma, S. Fan, D. Zhen, X. Wu, S. Liu, J. Lin, S. Huang, W. Chen, G. He, Electrochemical reduction of CO_2 in proton exchange membrane reactor: the function of buffer layer, Ind. Eng. Chem. Res. 56 (2017) 10242–10250, https://doi.org/10.1021/acs.iecr.7b00819.
[200] H. Wu, J. Song, C. Xie, Y. Hu, B. Han, Highly efficient electrochemical reduction of CO_2 into formic acid over lead dioxide in an ionic liquid–catholyte mixture, Green Chem. 20 (2018) 1765–1769, https://doi.org/10.1039/C8GC00471D.
[201] A. Hailu, A.A. Tamijani, S.E. Mason, S.K. Shaw, Efficient conversion of CO_2 to formate using inexpensive and easily prepared post-transition metal alloy catalysts, Energy Fuels 34 (2020) 3467–3476, https://doi.org/10.1021/acs.energyfuels.9b03783.
[202] W. Zhang, Y. Hu, L. Ma, G. Zhu, P. Zhao, X. Xue, R. Chen, S. Yang, J. Ma, J. Liu, Z. Jin, Liquid-phase exfoliated ultrathin Bi nanosheets: uncovering the origins of enhanced electrocatalytic CO_2 reduction on two-dimensional metal nanostructure, Nano Energy 53 (2018) 808–816, https://doi.org/10.1016/j.nanoen.2018.09.053.
[203] Y. Liu, M. Fan, X. Zhang, Q. Zhang, D. Guay, J. Qiao, Design and engineering of urchin-like nanostructured SnO_2 catalysts via controlled facial hydrothermal synthesis for efficient electro-reduction of CO_2, Electrochim. Acta 248 (2017) 123–132, https://doi.org/10.1016/j.electacta.2017.07.140.
[204] N. Han, Y. Wang, H. Yang, J. Deng, J. Wu, Y. Li, Y. Li, Ultrathin bismuth nanosheets from in situ topotactic transformation for selective electrocatalytic CO_2 reduction to formate, Nat. Commun. 9 (2018) 1320, https://doi.org/10.1038/s41467-018-03712-z.
[205] J. Huang, X. Guo, Y. Wei, Q. Hu, X. Yu, L. Wang, A renewable, flexible and robust single layer nitrogen-doped graphene coating Sn foil for boosting formate production from electrocatalytic CO_2 reduction, J. $_{CO2}$ Util. 33 (2019) 166–170, https://doi.org/10.1016/j.jcou.2019.05.026.
[206] K. Natsui, H. Iwakawa, N. Ikemiya, K. Nakata, Y. Einaga, Stable and highly efficient electrochemical production of formic acid from carbon dioxide using diamond electrodes, Angew. Chem. Int Ed. Engl. 57 (2018) 2639–2643, https://doi.org/10.1002/anie.201712271.
[207] K. Bejtka, J. Zeng, A. Sacco, M. Castellino, S. Hernández, M.A. Farkhondehfal, U. Savino, S. Ansaloni, C.F. Pirri, A. Chiodoni, Chainlike mesoporous SnO_2 as a well-performing catalyst for electrochemical CO_2 reduction, ACS Appl. Energy Mater. 2 (2019) 3081–3091, https://doi.org/10.1021/acsaem.8b02048.
[208] C.W. Lee, J.S. Hong, K.D. Yang, K. Jin, J.H. Lee, H.-Y. Ahn, H. Seo, N.-E. Sung, K. T. Nam, Selective electrochemical production of formate from carbon dioxide with bismuth-based catalysts in an aqueous electrolyte, ACS Catal. 8 (2018) 931–937, https://doi.org/10.1021/acscatal.7b03242.
[209] H. Xiang, H.A. Miller, M. Bellini, H. Christensen, K. Scott, S. Rasul, E.H. Yu, Production of formate by CO_2 electrochemical reduction and its application in energy storage, Sustain. Energy Fuels 4 (2020) 277–284, https://doi.org/10.1039/C9SE00625G.
[210] R. Sinha, A. Bisht, S. Rarotra, T.K. Mandal, Continuous semi-micro reactor prototype for the electrochemical reduction of CO_2 into formic acid, Ind. Eng. Chem. Res. 59 (2020) 1737–1745, https://doi.org/10.1021/acs.iecr.9b03304.
[211] R.I. Masel, Z. Liu, H. Yang, J.J. Kaczur, D. Carrillo, S. Ren, D. Salvatore, C. P. Berlinguette, An industrial perspective on catalysts for low-temperature CO_2 electrolysis, Nat. Nanotechnol. 16 (2021) 118–128, https://doi.org/10.1038/s41565-020-00823-x.
[212] L. Fan, C. Xia, F. Yang, J. Wang, H. Wang, Y. Lu, Strategies in catalysts and electrolyzer design for electrochemical CO_2 reduction toward C^{2+} products, Science Advances, 6 eaay3111, https://doi.org/10.1126/sciadv.aay3111.
[213] M. Sassenburg, M. Kelly, S. Subramanian, W.A. Smith, T. Burdyny, Zero-gap electrochemical CO_2 reduction cells: challenges and operational strategies for prevention of salt precipitation, ACS Energy Lett. 8 (2023) 321–331, https://doi.org/10.1021/acsenergylett.2c01885.
[214] T. Saberi Safaei, A. Mepham, X. Zheng, Y. Pang, C.-T. Dinh, M. Liu, D. Sinton, S. O. Kelley, E.H. Sargent, High-density nanosharp microstructures enable efficient CO_2 electroreduction, Nano Lett. 16 (2016) 7224–7228, https://doi.org/10.1021/acs.nanolett.6b03615.
[215] M.B. Ross, C.T. Dinh, Y. Li, D. Kim, P. De Luna, E.H. Sargent, P. Yang, Tunable Cu enrichment enables designer syngas electrosynthesis from CO_2, J. Am. Chem. Soc. 139 (2017) 9359–9363, https://doi.org/10.1021/jacs.7b04892.
[216] J.M. Jani, H. Can Aran, M. Wessling, R.G.H. Lammertink, Modeling of gas–liquid reactions in porous membrane microreactors, J. Membr. Sci. 419–420 (2012) 57–64, https://doi.org/10.1016/j.memsci.2012.06.044.
[217] B.S. Crandall, F. Jiao, Knowledge transfer between liquid- and gas-fed CO_2 electrolysis, Chem. Catal. 2 (2022) 2833–2834, https://doi.org/10.1016/j.checat.2022.10.009.
[218] P. Senthilkumar, M. Mohapatra, S. Basu, The inchoate horizon of electrolyzer designs, membranes and catalysts towards highly efficient electrochemical reduction of CO_2 to formic acid, RSC Adv. 12 (2022) 1287–1309, https://doi.org/10.1039/D1RA05062A.
[219] G. Li, T. Yan, X. Chen, H. Liu, S. Zhang, X. Ma, Electrode engineering for electrochemical CO_2 reduction, Energy Fuels 36 (2022) 4234–4249, https://doi.org/10.1021/acs.energyfuels.2c00271.
[220] J.E. Huang, F. Li, A. Ozden, A. Sedighian Rasouli, F.P. García de Arquer, S. Liu, S. Zhang, M. Luo, X. Wang, Y. Lum, Y. Xu, K. Bertens, R.K. Miao, C.-T. Dinh, D. Sinton, E.H. Sargent, CO_2 electrolysis to multicarbon products in strong acid, Science 372 (2021) 1074–1078, https://doi.org/10.1126/science.abg6582.
[221] Z. Kou, X. Li, T. Wang, Y. Ma, W. Zang, G. Nie, J. Wang, Fundamentals, on-going advances and challenges of electrochemical carbon dioxide reduction, Electrochem. Energy Rev. 5 (2022) 82–111, https://doi.org/10.1007/s41918-021-00096-5.
[222] G.O. Larrazábal, P. Strøm-Hansen, J.P. Heli, K. Zeiter, K.T. Therkildsen, I. Chorkendorff, B. Seger, Analysis of mass flows and membrane cross-over in CO_2 reduction at high current densities in an MEA-type electrolyzer, ACS Appl. Mater. Interfaces 11 (2019) 41281–41288, https://doi.org/10.1021/acsami.9b13081.
[223] A.A. Samu, A. Kormányos, E. Kecsenovity, N. Szilágyi, B. Endrődi, C. Janáky, Intermittent Operation of CO_2 electrolyzers at industrially relevant current densities, ACS Energy Lett. 7 (2022) 1859–1861, https://doi.org/10.1021/acsenergylett.2c00923.